Functional characterization of Satb 1 and Satb2 genes in developing neocortex

Disputation

zur Erlangung des Doktorgrades

der Mathematisch-Naturwissenschaftlichen Fakultäten

der Georg-August-Universität zu Göttingen

vorgelegt von

Meury del Camino de Juan Romero

aus León, Spanien

Göttingen 2008

D7

Referent: Prof. Dr. Ernst A Wimmer

Korreferent: Prof. Dr. Thomas Pieler

Tag der mündlichen Prüfung: 28.10.2008

This thesis is dedicated to my family

Contents

Abbreviations

a.c	anterior commissure
ATP	adenosine triphosphate
BrdU	5-bromo-2-desoxy-uridine
bp	Base pair
BSA	Bovine serum albumin
BUR	Base unpairing regions
cDNA	Complementary DNA
CDS	Coding sequence
CFN	Corticofugal neurons
ChIP	Chromatin immunoprecipitation assay
CMV	Cyto-megalo virus
CNS	Central nervous system
CSMN	Corticospinal motor neurons
CP	Cortical plateral
Cp	cerebral peduncle
CR	Cajal retzius cells
CUX	Cut domain transcription factor
d	day
DAPI	4'-6'-diamidino-2-phenylindole
DEPC	Diethyl pyrocarbonate
DiI	1,1′-dioctadecyl-3,3,3′,3′-tetramethylindocarbocyanine perchlorate
DIG	Digoxigenin
DL	Deep layer
DMSO	dimethylsulfoxide
DNA	Deoxyribonucleic acid
DNase	Deoxyribonuclease
dNTP	Deoxynucleotides
DTT	Dithiothreitol
E	Embryonic day
EDTA	Ethylene diamine tetra acetic acid

ES cell	embryonic stem cell
et al.	*et altera*
FCS	Fetal calf serum
FGFR	Fibroblast growth factor receptor 1
Fig.	Figure
g	grams
G1	G1-phase of cell cycle
G2	G2-phase of cell cycle
G418	geneticin
GABA	γ-amino butyric acid
GAPDH	Glyceraldehyde-3-phosphate dehydrogenase
GFAP	Glial fibrillary acidic protein
h	Hour
HAT	Hystone acetyl transferese
HCL	Hydrochloric acid
HD	Homeodomain
HDAC	Histone deacetylase
HEPES	4-(2-Hydroxyethyl)-piperazin-1-ethansulfonic acid
h.p	hippocampal commissure
HPRT	Hypoxanthine guanine phosphoribosyl transferase
HRP	Horse radish peroxidase
Hybmix	Hybridization mix
Ic	internal capsule
IHC	Immunohistochemistry
IPC	Intermediate progenitor cell
IRES	Internal Ribosome Entry Site
ISH	*In situ* hybridization
IZ	Intermediate zone
IVT	*in vitro* transcription
IUE	in utero eletroporation
Kb	kilobase
kDa	kilodalton
ko	Knock-out
ki	Knock-in

l	litter
LB	Luria-Bertani
LI	Labeling index
LIF	leukemia inhibitory factor
LGE	Lateral ganglionic eminence
LP	Lens placoid
M	Molar
mAB	Monoclonal antibody
MARs	Matrix attachment regions
MGE	Medial ganglionic eminence
Min	minute
Ml	milliliter
mM	millimolar
μM	micromolar
MEM	Modified Eagle Medium
mRNA	Messenger ribonucleic acid
MW	Molecular weight
MZ	Marginal zone
n	Sample number
NaAc	Sodium acetate
NaCl	Sodium chloride
NADPH	Reduced nicotinamide adenine dinucleotide phosphate
NaOH	Sodium hydroxide
NE	Neuroepithelium
neoR	neomycin resistance gene
NTE	NaCl-tris-EDTA
oN	overnight
P	Postnatal day
pAB	Polyclonal antibody
PBS	Phosphate buffered saline
pBS KS	Plasmid bluescript KS
PBT	PBS containing 0.05% Tween-20
PCR	Polymerase chain reaction
pcDNA	Plasmid-cDNA

PD	Paired domain
Pen/Strep	Penicillin/Streptomycin
PFA	Paraformaldehyde
pH	*potentium hydrogenii*
PH3	Phosphorylated histone H3
PRD	Bipartite paired domain
PSPB	Pallial-subpallial boundary
RNA	Ribonucleic acid
RNase	Ribonuclease
RC2	Radial cell 2
rln	Reelin
rpm	Rounds per minute
RT	Room temperature
SDS	Sodium dodecyl sulfate
s.d.	Standard deviation
siRNA	Small interfering RNA
SP	Subplate
SpC	Spinal Cord
SP6	Bacteriophage sp6
SEM	Standard error of the mean
SFRP	Secreted frizzled related protein
S-phase	DNA-synthesis phase of the cell cycle
SSC	Sodium chloride-Sodium citrate
SUMO	Small ubiquitive related modifier
Svet1	Subventricular tag1
SVZ	Subventricular zone
T7	Bacteriophage T7
TAD	Transactivating domain
TAE	Tris-acetate-EDTA
TBE	Tris-borate-EDTA
TBS	Tris-buffered saline
Tbr	T-domain transcription factor
TCA	Thalamicocortical axons
TF	Transcription factor

TK	Thymidin Kinase
Tris	Tris-(hydroxymethyl)-aminomethane
TSA	Trichostatin A
Tween 20	Polyoxyethylene sorbitan monolaurate
U	unit (enzymatic activity)
UL	Upper layer
UV	Ultraviolet
V	Volt
Vol	Volume
VZ	Ventricular zone
W	Watt
wt	Wild type

1. Introduction

1.1 Cortex development.

1.1.1 Early cortical development in mouse.

Development of the central nervous system (CNS) begins with the specification of a group of cells of the presumptive ectoderm into the neural plate, which invaginates under the influence of signals from the notochord to give rise to the neural tube. The most rostral portion of this neural tube, telencephalon, is divided into two cerebral cortices. The mammalian neocortex, the top layer of the cerebral hemispheres, is a very complex structure consisting of six layers. This elaborate organization of the neocortex appears in stages, with the sequential formation of the marginal zone (MZ), intermediate zone (IZ) and subventricular zone (SVZ). After the generation of the ventricular zone (VZ), the layer adjacent to the lateral ventricle, an additional proliferative layer known as the subventricular zone (SVZ) forms above the VZ. Progenitors residing in these two layers produce projection neurons of the different neocortical layers

in a tightly controlled temporal order from embryonic day (E) 11.5 to E17.5 in mice (Angevine and Sidman, 1961; Caviness et al., 1995; Rakic, 1974).The earliest-generated cortical neurons, that appear around E10.5 in mice, migrate away from the VZ to form the preplate, which subsequently splits into the marginal zone and the subplate (SP) (Allendoerfer and Shatz, 1994)

During the formation of the cortical plate, neurons in different layers are generated in an orderly inside- first, outside-last fashion. The most superficial layers of the cortex are populated by late born neurons with the exception of the Cajal-Retzius cells, located in the marginal zone, that are the first ones to be generated. Early-born cortical plate cells populate the deepest layers, and later generated neurons migrate past older cells and settle into progressively more superficial positions (Luskin and Shatz, 1985) The newly postmitotic neurons are specified to adopt the laminar positions characteristic of their birthdays (McConnell, 1995) neurons that end up in the same laminar position tend to share similar functional properties and patterns of connectivity (O'Leary, 1993).
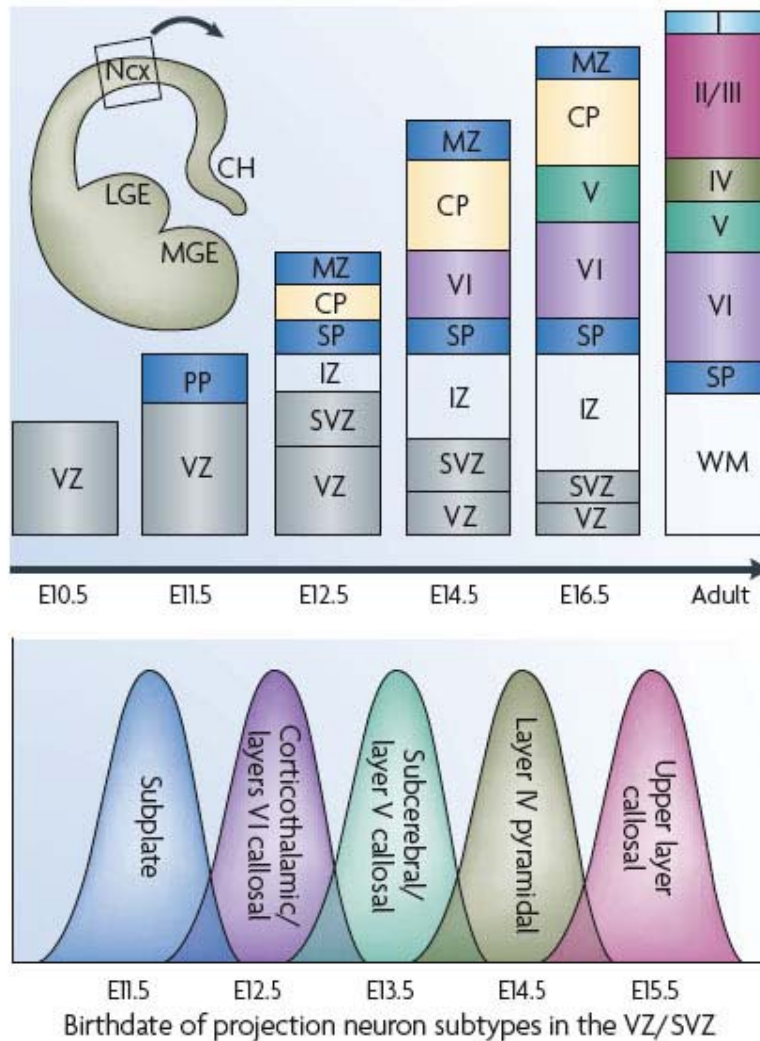
Fig.1 Schematic diagram depicting how progenitors residing in the VZ and SVZ in mice produce projection neurons in an 'inside-out' fashion. The earliest born neurons form the preplate (PP), which is later split into the more superficial marginal zone (MZ) and the deeply located subplate (SP). The cortical plate (CP), which will give rise to the multilayered neocortex, develops in between these two layers, such that later born neurons arriving at the cortical plate migrate past earlier born neurons. Different classes of projection neuron are born in overlapping temporal waves. All times listed are approximations given the neurogenic gradients that exist across the cortex, where caudomedial neurogenesis lags behind rostrolateral neurogenesis. CH, cortical hem; E, embryonic day; Ncx, neocortex; IZ, intermediate zone; LGE, lateral ganglionic eminence; MGE, medial ganglionic eminence; SVZ, subventricular zone; VZ, ventricular zone; WM, white matter. Modified, with permission, from REF. 131© (2002) Elsevier Science. (Molyneaux et al., 2007)

There are three basic types of neurogenic progenitors within the developing neocortex: neuroepithelial cells, radial glia and intermediate progenitors (Gotz and Barde, 2005). A single sheet of pseudostratified neuroepithelial cells undergo symmetric cell divisions in order to expand the pool of multipotent progenitors as well as a smaller percentage of asymmetric cell divisions to generate the earliest born

neurons (Gotz and Barde, 2005; McConnell, 1995; Smart, 1973). After the onset of cortical neurogenesis, neuroepithelial cells give rise to bipolar radial glial cells, the progenitors of cortical neurons and astrocytes. In contrast, progenitors in the retina and spinal cord mostly maintain neuroepithelial properties and to a lesser extent radial glial properties during neurogenesis.

Radial glia cells have a crucial role in guiding neurons to their final locations in the cortical plate owing to their long processes that extend from the ventricular wall to the pial surface that serve as a migratory scaffold for young neurons (Rakic, 1972; Rakic, 2003). The nuclei of these cells move through these processes within the limits of the ventricular zone limits (basal and ventral) during the cell cycle. During the M-phase of the cell cycle, the soma reaches the most ventral part, whereas during the S-phase it moves away from the ventral to the basal side of the ventricular zone. The radial glial cells undergo two different types of mitotic divisions: Symmetric cellular divisions creating two identical daughter cells which are both again radial glia cells, or, the asymmetric cellular divisions creating one radial glia cell and one post-mitotic neuron or neuronal progenitor cell of the subventricular zone. In the case of asymmetric cellular divisions, the post-mitotic neurons, which do not have processes like radial glia cells, start to move through the developing cortical tissue by climbing over the latter. (Rakic, 2003; Weissman et al., 2003).

Intermediate or basal progenitors are another class of cortical progenitors located in the SVZ and in the basal VZ. (Miyata et al., 2004; Noctor et al., 1992; Smart, 1973). VZ progenitors divide asymmetrically to self-renew and produce rounded daughter cells called the Intermediate progenitor cell (IPC). However, It has been shown that cells located in the basal side of the VZ (the developing SVZ) undergo symmetric cell divisions giving rise to two postmitotic neurons (Haubensak et al., 2004) the SVZ thus contributes to the generation of upper-layer neurons. Multipolar IPCs also divide symmetrically at a nonsurface position to produce two immature multipolar neurons (Cai et al., 2002). These immature neurons migrate into the cortical plate (Noctor et al., 2004) and differentiate into projection neurons. IPC's appear to produce the majority of neurons during early neurogenesis when deep layers are generated (Haubensak et al., 2004) Basal progenitors or IPCs express markers like subventricular tag1 (Svet1), T-domain transcription factor (TF; Tbr2), and the homeobox proteins Cux1 and Cux2 (Englund et al., 2005; Nieto et al., 2004; Tarabykin et al., 2001; Zimmer et al., 2004)

Time-lapse microscopy revealed that a progenitor can continue to divide *in vitro* and produce neurons that express laminar markers after the same number of cell divisions as their *in vivo* counterparts, suggesting that the temporal sequence of the genetic program required to produce a given subtype of projection neuron is at least partially intrinsic to progenitors (Shen et al., 2006). However, experiments involving transplantation of early progenitors into later environments has shown that extracellular signals can alter this programme as long as their influence occurs before the S phase of the cell cycle (McConnell and Kaznowski, 1991; Nguyen et al., 2006).

1.1.2 Cortical neurons.

There are two broad classes of cortical neurons: interneurons, which make local connections; and projection neurons, which extend axons to distant intracortical, subcortical and subcerebral targets. Projection neurons are glutamatergic neurons characterized by a typical pyramidal morphology that transmit information between different regions of the neocortex and to other regions of the brain. GABA (γ-aminobutyric acid) containing interneurons are generated primarily from progenitors in the ventral telencephalon while the Cajal-Retzius cells and the MZ are produced by cortical hem and the pallial-subpalial boundary. Both of these cell types migrate long distances to their final locations within the neocortex. Early in development, the presumptive forebrain is subdivided into two separate domains: the ventral telencephalon, and the dorsal telencephalon which eventually develops into the cerebral cortex, responsible for cognitive function, sensory perception and consciousness. The ventral telencephalon is formed by two distinct proliferating cell masses: medial ganglionic eminence and lateral ganglionic eminence (MGE and LGE), where most inhibitory interneurons and a large population of oligodedrocytes originate. These interneurons and oligodendrocytes enter the developing cortical plate by tangential migration. In contrast, projection neurons of the developing cerebral cortex are generated from progenitors of the neocortical germinal zone located in the dorsolateral wall of the telencephalon and subsequently migrate radially to the developing cortical plate (Marin et al., 2003; Nadarajah et al., 2003). However, a subpopulation of cortical projection neurons, derived from Emx1+ cortical progenitors, migrate tangentially over long distances. These neurons express upper

layer cortical marker Satb2 and not GABA or oligodendrocyte marker Olig1 (Britanova et al., 2005).

1.1.3. Axonal connectivity.

In the mammalian cerebral cortex, projection neurons comprise of three broad classes. First, are the commissural projection neurons, that project across and within the telencephalon but never outside. This group includes callosal projection neurons, which extend axons across the corpus callosum to the contralateral hemisphere. Corticofugal neurons (CFN) are the second type of projection neurons. They send their axons away from the cortex forming connections with subcortical targets, including the thalamus, midbrain, hindbrain, and spinal cord (McConnell, 1995; Molyneaux et al., 2007). There are two different kinds of CFNs, corticothalamic neurons (CTN) that project subcortically to different nuclei of the thalamus and, subcerebral projection neurons. The latter include pyramidal neurons located in layer V that extend projections to the brainstem and spinal cord. These can be further subdivided into:1) corticotectal neurons, located in the visual area of the cortex and responsible for primary projections to the superior colliculus with secondary collateral projections to the rostral pons; 2) corticopontine neurons that maintain primary projections to the pons and finally, 3) corticospinal motor neurons (CSMNs), located in the sensorimotor area of the cortex, that responsible for primary projections to the spinal cord, with secondary collaterals to the striatum, red nucleus, caudal pons and medulla.

CSMNs are located primarily in cortical layers 5 and 6. While neurons of layer 6 project to the thalamus, projections to the midbrain, hindbrain, and spinal cord originate from layer 5 neurons. Cortical and callosal projections are found in all layers but are particularly abundant in layers 2 through 4 (O'Leary, 1993). Also, neurons generated at the same time can project differently, for example different subpopulations of layer 5 neurons that form callosal versus subcortical projections. They migrate and differentiate in parallel, but their axonal trajectories diverge, extending toward the midline and internal capsule, respectively (Koester and O'Leary, 1993; O'Leary et al., 1994). Transplantation studies suggest that a neuron acquires a laminar identity, which specifies the layer to which it will migrate, by the time of terminal mitotic division (Desai and McConnell, 2000; McConnell, 1995).

1.1.4 Laminar specification in the cerebral cortex.

Several genes, *Pax6, Emx2, Lhx2* and *Foxg1*, have been found to be involved in the initial specification of neocortical cell fate, controlling the early aspects of cortical progenitor specification (Mallamaci and Stoykova, 2006). These four genes establish neocortical progenitor domain by repressing dorsal midline (*Lhx2* and *Foxg1*) and ventral (*Emx2* and *Pax6*) fates.

Other genes, *Tbr1, Fezf2*, and *Ctip2* are involved in postmitotic specification of DL neurons. *Tbr1* is expressed by multiple types of cortical neurons and regulates the differentiation of layer 6 and subplate. Its absence produces abnormalities in projection neuron migration and defects in axonal growth of subplate, corticothalamic, subcerebral and cortico-cortical projection neurons (Hevner et al., 2001). Fez family zinc finger 2 (*Fezf2*, also known as *Fezl*) and *Otx1* are expressed in a subpopulations of progenitors in the VZ and SVZ prior to genesis and layers V and VI, subsequently in early posmitotic and differentiated neurons of the same layers. B-cell leukaemia/ lymphoma 11B (*Ctip2*, also known as *Bcl11b*) is expressed at high levels in subcerebral neurons of layer V and at much lower levels in corticothalamic neurons of layer VI (Arlotta et al., 2005).

The identity of genes controlling the postmitotic specification of UL neurons remains unknown. A reduction in UL neuron production can be seen after the deletion of transcription factors *Pax6* or *Tlx,* and in the double knockout of Brn1 and Brn2 (McEvilly et al., 2002; Roy et al., 2004; Sugitani et al., 2002; Tarabykin et al., 2001). *Pax6* is expressed in the mitotically active ventricular zone and has previously been shown to control specification, regionalization and arealization of the cerebral cortex (Walther and Gruss, 1991). *Brn1* (also known as *Pou3f3*) and *Brn2 (Pou3f2)*, which are expressed primarily by neurons of layers II–V, are involved in directing the differentiation and migration of neurons within these layers.

Cux1 (*Cutl1*) and *Cux2* (*Cutl2*), cut domain transcription factors are expressed by young UL neurons during the initial steps of their specification and continue to be expressed postmigration in all UL neurons, *Satb2* is expressed only in a subgroup of UL cells (Britanova et al., 2005; Britanova et al., 2006a; Nieto et al., 2004; Zimmer et al., 2004).The pattern of *Satb2* expression, predominantly in young UL neurons but

not in SVZ progenitors, suggests that it may be involved in the control of early aspects of UL neuron specification (Britanova et al., 2005).

Transcription factors function by regulating chromatin accessibility via recruitment of histone-modifying enzymes or nucleosome-remodeling complexes and stimulation of RNA polymerase via interaction with the mediator complex (Freiman and Tjian, 2003; Zhang and Reinberg, 2001). Enhancers, promoters and nuclear matrix attachment regions (MARs) have been implicated in the regulation of gene expression by altering the organization of eukaryotic chromosomes and augmenting the potential of enhancers to act over large distances (Bode et al., 2000; Scheuermann and Garrard, 1999). The association of MARs with the nuclear matrix serves to structurally define the borders of chromatin domains and participate in the regulation of transcription. *Satb1* and *Satb2* are a family of transcription factors with the ability to bind MARs.

1.2 Special AT-rich binding protein 1 (Satb1): The beginning of the story.

The nuclear matrix or skeleton, defined as the insoluble material left in the nucleus after a series of biochemical extraction steps (Nelson et al., 1986), is the intranuclear frame where the independent loop domains of eukaryotic chromosomes seems to be periodically anchored. Matrix attachment regions (MARs) are specific DNA sequences that form the base of chromosomal loops and can bind to the nuclear matrix *in vitro* (Earnshaw, 1988; Gasser and Laemmli, 1987) . MARs are often located in close proximity to regulatory sequences including enhancers (Cockerill and Garrard, 1986; Gasser and Laemmli, 1987; Jarman and Higgs, 1988; Klehr et al., 1991; Mielke et al., 1990; Poljak et al., 1994), and some MARs can increase transcription from certain promoters (Bode et al., 1992; Dietz et al., 1994; Klehr et al., 1991; Mielke et al., 1990) suggesting that MARs may play a role in tissue-specific gene expression.

Satb1 is a transcription factor that was originally cloned by virtue of its ability to bind to a core unwinding element, a MAR, located in the *immunoglobulin* μ *heavy chain* (*IgH*) gene enhancer (Dickinson et al., 1992). Satb1 can mediate the attachment of chromatin to the nuclear matrix, thereby folding chromatin into topologically independent loop domains in order to form higher order chromatin structure (Cockerill and Garrard, 1986; Dickinson et al., 1992; Gasser and Laemmli, 1987).

Satb1 was the first cell-type-restricted MAR-binding protein to be identified and is expressed in a lineage-specific manner, primarily in T-cells and other tissue-specific precursors in testis, fetal brain, and osteoblasts (Alvarez et al., 2000; Dickinson et al., 1992; Hawkins et al., 2001) Satb1 recognizes double-stranded DNA characterized by a unique group of AT-rich sequences. Such regions are usually 100–150 bp in length and contain a high degree of base-unpairing, which is characterized by the present of several base-unpairing regions (BURs) This specialized DNA context (an ATC sequence context) where Gs and Cs are located only in one strand gives Satb1 the property of unwinding by base unpairing under negative superhelical strain (Dickinson et al., 1992; Kohwi-Shigematsu and Kohwi, 1992; Leonard et al., 1984) *Satb1* also contains an atypical homeodomain and two cut domains. The *Satb1* homeodomain is unique among other homeodomains since, in the highly conserved aminoacid position 49, tryptophan is replaced by phenylalanine. This homeodomain together with the BUR-binding domain is necessary for recognition of the core unwinding element within a BUR. The isolated homodomain exhibits only very weak nonspecific binding activity to base-unpairing sequences, similar to the homeodomains of the POU transcription factors. POU proteins are eukaryotic transcription factors containing a bipartite DNA binding domain referred to as the POU domain. The acronym POU is derived from the names of three mammalian transcription factors, the pituitary-specific *Pit-1*, the octamer-binding proteins *Oct-1* and *Oct-2*, and the neural *Unc-86*. The homeodomain in these transcription factors cannot bind independently or bind with low affinity and relaxed specificity (Rosenfeld, 1991). In case of POU transcription factors, both the POU domains and the homeodomains are equally necessary for high affinity binding, and together they form a bipartite binding domain (Sturm et al., 1988). Similarly, association of *Satb1* homeodomain with the MAR-binding domain enhances binding specificity toward the core unwinding element of a MAR. Also, when the core unwinding element of a BUR is mutated to abolish its unwinding property, *Satb1* binding is eliminated (Dickinson et al., 1992; Nakagomi et al., 1994; Wang et al., 1995).

The fact that *Satb1* contains Cut-like repeats and a homeodomain, suggests structural similarity to the Cut proteins identified from various species (Andres et al., 1992; Blochlinger et al., 1988; Neufeld et al., 1992; Valarche et al., 1993). However, the *Satb1* homeodomain shares more homology with other homeodomains like engrailed (33% identity) than with Cut proteins (26% identity). Furthermore, Cut repeats were

shown to be specific DNA-binding domains (Andres et al., 1992; Harada et al., 1994) whereas the Cut-like repeats in *Satb1* did not appear to bind *Satb1*-binding DNA sequences.

The other important region is the N-terminal PDZ-like domain, a putative region for facilitating interactions with other proteins, it also assist in the formation of *Satb1* homodimer and is essential for DNA binding (Galande et al., 2001).
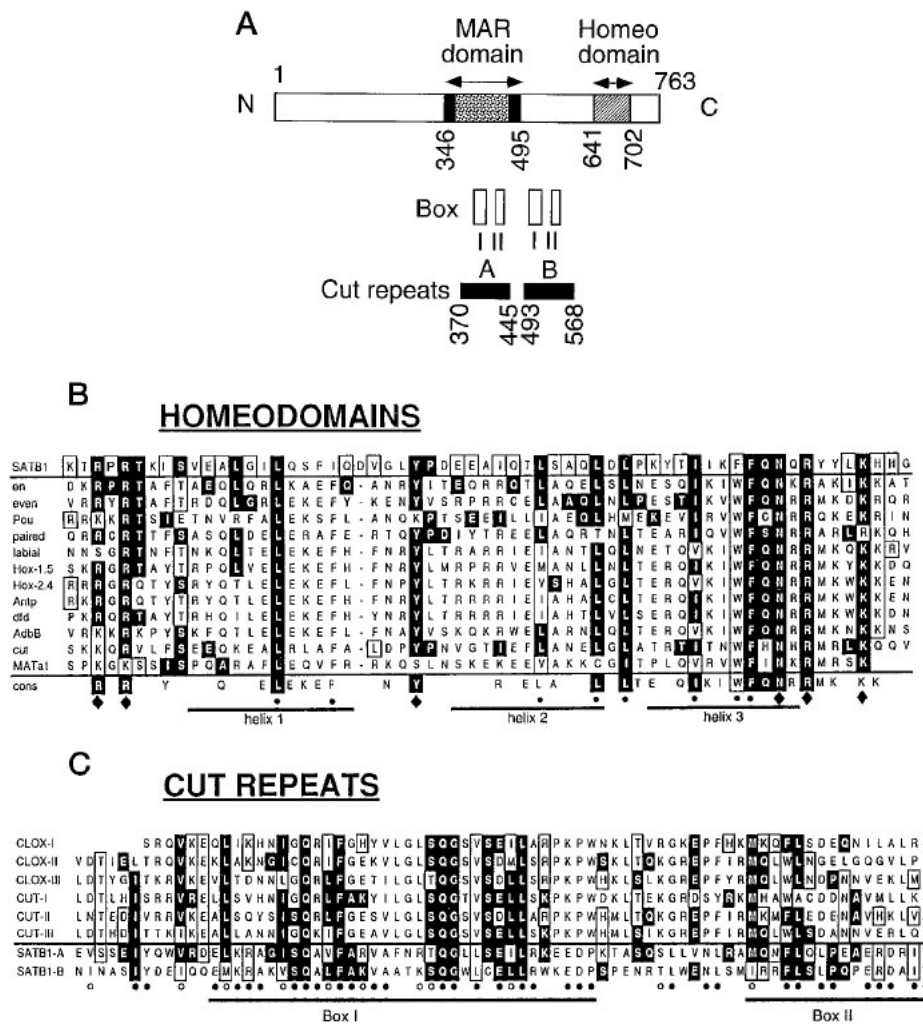
FIG. 2. *Satb1* **contains a homeodomain and Cut-like repeats in addition to its MAR binding domain.** *A,* schematic representation of the overall structure of *Satb1*, indicating the positions of the MAR-binding domain including the amino acids at each end that are essential for MAR binding (shown in *black*), the homeodomain, the two Cut-like repeats, and the previously identified repeats box I and box II. *B,* alignment of the homeodomain in *Satb1* with representative members of the different classes of homeodomain-containing proteins, defined by Scott *et al.(Scott et al., 1989)* (*Single letter amino acid code*). Identical amino acids between *Satb1* and other homeodomains are shown in *closed boxes*; *open boxes* indicate similar amino acids or residues in *Satb1* that are identical to only one or two other members. A consensus sequence derived from the alignment is given at the *bottom*. The positions of the three helical regions are indicated. *Dots* represent residues important for structure; *diamonds* indicate amino acids contacting DNA, as derived from the crystal structure of the engrailed homeodomain-DNA complex (Kissinger et al., 1990). *C,* alignment of the Cut-like repeats A and B in *Satb1* with the Cut proteins from *Drosophila melanogaster* (*CUT I–III*) and the mammalian Clox

proteins (*CLOX I–III*). *Box I* and *box II* in *Satb1* are *underlined*. Identical and similar amino acids are shown in *closed* or *open boxes*, respectively. Amino acids indicated by *dots* are identical or conserved in both *Satb1* repeats (adapted from Dickinson et al., 1992).

Satb1 forms a functional nuclear architecture that has a 'cage-like' protein distribution in thymocytes surrounding heterochromatin and demarcating it from euchromatin (Cai et al., 2003). This is called, the '*Satb1* regulatory network', and it pertains to the fact that *Satb1* regulates distant gene expression (Alvarez et al., 2000; Cai et al., 2003; Dickinson et al., 1992; Yasui et al., 2002) by recruiting chromatin remodelling/modifying enzymes and transcription factors to genomic DNA, which it tethers via BURs (Bode et al., 1992; Kohwi-Shigematsu et al., 1998; Kohwi-Shigematsu and Kohwi, 1990).

Satb1 can act as a transcriptional repressor (Kohwi-Shigematsu et al., 1997; Liu et al., 1997) by binding to MARs at multiple sites where chromatin is fastened to form loop domains and dictating the organization and structure of chromatin domains. Thereby, *Satb1* can control the transcription potential of multiple genes in specific cell lineages, a property that can be critical during development. *Satb1* can also regulate gene expression in other ways, for instance, in case of globin gene where it directly influences the promoter activity by interacting with CBP (Wen et al., 2005), or in case of regulation of IL-2 and IL-2Ra expression by recruiting HDAC1 (Kumar et al., 2005).

Satb1 can be expressed in breast cancer cells and where it coordinates the expression of a large number of genes to induce metastasis. Satb1 seems to play a key role in breast cancer progression since the removal of *Satb1* from aggressive breast cancer cells not only reverses metastatic phenotypes but also inhibits tumor growth. (Han et al., 2008)

1.3 Special AT-rich binding protein 2 (Satb2)

Satb2, a close homologue of *Satb1* (61% homology to Satb1 at amino acid level), was identified in a cDNA subtraction screening in a search for genes controlling neural differentiation. Expression of *Satb1* and *Satb2* was detected in different subpopulations of developing mouse CNS in a mutually exclusive manner. In the developing neocortex, *Satb2* expression is largely confined to subsets of postmitotic cells in the superficial layers that extend axons across the corpus callosum. In the

developing spinal cord *Satb2* expression marks a subpopulation of *Lbx1*-positive neurons dorsally and a subgroup of *Isl1*-positive neurons ventrally.

Similar to Satb1, Satb2 was found in a nuclear protein complex that can bind to MARs with high affinity in the developing neocortex, but not basal ganglia, this suggest that Satb2 may be involved in regulating differentiation of neurons at the level of higher order chromatin structure, via binding to MARs (Britanova et al., 2006a; Dobreva et al., 2003).

Satb2 is a target for SUMOylation, a reversible modification of the protein that modulates its activity as a transcription factor. The small ubiquitin related modifier (SUMO) modifies several lysine residues, which makes *Satb2* differs from *Satb1*. These modifications are augmented specifically by the SUMO E3 ligase PIAS1. Mutations of the SUMO conjugation sites of *Satb2* enhance its activation potential and association with endogenous MARs in vivo, whereas N-terminal fusions with SUMO1 or SUMO3 decrease *Satb2*-mediated gene activation. This sumoylation targeting *Satb2* to the nuclear periphery may contribute to the modulation of subnuclear DNA localization (Dobreva et al., 2003).

In the nucleus, regulation of gene expression involves a temporally coordinated interaction between cis-regulatory DNA elements and nuclear proteins that are expressed in a developmental and cell-specific manner (Agoston and Dobi, 2000; Jaenisch and Bird, 2003). *Satb2* specifically interacts with, histonedeacetylase (HDAC) 1 and metastasis-associated protein (MTA) 2, members of the nucleosome remodelling and HDAC (NuRD) complex (Gyorgy et al., 2008). The AT-rich DNA-dependent repressor function of Satb2 can be reversed by the treatment of trichostatin A (TSA), that blocks histone acetylations (Dobreva et al., 2003; Gyorgy et al., 2008).

 Satb2 was also identified as a candidate gene responsible for craniofacial dysmorphologies associated with deletions and translocations at 2q32-q33 in humans, one of only three regions of the genome for which haploinsufficiency has been significantly associated with isolated cleft palate (FitzPatrick et al., 2003). Full functional loss of *Satb2,* and also haploinsufficiency, phenocopy these craniofacial abnormalities in mice. There is also increased apoptosis in the discrete, complementary regions of the developing jaw primordia where Satb2 is expressed and the subsequent arrest of regional development, changes in the pattern of expression of three genes implicated in the regulation of craniofacial development in humans and mice: *Pax9, Alx4,* and *Msx1* is seen (Beverdam et al., 2001; Britanova et al., 2006b;

Gyorgy et al., 2008; Jezewski et al., 2003; Park et al., 2006; Peters et al., 1998; Satokata and Maas, 1994; Schuffenhauer et al., 1999; van den Boogaard et al., 2000). Coupled with its spatiotemporal expression profile, this marks *Satb2* as a potentially key gene coordinating the elaboration of the functional design of jaws, including that of the mammalian palate.

Satb2 is expressed also in cells of the osteoblast lineage, playing an important role in osteoblast differentiation, and moreover in vertebrate skeletogenesis. *Satb2* not only positively regulates expression of multiple osteoblast-specific genes, it also repress the expression of several Hox genes including *Hoxa2*, an inhibitor of bone formation and regulator of branchial arch patterning. Furthermore, *Satb2* directly interacts with and enhances the activity of several transcription factors involved in osteoblast differentiation (Britanova et al., 2006b; Dobreva et al., 2006). Examples include *Runx2*, a gene required for early and late stages of osteoblast differentiation and *ATF4*, a factor that regulates terminal differentiation and function of osteoblasts including the synthesis of the most abundant bone extracellular matrix protein, Type I collagen (Nakashima et al., 2002; Yang and Karsenty, 2004).

1.4 Coup TF interaction protein 2 (CTIP2)

Ctip2 (Bcl11b, Rit-1b) and the highly related *Ctip1* (Bcl11a, Evi9) are the two members of a family of transcription factors that were found to interact directly with chicken ovalbumin upstream promoter transcription factor (COUP-TF) family members (Avram et al., 2000) They have been demonstrated to modulate transcription by at least two mechanisms, both of which are independent of trichostatin A-sensitive histone deacetylation independent (Avram et al., 2000; Senawong et al., 2003). *Ctip*s may either be recruited to the template by a COUP-TF family member or bind directly in a sequence specific manner to a motif that is related to the canonical GC box (Avram et al., 2002).

Ctip2 and *Ctip1* mediated transcriptional repression may involve the action of NAD^+-dependent, TSA-insensitive histone deacetylase known as sirtuin 1 (SIRT1). The NuRD complex is considered to play a key role in transcriptional repression mediated by sequence-specific transcription factors (Hong et al., 2005; Kehle et al., 1998; Luo et al., 2000; Murawsky et al., 2001; Sasaki et al., 2008). It harbors ATP-

dependent, nucleosome remodeling and histone deacetylase activities, and consists of several subunits, including RbAp46, RbAp48,HDAC1, HDAC2, MTA1, MTA2, MTA3, MBD3, and Mi-2 (Fujita et al., 2004; Xue et al., 1998; Yao and Yang, 2003; Zhang et al., 1999). *Ctip2*-mediated transcriptional repression seems to need the recruitment of the NuRD complex to the template of a subset of genes, and in a neuron-like context.

Ctip2 (COUPTF1-interacting protein 2) is a transcription factor expressed at a high level in the central nervous system (CNS) of pre- and postnatal mouse brain. It is expressed specifically in developing cerebral cortex, including layer V neurons of the cortical plate, striatum, olfactory bulb, hippocampus, limbic system, basal ganglia, and intermediate region of the spinal cord (Arlotta et al., 2005; Chen et al., 2005a; Leid et al., 2004). *Ctip2* transcripts have been detected in mouse embryo at 10–12.5(Avram et al., 2000).

Within the striatum, it is specifically expressed by GABAergic medium-sized spiny neurons (MSN). It specifically labels this critical neuronal population at early postmitotic stages, this can be concluded from the earliest detection of *Ctip2* expression in Doublecortin-expressing immature neurons at the interface between SVZ and mantle zone (Leid et al., 2004). It plays critical lineage-specific roles in the development of corticospinal motor neurons (CSMNs), axon extension and pathfinding of subcerebral projection neurons, differentiation of MSN (Arlotta et al., 2005). Loss of *Ctip2* function results in a failure of MSN differentiation of both patch and matrix compartments, and leads to changes in expression of several known and novel striatal genes involved in cellular repulsion. Lack of *Ctip2* also leads to a disruption of the patch-matrix organization of MSN since afferent dopaminergic innervation are repelled from distinct areas within the mutant striatum and defects in patch aggregation prevent them from targeting striatal patches.

In the neocortex, *Ctip2* is expressed at high levels in postmitotic neurons in the cortical plate and not in progenitors of the VZ/SVZ (Arlotta et al., 2005). *Ctip2*-null mice exhibit defective axonal projections of CSMNs, consistent with the fact that within the cortex, expression of *Ctip2* is restricted to MSN (the striatal output projection neurons) with lineage-restricted high-level expression in corticospinal and cortico-brainstem projection neurons.

Ctip2 controls lineage-restricted pathways of gene regulation in specific projection neuron populations of the brain. It is likely to act downstream of genes involved in

specification and differentiation of medium spiny neurons and those specifying ventral telencephalic identity of progenitors in the VZ and/or SVZ, such as *Gsh2*, *Dlx1/2*, *Mash1*, and *Islet1* (Casarosa et al., 1999; Coussens et al., 2008; Stenman et al., 2003; Yun et al., 2003). These genes are expressed much earlier in the progenitors that give rise to MSN, whereas *Ctip2* expression is first detected in migrating MSN.

1.4 Eph receptor /ephrin signalling: guiding the axons.

Neurons are often located far away from their synaptic target cells. Neuronal connections are established via extensions of long axons that contain sensing devices on their tips (*growth cones*). In order to find the right pathway these growth cones sense and interact with axon guidance molecules within the environment that they are growing through. The interaction of the axon guidance ligands with their receptors, directly or indirectly regulate many different types of actin-associated proteins as well as the structure and dynamics of the actin-cytoskeleton of the growing axon in order to cause attraction, repulsion or collapse (Chilton, 2006; Dent and Gertler, 2003; Plachez and Richards, 2005).

During development, the connections between neurons of two distant regions are established using 'pioneering axons', intermediate targets of axon pathfinding and 'Glial Guidepost' cells (Chilton, 2006; Plachez and Richards, 2005). First, a small set of '*pioneering axons'* create a 'path' which will later guide the main set of axons. In the neocortex, subplate neurons have been shown to serve as pioneering axons for thalamocortical and corticothalamic axons (De Carlos and O'Leary, 1992; Ghosh et al., 2007). Also during establishment of the medial cortical projection, the first axons that cross the rostral cortical midline are derived from neurons in the cingulate cortex. They are then followed by neocortical axons, which mainly grow within the tract of pioneering cingulate cortex axons, and possibly fasciculate with them (Rash and Richards, 2001). Guidepost glial cells secrete guidance cues and also express cellular cues on their surface that guide axonal outgrowth during the development of spinal cord, the ventral roots, the optic nerve, the auditory system, and the corpus callosum. During embryonic development of CNS, these cells are vital in defining boundaries between different brain areas or between functional subdomains within the same area. These glial boundaries act in order to prevent axons from straying from their correct

elongation path (Chilton, 2006; Plachez and Richards, 2005).

There are several groups of guidance molecules: *Slits, Semaphorins, Ephrins,* and *Netrins* and a number of other molecules, like morphogens, steroids, extracellular matrix proteins and cellular adhesion molecules (Chilton, 2006; Plachez and Richards, 2005).

Eph receptors (erythropoietin-producing human hepatocellular carcinoma) in concert with ephrin ligands (Eph family receptor interacting proteins), comprise the largest family of vertebrate receptor tyrosine kinases. Eph receptors have been divided on the basis of sequence similarity and ligand affinity into two subclasses: EphA (8 members) and EphB (6 members) (Gale et al., 1996). Ephrin ligands have also been divided into two subclasses: GPI-linked ephrin As (5 members) and transmembrane ephrin B (3 members). Ephrin A ligands preferentially bind to EphA receptors, while ephrin B ligands bind preferentially to EphB receptors, although other combinations have also been observed (Heroult et al., 2006). Ephs and ephrins form a cell-cell communication system capable of bi-directional signaling, where the eph receptor mediated signaling is designated as "forward" and ephrin signaling is considered "reverse" (Fig.3; (Heroult et al., 2006; Kullander and Klein, 2002).
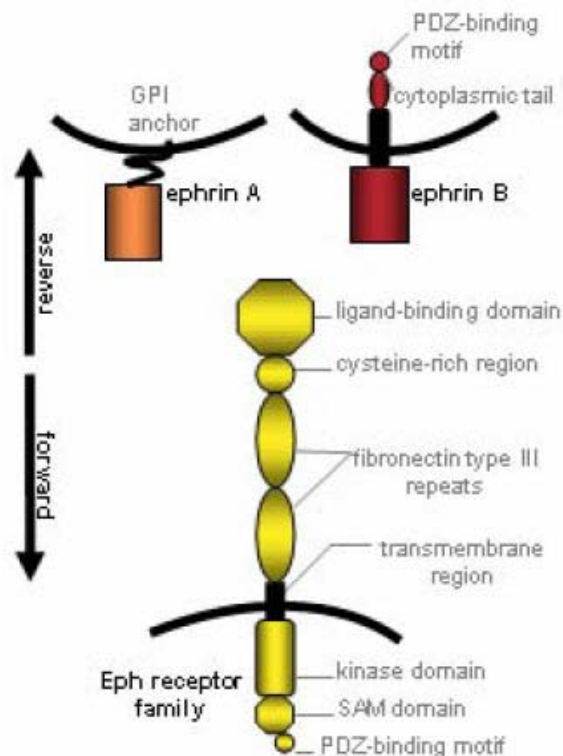
Fig. 3. Bi-directional signalling in the Eph receptor/ephrin communication system.
(Campbell and Robbins, 2008)

This system directs the positioning, adhesion and migration of cells and cell layers during development by providing graded molecular tags which translate the density of their cognate partner on opposing membranes into precisely graded cellular responses, resulting in cell contact-repulsion or cell-cell adhesion (Wimmer-Kleikamp and Lackmann, 2005).

Gradients of ephrin/Eph genes were proposed to control several aspects of thalamocortical (TC) mapping (Britanova et al., 2008; Lee et al., 2007; Mackarehtschian et al., 1999; Prakash et al., 2000; Vanderhaeghen et al., 2000).

Eph receptors in the thalamus and ephrins in the cortex control *intraareal* topographic mapping of thalamocortical (TC) axons.In particular, ephrin-A5 and its receptor EphA4 that are expressed in complementary gradients in the rodent primary somatosensory cortex (S1) and in the primary somatosensory thalamus are required for the topographic mapping of TC axons within the somatosensory area (Prakash et al., 2000; Vanderhaeghen et al., 2000). And the same ephrin/Eph genes unexpectedly control the *inter-areal* specificity of TC projections through the early topographic sorting of TC axons in an intermediate target, the ventral telencephalon.

The Eph receptor/ephrin system has classically been demonstrated to play a role in development but also seems to be implicated in immune regulation (Wu and Luo, 2005), as well as in CNS injury and disease (Goldshmit et al., 2006). It also plays a role in several biological processes. Emerging evidence has revealed differential expression of Ephs and ephrins in numerous form of cancer, suggesting a role in invasive behaviour or methastasis.

2. Materials and Methods

2.1 Molecular biology procedures

2.1.1 Mouse genotyping

2.1.1.1 DNA Isolation

Tail or yolk sac (from young mice or embryo's respectively) was incubated in 0.5ml PK- lysis buffer (100mM Tris- HCl pH8.5, 5mM EDTA, 200mM NaCl, 0.2% SDS, 100μg/ml Proteinase K), shaking at 55ºC overnight. After a 10 min centrifugation at 13,000 rpm, the DNA in the supernatant was precipitated by the addition of isopropanol to a final concentration of 50%. Genomic DNA was collected by centrifugation, washed twice in 80% ethanol and resuspended in water at 40ºC for 1 hr.

2.1.1.2 Polymerase chain reaction (PCR)

All PCR reactions were carried out in an end volume of 20μl that contained:

10x Buffer (Genecraft) 2μl

10mM dNTPs (Invitrogen) 0.4μl (20pmol/ml)

Primer1/Primer2 (IBA) 0.8μl (40pmol/ml) each

TAQ polymerase (Genecraft) 0.4μl (0.5 units)

Template DNA 1μl

dH$_2$O 13μl

To detect wt and Satb2 ko alleles(Britanova et al., 2006b), mice were genotyped using specific primers (94ºC 10sec, 55ºC 30sec, 72ºC 40sec; 30 cycles);

A primer against RCb

5'- CAAGAGAGCCATCCAACTGC- 3'

a reverse primer that recognizes Cre

5'- CCAGACCGCGCGCCTGAAGA- 3'

and a primer against Avr:

5'- AACCATCAGGCTCAACC3'

were used.

In wt mice, the PCR generated a fragment of ~400 bp whereas mutant alleles generated a fragment of ~200 bp.

To identify Cre recombinase gene, a 500 bp fragment was amplified (94ºC 10sec, 55ºC 30sec, 72ºC 40sec; 30 cycles) using the following primers:

5'-TCGATGCAACGAGTGATGAG- 3' (forward)

5'-TTCGGCTATACGTAACAGGG-3' (reverse).

To identify wt and ROSB knock in mice, genotyping was done using the following primers (Soriano, 1999) (95°C 3 min, 56°C 30sec, 72°C 45sec; 95°C 30 sec 39 cycles 56°C 60sec, 72°C 10 min 4°C pause):

5' -AAAGTCGCT CTGAGTTGTTAT- 3'

5' -GCGAAGAGTTTGTCCTCAACC- 3'

5'-GGAGCGGGAGAAATGGATATG -3'

To genotype A11 transgenic line , GFP fragment was amplified (94ºC 10sec, 55ºC 30sec, 72ºC 40sec; 30 cycles) using the following primers:

5'-TCGATGCAACGAGTGATGAG- 3' (forward)

5'-TTCGGCTATACGTAACAGGG- 3' (reverse).

To identify CTIP2 gene, a 500 bp fragment was amplified (94ºC 10sec, 55ºC 30sec, 72ºC 40sec; 30 cycles) using the following primers:

5'-TCGATGCAACGAGTGATGAG- 3' (forward)

5'-TTCGGCTATACGTAACAGGG- 3' (reverse).

5. -5713 to -5441 bp upstream (272 bp fragment)

5'-TGCTAAGGTGTTAACAGGCC- 3' (forward)

5' -CTGGCACTGGGATTACAAATG- 3' (reverse);

PCR conditions were as follows: 2min at 94 ºC followed by 34 cycles of 30sec at 94 °C, 30sec at 60 °C, 30sec at 72 ºC.

All PCR products were separated by 1.5% agarose gel electrophoresis at 5V/cm (chamber length). Agarose gels were prepared in TAE buffer (40mMTris- acetate, 1mMEDTA, pH 8) containing 0.5μg/ml ethidium bromide (Fulka) and visualized under ultra violet light. DNA was loaded using OrangeG buffer, and 100 bp or 1kb plus DNA markers (Invitrogen) were used at a concentration of 50ng/μl.

2.1.1.3 Gel electrophoresis

DNA fragments amplified by PCR were separated by agarose gel electrophoresis at ~5V/cm (chamber length). The 1-2% agarose (Gibco) gels were prepared in TAE buffer (40mM Tris-acetate, 1mM EDTA, pH8) containing 0.5 μg/ml ethidium bromide (Fluka), which allowed for the proper visualization of DNA under ultraviolet light. OrangeG (Sigma) was used as loading buffer and 100bp and 1kb-DNA markers (Invitrogen) were used at a concentration of 50ng/μl.

2.1.2 Transformation

Amplification of the desired cDNA plasmid was carried out using competent cells (DH5α- E. Coli). An aliquot (about 20μl) of E.Coli was defrosted on ice for 30 mins. Plasmid of interest (1 μl) was added to the bacterial cells and incubated on ice for 10 mins. Cells were transformed by heat shock (42ºC., 30 sec) and placed on ice for 5 mins. They were then incubated in LB medium for 1hr with slight agitation and finally plated on selective LB- agar plates containing appropriate antibiotics (penicillin 100mg/ml). Such plates were incubated at 37ºC overnight for the growth of individual colonies.

2.1.3 Plasmid isolation (mini prep)

Individual colonies developed on agar plates were inoculated in 3 ml LB medium containing appropriate antibiotics for 10- 16 hrs at 37ºC, 220rpm. The bacterial pellet was obtained by centrifugation (10 mins, 3000rpm). Plasmid isolation was performed using a Macherey- Nagel NucleoSpin™ plasmid Kit, according to the manufacturer's specifications.

2.1.4 Plasmid linearization and purification

Purified plasmids were linearized using specific restriction enzymes (New England biolabs), according to the orientation of the cDNA fragment and the characteristics of the vector. Plasmid DNA was diluted in dH$_2$O to a concentration of 50ng/μl and the following components were added: 1:10 of 10x Buffer, 1-5μl/ml of restriction enzyme

and 1:100 of 100x BSA (if required). Reactions were normally at 37ºC for few hours or even overnight until complete restriction, as verified by gel electrophoresis.

To purify DNA from proteins, an equal volume of Tris-saturated phenol-chloroform/isoamyl alcohol pH8 (Invitrogen) was added to the complete reaction mixture. This mixture was then vortexed gently and centrifuged (10 min, 13000rpm). The upper aqueous phase was transferred to a new tube and 0.1 volume of 3M sodium acetate (pH5.5) was added. After vortexing, DNA was precipitated with 3 volumes of 100% ethanol for 1 hr at -20°C, washed twice in 70%ethanol and resuspended in H_2O to a final concentration of 0.1- 1µg/µl.

2.1.5 Chromatin Immunoprecipitation (ChIP) Assay

Mouse embryonic cortex (P0) was used as a tissue source of chromatin. Cortex tissues were homogenized in 1x phosphate-buffered saline (10ml for 10-14 hemispheres of cortex tissue) with protease inhibitors (Roche Applied Science). Proteins were cross-linked in 1% formaldehyde for 10 min at 37ºC in a water bath incubator. Cross-linking was terminated with three washes in 1x phosphate-buffered saline. Samples were then processed using a ChIP assay kit, essentially as described by the manufacturer (Upstate biotechnology, Lake Placid, NY). In brief, the cells were lysed in SDS lysis buffer with protease inhibitors, then sonicated using a waterbath sonicator, super RK 103H from Schött labortechnik (Goettingen, Germany) to shear DNA to fragments with a length of 100–1000 bp. To reduce nonspecific background, the cell lysates were precleared by incubation with salmon sperm DNA/protein A-agarose slurry. The agarose beads were pretreated with 2% BSA before the preclearing step as suggested by the company. Supernatants from the preclearing step were incubated with (1: 500) rabbit anti-Satb1 polyclonal IgG (Lab) and (1: 1000) rabbit anti-Satb2 polyclonal IgG (Lab), at 4ºC overnight. Cortex from Satb2 [Cre/Cre] and Satb2 [Cre/Satb1] mutant mice were used. Chromatin-antibody complexes were precipitated by incubation with Protein A-agarose beads. Chromatin was eluted from the beads after washes in several buffers provided with the kit. The DNA-protein cross-links in all samples were reversed by incubation for 4 h at 65 ºC followed by incubation with proteinase K for 1 h at 45 ºC. DNA was isolated by phenol/chloroform extraction and ethanol precipitation. PCR was performed with different set of primers.

2.1.6 *Ex vivo* electroporation experiments

For over-expression experiments, the vector pCAG-Satb2 was constructed by cloning the full-length mouse Satb2 cDNA (BC098136) into the EcoRI site of pCAGEN. The ability of this vector to express Satb2 protein was confirmed both *in vitro* and *in vivo* by Western blot and immunostaining. For *ex vivo* electroporation experiments, introduction of plasmid DNA into the neuroepithelial cells of mouse embryos *ex utero* was performed. Plasmid DNA for pCAG-Satb2 (approximately 2µl of maxi-prep DNA) overexpression and pCAG-GFP as a control were injected into the lateral ventricles of each littermate at E13.5. Electrodes were placed flanking the equivalent ventricular region of each embryo, covered with a drop of PBS and pulsed 5 times at 40 V for 50 ms separated by intervals of 950 ms with an electroporator (BTX Harvard Apparatus) (Chen et al., 2005b).

After electroporation, the brains were removed and embedded in agarose. Coronal sections were prepared by cutting the brain with a vibrotome (LeicaVT 1000S) at a thickness of 50 µm and cultured for two days *in vitro*.

2.2 Histological procedures

2.2.1 Tissue preparation

The day of vaginal plug was considered embryonic day (E) 0.5. Pregnant females were sacrificed by cervical dislocation. Brains were fixed either by immersion (embryonic and perinatal brains) into or perfused (adult brains) by freshly prepared 4% paraformaldehyde (PFA, Sigma) in PBS (pH 8) overnight at 4°C and then washed in PBS. Dehydratation was done with a series of ethanol wash steps (30%, 50%, 70%, 80%, 90%, 95% and 100%) for at least 2 hrs each, transferred to toluol for 6 hrs, soaked in fresh paraplast, twice, overnight and then embedded in wax according to standard procedures. Sections (10µm thick) were mounted on Marienfeld Histobond slides and dried overnight at 37°C. Alternatively, upon 4% paraformaldehyde-PBS fixation, brains were cryoprotected by 30% sucrose-PBS, included in OCT (TissueTeck) and cut at 10µm with a cryostat. Cryosections, mounted on Menzel-

Gläser SuperFrost Plus slides, were dried for 20 min. and kept at -80°C until used. Paraffin sections were subsequently dewaxed by histoclear (xylene substitute), rehydrated in descending ethanol series, and processed for Nissl staining, immunohistochemistry or in situ hybridization.

2.2.2 Nissl staining

After rehydratation, paraffin sections were washed in H_2O for 5min., incubated in 50% (w/v) potassium sulfite solution for 15min. and washed again. Sections were stained for 20min. in cresylviolet solution (1.5% cresylviolet in acetate buffer) and cleared in two washes of acetate buffer (10mM sodium acetate, 10mM acetic acid in H_2O) for 2min (or until desired coloration was achieved). Sections were finally rinsed in H_2O, dehydrated in a series of ethanol dilutions (70%, 80%, 100%, 100%; 2min. each) and immersed in histoclear for 10min. Nissl-stained sections were mounted using Eukitt mounting media (E. Kindler GmbH).

2.2.3 Immunohistochemistry

Embryos were sectioned at 10 μm with a cryostat (Leica), air dried for 20 min, washed in PBS and fixed for 5 min in 4% paraformaldehyde (PFA)∕PBS. After three washes in PBS, sections were preblocked in 1% BSA∕0.1% Tween 20∕PBS (1 h), and incubated with primary antibodies overnight at 4ºC in the same solution. Sections were then washed in PBS and incubated with a diluted (1:800) secondary antibody (Molecular Probes) for 1 h at room temperature, rinsed with PBS and visualized under a fluorescence microscope after mounting with DAKO.
The following antibodies were used:

Antigen	Source	Class	Provider
anti Acetil H4	rabbit	polyclonal	Upstate 06-866
anti Histone H4 (acetylK12)	rabbit	polyclonal	Abcam ab1761
anti Histone H4 (mono methylK20)	rabbit	polyclonal	Abcam ab9051
anti Histone H3 (acetylK9)	rabbit	polyclonal	Abcam ab4441

Antigen	Source	Class	Provider	Concentration
anti-Cre recombinase	mouse	monoclonal	Sigma#c7988	1:200
anti-BrdU	mouse	monoclonal	Chemicon #mab3424	1:200
anti-Brn2	goat	polyclonal	Santa Cruz #SC-6029	1:300
anti-Nurr1	rabbit	polyclonal		1:45
anti-Ctip2	rat	polyclonal	Abcam#ab18465	1:300
anti-L1	rat	monoclonal	Chemicon #mab5272	1:300
anti-KI67	mouse	monoclonal	novocastra	1:500
anti Tbr 1	rabbit	polyclonal	Chemicon	1:1000
anti-Cre	mouse	monoclonal	Covance	1:300
anti Acetil H4	rabbit	polyclonal	Upstate 06-866	
anti Satb1	rabbit	polyclonal	Our Lab	1:1000
anti Satb2	rabbit	polyclonal	Our Lab	1:100

In case of double ISH/IHC, ISH was performed without proteinase treatment and was followed by IHC.

For BrdU migration experiments, BrdU (100 mg ∕ g body weight) (Sigma) ∕ PBS was injected intraperitoneally at E13.5, 15.5 and 17.5 and brains taken at P0 Incorporated BrdU was detected with mouse anti-BrdU mAb (Sigma) or rat anti-BrdU pAb (Abcam). Sections were treated with 0.3%H_2O_2 in 50%Methanol to block the endogenous peroxidase and then wash in PBS for two times, then the section were incubated in 2 N HCl at room temperature for 1 h, rinsed in 0.1 M Borate buffer and processed for immunohistochemistry. Following washes in PBT, the reaction was revealed using DAB reaction kit (VEKTOR) at room temperature for 5-10 min, inactivate with water and mounted in Mowiol.

2.2.4 Cold *In situ* hybridization.

2.2.4.1 Tissue preparation

Isolated mouse brains (E13.5 up to P0), and entire heads at E10.5 were fixed several hours in DEPC-PBS buffered 4% paraformaldehyde at 4°C and cryoprotected in 25% sucrose in DEPC-PBS (solution not autoclaved), keep @ 4°C overnight, shaking .

Tissue was embedded in Tissue Freezing Medium (Leica, Nussloch, Germany) and store @ -80°C .The brains were cut at 10 μm on a cryostat (Leica) and collected in superfrost slides. The sections were stored at -80°C.

2.2.4.2 Dig-Labelling of RNA probes:

Linearization of approx. 5μg of plasmid DNA with the appropriate enzyme was done for 2 hours or overnight and then a control of the digestion on gel for complete linearization.

A Phenol-CHCl$_3$ extraction was done in order to remove the rest of the enzyme. For that we have filled the volume of the digest up to 200μl with H$_2$O. 200μl of saturated phenol-chloroform was added, vortex, spin 5 min, 13000 rpm and transferred upper phase to new e-cup without disturbing the interphase. Finally, DNA was precipitated with 20μl NaAc pH 3.5, 1μl of paint pellet and 400μl 100% EtOH for 2hours to overnight. Spin 20 min, 13000rpm, 4°C; discard supernatant. 70μl of 70% EtOH was added and spin as above, discarding supernatant and leaving to air dry. The pellet was dissolved in 14μl H$_2$O.

The concentration of the plasmid was checked with a spectrophotometer OD$_{260}$ with 1/100 dilution.

For the in vitro transcription (IVT), approx. 2μg of linearised plasmid was used:

X μl linearised plasmid (~2μg)

2 μl Dig RNA labelling mix

2 μl 10x transcription buffer

2 μl RNA polymerase (Sp6, T3, or T7)

X μl DEPC-treated H$_2$O up to 20 μl total volume

Incubate @ 37 °C for 2 hours. Add 2 μl DNase (RNase free) Incubate @ 37 °C for 15 minutes. Add:

2 μl 0.2M EDTA pH 8.0

2.5 μl 4M LiCl

75 μl 100% EtOH

Precipitate @ -20 °C for overnight.

Finally we spin 20 min, 13000 rpm, 4°C; discarded supernatant. Added 70μl 70% EtOH, spin as above, discarded supernatant and leaved to air dry. Dissolve in 50μl H$_2$O. Checked OD$_{260}$ with 1/100 dilution and loaded 1μl on gel.

2.2.4.3 *In situ* hybridization.

Sections were transferred from –80°C into a dry slide box and brought to room temperature. Meanwhile 4% PFA in PBS-DEPC from –20°C was taken and put into a beaker with hot water. A circle with ImagePen around the slide was draw, let dry and put into empty cuvette. Sections were fixed in 4% PFA/PBS-DEPC for 15min at RT (These PFA was reused for Postfix by adding glutaraldehyde) and washed two times in PBS. A proteinaseK treatment was applied for 2-3min at RT where proteinase K (20μg/mlof stock10mg/ml; 300μl /150ml buffer) was dissolved in Proteinase K buffer (20mM Tris pH 7.5, 1mM EDTA pH 8). After that the slides were transferred in to a chamber with 0.2% Glycine (Stock: 20%; 1.5 ml in 150 ml) in PBS-DEPC for 5 min and wash twice in PBS. Sections were then re-fixed for 20 min in 4% formaldehyde/0.2% glutaraldehyde (Stock of Glutaraldeyde can be either 25% (1.2ml/150ml) or 50% (600μl/150ml) dissolved in PBS to ensure firm attachment of the sections to the microscope slides.

Needed hybmix was aliquoted and the RNA in it denatured by incubation @ 65°C for 3min. Then transferred on ice until it was applied on sections. Sections were pre-hybridized in hybridization mix (150μl per slide) without probe for 2 hr at 70°C and then hybridized overnight at 70°C in humid incubation boxes that were prepared by putting tissue in the box and applying 20ml 50%FA/5xSSC in each compartment. Hybridization mix is composed of 50% formamide, 5 x SSC, 1% block solution (Roche), 5 mM EDTA, 0.1% Tween-20, 0.1% Chaps (Sigma; St. Louis, MO), 0.1 mg/ml heparin (Becton-Dickinson; Mountain View, CA), and 1 mg/ml yeast total RNA (Roche). Probe concentration was about 1 ng/μl and it was pipetted into hybmix and denatured as above shortly before using it and kept on ice. Approximately 6 μl hybridization mix was applied to the sections and no coverslips were used. After hybridization sections were rinsed at RT in 2xSSC pH 4.5, washed three times for 30 min at 65°C in 50% formamide/2 x SSC, pH 4.5, followed by two 10-min washes in KTBT (50mM Tris pH7.5; 150mM NaCl; 10mM KCl; 1% Triton X-100 up to 1l with water). Probe bound to the section was immunologically detected using sheep anti-digoxigenin Fab fragment covalently coupled to alkaline phosphatase (1:2000 – 1:5000 in blocking solution). The antibody solution was discarded and sections were transferred to KTBT buffer. Sections were washed in this buffer three times for 5 min, followed by three 30-min washes. Finally three 5 min washes in NT (M) T (100mM

Tris pH9.5; 100mM NaCl; 50mM MgCl$_2$; 0.05% Tween-20u p to 500ml with water) at RT were done prior the developing of the sections with NBT/BCIP as chromogenic substrate, essentially according to the manufacturer's protocol (Roche). The reactions for sense and antisense probes were stopped at the same time. Slides were stored in PBS after the fixation and mounted when all slides are ready.

2.2.5 Hot *In situ* hybridization

2.2.5.1 Tissue preparation

Freshly isolated brains were dehydrated with a series of ethanol wash steps (30%, 50%, 70%, 80%, 90%, 95% and 100%) for at least 2 hrs each, transferred to toluol for 6 hrs, soaked in fresh paraplast, twice, overnight and then embedded. The brains were cut at 10 μm on a microtome (Leica) and collected in coated slides (Menzel). The sections were stored at RT.

2.2.5.2 Synthesis of radioactive riboprobes

In vitro transcription of the linearized cDNA was carried out by incubating at 37°C for 1.5 hrs with the following reagents:

Linearized DNA (>0.25μg/μl) 1- 3μl (0.5- 1μg)

Transcription Buffer 10x (Boehringer) 1μl

-U dNTPs (Boehringer) 1μl

RNase inhibitor (Promega) 0.5μl (1U/μl)

T3/T7/SP6 RNA polymerase (Promega) 0.5μl (0.5U/μl)

[α]35 S- UTP (Amersham) 2μl (10mCi/ml)

DEPC- H$_2$O up to 10μl

Riboprobes bearing a sequence complementary to the mRNA of interest (antisense) were synthesized using the following cDNA templates:

cDNA Size (bp)	Vector	Enzyme	Pol	Provider
Cad8 400	pGEM-Teasy	SpeI	T7	Lab stock
Cux2 530	pGEM-T	SpeI	T7	Lab stock
Er81 300	pGEM-Teasy	SacII	SP6	Lab stock

cDNA Size (bp)	Vector	Enzyme	Pol	Provider
Id2 350	pGEM-Teasy	SpeI	T7	Lab stock
Lmo4 600	pGEM-T	SpeI	T7	Lab stock
Svet1 900	pBluescript	XhoI	T7	P.Gruss
EphA2 300	pBluescript	BamHI	T7	Lab Stock
EphrinA2 300	pBluescript	SacI	T7	Lab Stock
EphA3 300	pBluescript	BamHI	T7	Lab Stock
EphA4 300	pBluescript	SacI	T7	Lab Stock
Ephrin A2 300	pBluescript	EcoRI	T7	P. Gruss
Ephrin a5 500	pBluescript	KpnI	T7	FrancoWeth
Eprhin a5 700	pBluescript	XbaI	T7	P. Vanderhaegen
EphA7 300	pBluescript	NotI	T3	Lab Stock
Ephrin B1	pBluescript	Hind III	Sp6	P. Vanderhaegen
Ephrin B2	pBluescript	Hind III	Sp6	P. Vanderhaegen
Ephrin B3	pBluescript	Hind III	Sp6	P. Vanderhaegen
EphB1 1.7	pBluescript	BamHI	T7	P. Vanderhaegen
EphB2	pBluescript	KpnI	T7	P. Vanderhaegen
EphB4 1.2	pGem 37	Hind III	T7	P. Vanderhaegen
Fezl 1.3	pBluescript	NotI	Sp6	Lab stock
Satb21 600	pGEM-Teasy	ApaI	Sp6	Lab stock
Rorß 400	pBluescript	SalI	T3	Lab stock
Unc 544 1.4	pDrive	Xba I	T7	Lab stock

2.2.5.3 *In situ* Hybridization

Dewaxing of paraffin embedded tissue (sectioned cortex and whole embryo) was done using histoclear (twice for 10 mins). The tissue was rehydrated in a series of ethanol dilutions (100%, 100%, 95%, 90%, 80%, 70%, 50%, and 30%, for 2 mins each) and rinsed in saline (0.86% NaCl in DEPC autoclaved water) and PBS- DEPC. The sections were then fixed in cold 4% PFA/PBS and washed twice in PBS- DEPC for 5 mins. The sections were then Proteinase K treated (50mMTris-HCl; 5mM EDTA; 20µg/ml Proteinase K) followed by a PBS- DEPC wash step. These sections were treated with freshly prepared acetylation buffer (0.1M triethanolamine; 0.05M acetic anhydride in DEPC- H_2O), twice for 15 mins and washed in PBS- DEPC

followed by dehydrating ethanol wash steps.

Hybridization buffer was used for diluting the radioactive RNA probe:

50% Deionized Formamide (Fulka)

10% Hybridization salt stock (0.2% polyvinylpyrrolidone; 0.2% Ficoll; 0.1M NaH$_2$PO4; 50mM EDTA pH 6.8; 3M NaCl; 0.1M Tris- HCl pH8 in DEPC-H$_2$O

10% 1M DTT (Sigma/Promega)

20% Dextran sulfate 50% (Amersham)

500μg/ml tRNA (Sigma)

200μg/ml αSPthio- ATP (Roche)

Denaturation of the diluted radiolabeled RNA probes was done at 80% for 2 mins and placed on ice for 5 mins. About 12- 18μl of the diluted probe was applied on each section and covered with 15x20mm coverslips that were previously siliconized with SurfaSil™, according to the manufacturer's instructions. Sections were allowed to hybridize with the probe at 55°C in a completely sealed humid chamber containing 50% formamide in 2xSSC.

Hybridized sections were transferred to 2xSSC at 55°C and coverslips were removed with gentle agitation for about 5-10 mins. Sections were then washed in 50% Formamide/2xSSC at 75°C, then at 65°C (both in a shaking water bath). This wash step was again carried out in a fresh aliquot of the same solution for 30min-2hr at 37°C with slight agitation. Sections were then incubated twice in NTE buffer (0.5M NaCl; 10mM Tris-HCl; 5mM EDTA pH8) for 5 and 15 mins. The unbound radiolabeled RNA probe

2.3 Southern-blot screening of ES cell clones for homologous recombination

After the electroporation of the knock-in constructs into the ES-cells (MPI-II), they underwent a positive and negative selection for about 10 days with geneticin (G418) and gancyclovir, respectively. Individual ES-cells that survive during these selections were separately grown. While preparing the cryo-stocks of each clone, some from each were let to grow in 24-well plates without the feeder layers. The screenings for the homologous recombination were done by using these ES cell cultures.

2.3.1 Genomic DNA extraction from ES-cells

Genomic DNAs from these ES cells were extracted by proteolytic digestion with proteinase K (1 mg/ml) in Lysis Buffer at 56°C for overnight and then precipitating the genomic DNA with the addition of 1.5 x volumes Isopropanol onto the lysed samples. After vigorous shaking by hand, they were centrifuged for 20 minutes, and then the pellets were washed with 70% ethanol and finally dissolved in 100 µl of TE.
Lysis Buffer (final concentrations of the ingredients):
(100mM Tris-Cl (pH 8.0); 5mM EDTA (pH 8.0); 0.2% SDS; 200mM NaCl)

2.3.2 Digestions of genomic DNA

During the preparation of the knock-in construct, some Nsi I sites were introduced in specific regions of the construct. These NsiI sites are absent in the wild type genomic region. In case of homologous recombination, digestion with NsiI would therefore produce specific bands of expected sizes as shown in Figure 7.
With this idea, one third of each ES-clone genomic DNA sample was digested with NsiI (Promega) at 37°C overnight. Digested genomic DNA samples were loaded onto 0.7% Agarose gels and electrophoresed at 30V overnight

2.3.3 Southern blotting

Southern blot analysis was used to screen ES cell clones for homologous recombination events. Between 5 and 10 µg of genomic DNA were digested overnight with 20 units of restriction enzyme. The digested DNA was resolved on a 0.7 % agarose gel containing 0.5 µg per ml ethidium bromide. To confirm complete digestion of the genomic DNA, gel was exposed to UV-light and photographed. The gel was depurinated in 0.25 M HCl solution for 10 min. Then the gel was denatured by 45 min incubation with gentle shaking in a solution of 1.5 M NaCl and 0.5 M NaOH, followed by neutralization in a 1M Tris-HCl (pH 8) and 1.5 M NaCl solution for 45 mins. Finally the gel was then rinsed in water. A nylon membrane was cut with the size of the gel, washed in water and incubated for 10 min in 2X SSC. The gel was blotted overnight using 10X SSC, so as to transfer the DNA onto a nylon membrane

(Hybond N+, Amersham- Pharmacia) as described by Southern (Southern, 1975). On the next day, after transfer, the membrane was dried in Whatman paper and the DNA was cross-linked to the membrane using UV-light at 120 mJ/cm^2. Subsequently the membrane was hybridized with specific radioactive probes. DNA probes (20-50 ng) were radioactively labeled with 50 µCi γ32P-dCTP (Amersham-Pharmacia) using the 'Prime-It RmT Random- Primed Labelling Kit' (Stratagene). The labeled probes were purified over Sephadex- G50 spin columns (Probe Quant G50, Amersham Pharmacia). Before hybridization probes were denatured by boiling for 5 min. Prehybridization was carried out according to Denhardt (Denhardt, 1966) with modifications. The membranes were saturated in 20-25 ml hybridization solution (0.5M Na PO$_4$ pH 7, 2, 7% SDS) at 65ºC for at least 40 min in the hybridization oven (Biometra). The denatured probes were then added to the tubes incubating the membranes in prehybridization buffer. Hybridization was carried out at 65ºC for 16-24 hours. In order to remove the non-specifically bound probe, the following washing steps were carried out in a shaking water bath at 60°C: 4x 20 min in 40mM Na PO$_4$ pH 7, 1% SDS. The membranes were then sealed in plastic foil and exposed to a Biomax MS autoradiographic films (Kodak) at –80°C for overnight.

2.4 Cell culture

2.4.1 Preparation and culture of embryonic fibroblast

All cell culture procedures were based on protocols according to "Gene Targeting: A Practical Approach" (Joyner, 1999). To maintain the pluripotency, ES cells were cultured in the presence of leukemia-inhibitory factor (LIF) on a layer of growth arrested feeder cells derived from embryonic fibroblasts. Embryos (E13.5 E16.5) obtained from mating wild-type mice with homozygous transgenic strains, which contain a neomycin resistance cassette (*neoR*), were used for fibroblasts preparation. *neoR* feeder cells survive during positive selection of ES cells with G418. Embryos were dissected in sterile conditions and head as well as internal organs were removed. Such carcasses were washed in large volume of PBS++ (1.47 mM KH$_2$PO4, 8.1 mM Na$_2$HPO$_4$, 137 mM NaCl, 2.68 mM KCl, 0.9 mM CaCl$_2$, 0.5 mM MgCl$_2$, pH 7.2) to remove blood. Then carcasses were minced into small cubes and pressed though the

screen into a flask that contains 20 ml of glass beads. The suspension of cells was incubated at 37°C in 50 ml 0.05% Trypsin/0.02% EDTA solution together with 200 ml of DNase I (10 mg/ml), for 30 min with stirring. Then an additional 50 ml of trypsin/EDTA was added, stirred for another 30 min and the trypsinisation procedure was repeated. After decantation of glass beads, the cells were centrifuged at 1500g for 5min. The pellet was washed twice in PBS++ and resuspended in 5ml PBS (1.47 mM KH_2PO_4, 8.1 mM Na_2HPO_4, 137 mM NaCl, and 2.68 mM KCl, pH 7.2). Afterwards, feeder cells (5 x 10^6) were plated onto 150 mm tissue culture dish with 10 ml of fibroblast medium. In 3-4 days, when the cells reached confluence (ca. 4-5 x 10^6 cells/plate), the feeders were split 1:3 or 4 for additional expansion or frozen for storage. For splitting, the cell were twice washed with PBS, each plate was incubated with 3 ml of 1x trypsin/EDTA at 37°C for 5 min. Once the cells detached, they were gently pipetted up and down to break aggregates. Trypsinized cells were added to 6 ml of feeder medium in a conical tube and centrifuged at 3,000g for 2 min. The supernatant was discarded, the cell pellet re suspended in feeder medium and plated. Generally, embryonic fibroblasts were not passed more than 3 times, because they are not anymore suitable for ES-cell culture. The feeders can be stored for several days at -80°C or for longer time in liquid nitrogen. For freezing trypsinized cells have to be re-suspended in cold freezing medium A (ES-cells-Medium/50% FCS) and then an equal volume of cold freezing medium B (ES-cells-Medium/20% DMSO) is slowly added. The suspension was then transferred to cryo-tubes (Nalgene) and freeze down first at -20°C and later at −80°C. For thawing vials with feeders were warmed-up at 37°C for short time and then the cells were transferred to 10 ml of warm fibroblasts medium. After centrifugation (1000rpm, RT) cells were re-suspended in fresh medium and platted.

2.4.2 Growth-arrest of Embryonic Fibroblast by mitomycin C treatment

A confluent plate of embryonic fibroblasts was washed with PBS and incubated for 2 h with 100 μl of mitomycin C stock solution (1 mg/ml in PBS, 5% DMSO, Sigma) in 10 ml of feeder medium. Then the cells were washed two times with PBS, incubated with 3 ml of 1x trypsin/EDTA at 37°C for 5 min, re-suspended and centrifuged in feeder medium. The cell pellet was brought to a concentration 2-3x10^5cells/ml of feeder medium and plated on gelatinized plates.

2.4.3 ES cell culture, electroporation and neomycin-resistance selection

Frozen ES were thawed rapidly and DMSO-containing medium was immediately replaced with warm (37°C) ES medium. As a standard procedure, 10^7 ES cells were electroporated with 20 μg of linearised targeting vector in 0.8 ml PBS (240 V, 500 μF, BioRad Gene Pulser). The transfected cells were then plated out on growth-arrested neomycin resistant mouse embryonic primary fibroblasts (see 2.5.1 and 2.5.2) at a density of 2.5×10^6 cells per 10-cm dish and cultured in ES cell medium. Selection with 400 μg/ml G418 (Geneticin) was started 48 hours later. Fresh selection media was added daily to the ES cells. After further 5-7 days culture with selective medium single, undifferentiated ES cell colonies were picked and cultured for additional 3-4 weeks in 24 well plates with layer of feeder cells. Then ES cell colonies were trypsinised and frozen; a little amount of the clone was cultured in a 24 well plate without feeder cells for screening. For freezing down, 1 volume of ice cold 2X freezing medium (ES medium plus 13.3% DMSO) was added to confluent, trypsinised 24 well plates that had 1volume of trypsin in them. The clones were carefully transferred to cryotubes and gradually frozen down to –80ºC and finally stored in liquid nitrogen tank. To screen the cells for homologous recombination by Southern analysis, a 24 plate was made with all the frozen clones. This plate was coated with 0.1% gelatine (Sigma) before seeding of ES cells. These plates were grown to confluence and used to extract DNA to screen for targeted clones as described earlier. The ES cells were electroporated with 10 μg of the construct. The ES cell suspension was diluted with ES cell medium, and up to 1×10^3 cells were placed in each 100 mm cell culture dish. Colonies were picked after 8-9 days in culture and processed as above. ES clones were screened by Southern analysis as described above.

2.5 TSA treatment in dissociated neuronal cell culture

2.5.1 Coating Plates with Laminin and Poly-L-lysine

One aliquot of Laminin (Sigma-Aldrich #L2020)Working Solution (1 mg of laminin diluted with sterile H_2O to a final volume of 1 ml to make a 1 mg/ml stock solution)

and one aliquot of Poly-L-Lysine (Sigma-Aldrich #P5899) Working Solution (20 mg of poly-L-lysine with sterile H_2O to a final volume of 20 ml to make a 1 mg/ml stock solution) was added to 12 ml of sterile ddH_2O to make a coating solution (enough for 12 inserts). One culture insert (Becton Dickinson #353102) was placed into each well of two six-well plates (Becton Dickinson #353502). Then 2 ml of sterile ddH_2O was added into the bottom of each well of the plate underneath the membrane of the insert, followed by 1 ml of the coating solution on top of the membrane. The plate was placed in a humidified incubator at 37°C 5% CO_2 overnight.

2.5.2 Dissociation of Cortical Neurons

The solutions were prepared in the following way:

Dissociation Medium (DM)

Stock Solution	Volume	Final Concentration
1 M Na_2SO_4	20.44 ml	98 mM
0.5 M K_2SO_4	15 ml	30 mM
1 M $MgCl_2$	1.45 ml	5.8 mM
100 mM $CaCl_2$	0.63 ml	0.25 mM
1 M Hepes (pH 7.4)	250 µl	1 mM
1 M glucose	5 ml	20 mM
Phenol red (0.5%)	0.5 ml	0.001%
0.1 N NaOH	0.5 ml	0.125 mN

Add sterile ddH_2O to a total volume of 250 ml. Store at 4°C. Sterile filter with a 0.2-µm bottle filter. The stock solutions of 1 M Na_2SO_4 and 0.5 M K_2SO_4 were kept at room temperature in order to avoid precipitate formation.

Enzyme Solution (ES)

20 ml of DM, Cysteine (Sigma-Aldrich #C-1276) 6.4 mg, Papain (Roche #108014) 400 units. Mix and let dissolve for 15 min in a 37°C water bath. Mix and adjust the pH with 0.1 N NaOH to about 7.4 (about 6 drops of 0.1 N NaOH). pH monitored by solution colour (Pink is too basic and yellow is too acidic). Filter through a 0.2-µm syringe filter. Solution prepared immediately before use.

Heavy Inhibitory Solution (HI)

DM 6 ml, Bovine serum albumin (BSA) (Sigma-Aldrich #A-7906) 60 mg, Trypsin inhibitor (Sigma-Aldrich #T-6522) 60 mg. Warm the DM to 37°C, then add BSA and

trypsin inhibitor and mix to dissolve. Adjust the pH with 0.1 N NaOH to about 7.4(12 drops aprox. of 0.1 N NaOH). Filter through a 0.2-μm syringe filter. Warm the solution in water bath at 37°C before use. Solution prepared immediately before use.

Light Inhibitory Solution (LI)

9 ml of DM and 1 ml of HI. Prewarm the DM to 37°C, and then add the HI. Filter through a 0.2-μm syringe filter. Warm the solution in a 37°C water bath before use. Solution should be prepared immediately before use.

Serum-Free Medium

100 ml of Basal Medium Eagle, 1 ml of N_2 supplement, 0.5 ml L-glutamine (200 mM), 1 ml of Penicillin (10,000 units/ml)-streptomycin (10 mg/ml). Warm the solution in water bath at 37°C and prepare under sterile hood immediately before use.

The area for dissection was prepared by spraying with 70% ethanol and wiping dry and the dissection instruments were sterilized by immersion in 70% ethanol for 10 min. Two 100-mm petri dishes with 15 ml of Complete HBSS (12.9 ml of 1 M, 1.35ml of 20mM D-glucose, 0.25 ml of 1 mM 200 mM L-glutamine, 0.5 ml of Penicillin-streptomycin (100 units/ml of penicillin and 0.1 mg/ml of streptomycin) sterile filtered with a 0.2-μm filter and heat-inactivated horse serum to a final concentration of 5%) were placed on ice. The P0 mouse brain were isolated and placed in this solution, where cortex was isolated without pia and hippocampus. The cortex was transferred into a new petri dish containing fresh Complete HBSS and cut with fine forceps into pieces of about 1 mm.

The pieces of cortex were transferred in a 50-ml tube containing 10 ml of Enzyme Solution by using a cut and flamed Pasteur pipette and incubated at 37°C. After 20 min, the remaining 10 ml of Enzyme Solution was added, and the tissue continued incubating at 37°C for an additional 20 min. The Enzyme Solution was gently removed by pipetting, leaving the tissue at the bottom of the tube. The tissue was rinsed once with 10 ml of LI and then incubated with 5 ml of HI at 37°C. After 2 min HI was removed and rinse once with 5 ml of Serum-Free Medium. The tissue was gently triturated in 5 ml of fresh Serum-Free Medium for about 10 to 20 times with a 5-ml pipette. The cell suspension was transferred to a new 50-ml conical tube and viable cells were count using a hemocytometer.

2.5.3 Multiple Immunofluorescence Protocol.

The coverslips were incubated for 4 to 6 hours in Permeabilization Solution (50 ml of 10x PBS, 450 ml H$_2$O, 15g BSA, 1.5 ml Triton X-100, 5 ml of 10% NaN3 in ddH$_2$0) at 4°C for at least 6 hours (or overnight) with gentle agitation. First antibody was diluted each in the appropriate volume of Permeabilization Solution, 1 ml per well in six-well plates was added and incubated overnight at 4°C with gentle agitation. The coverslips were washed eight times with 3 ml of 1x PBS for 15 min with gentle agitation at room temperature. One ml of diluted secondary antibodies was added to the wells and incubated overnight at 4°C with gentle agitation.

The coverslips were washed four times in 3 ml of 1x PBS for 15 min at 4°C with gentle agitation, wash twice in 3 ml of 1x PBS for 15 min at room temperature with gentle agitation and mounted microscopic slides with an appropriate mounting medium for fluorescence. The coverslips were seal with nail polish.

2.5.4 TSA treatment

Cells were platted in different under different densities (0.1, 0.5, 0.8) in order to see the optimal density of cells, which finally result to be 0.8, million cells per coverslip. Under these conditions we performed the experiment with increasing concentrations of TSA (0, 50, and 100) during 6h, 12h and 24h.

2.6 Generation of knockin mice

Two independent heterozygous ES cell clones were used to generate chimeras by injecting 10-15 ES cells into blastocysts obtained from C57BL/6 super-ovulated females (Hogan et al., 1994). Females (20-23 days old) were injected interperitoneally with 100 µl 50U/ml PMS in PBS („Pregnant Mare's Serum"= Intergonan, Intervet GmbH, Tönisvorst). This serum contains Follicle-Stimulating hormone (FSH). Two days later females were injected with 100µl 50U/ml hCG in PBS (human Chorionic Gonadotropin, Ovogest, Intervet GmbH, Tönisvorst) und then mated with C57Bl/6J males. Blastocysts were recovered on day 3.5 post-coitum by flushing the uterus with blastocyst medium (Fibroblasts-medium with 30 mM HEPES pH 7.2). Round ES

cells (12-15) were injected into the blastocoelic cavity and approximately 16 of such injected blastocysts were implanted into the uterine horns of time-matched pseudo-pregnant foster mice (day 2.5 post-coitum). Chimeras were identified by coat colour and backcrossed to C57BL/6 mice to achieve germ-line transmission. The offspring with brown coat colour was analyzed for heterozygosity by genotype PCR and by Southern blot analysis.

2.7 Carbocyanine Dye Tracing

All tract tracing were performed in P0 animals. Single DiI crystal (Molecular Probes, Eugene, Oregon, USA) was placed either in the ventrobasal complex of the thalamus or presumptive primary somatosensory cortex to trace TCAs and CFAs. Four DiI crystals were placed in the cerebral peduncle or internal capsule to study the distribution of projection neurons in the cortex. The number of DiI-labeled cells in the upper or lower layers was counted under 40x objective.

To study the origin of neurons projecting to the corpus callosum or anterior commissure, brains were bisected sagittally. In normal brains, DiI crystals were placed along the entire length of the corpus callosum and DiD in the anterior commissure. In KO, which the corpus callosum is missing, only DiD was placed in the anterior commissure.

All brains were kept in dark for 3 weeks at room temperature for DiI diffusion, then sectioned at 50-80μm on a vibrating microtome (Leica).

2.8 Image acquisition

Bright and dark field images were obtained with a light microscope (Olympus). For fluorescence images, a Leica inverted microscope equipped with a TCS-SP2 confocal scan head was used. Confocal pictures of 1-2μm thickness were acquired by sequential 4-line averaging. Fluorophors were excited with an Argon laser (488nm) or with diode lasers (561 and 405nm). Pictures were analyzed with the Leica software and further merged and refined with Adobe Photoshop CS2^{+}.

3. Aim of the project

We investigated the regulatory role of transcription factor *Satb2* and the other member of the same family, *Satb1*, in cortical development. It is well known that *Satb1* is involved in the regulation of tissue-specific organization of chromatin. We found that *Satb2*, a close homologue, can also bind matrix attachment regions (MAR) of genomic DNA. In this study, we focus on the functional relationship between *Satb1* and *Satb2*.

It has been previously reported that loss of Satb2 expression in the branchial arches leads to craniofacial abnormities and eventually causes postnatal death at P0 (right after birth). In the current study, we analyzed the function of Satb2 in the neocortex.

Here we analyzed the functional replacement of Satb2 by Satb1 in the neocortex and in the first branchial arches using a mouse line where the *Satb2* coding sequence has been replaced by *Satb1* cDNA. The Satb2^{Satb1} "knock-in" mutants not only lack Satb2, but also ectopically express Satb1 in cells under the influence of the *Satb2* promoter. The work presented here also describes generation of the Satb2^{Satb1} mouse line.

.

4. Results

4.1 Satb1 and Satb2 expression during cortical and craniofacial development.

4.1.1 Satb1 labels a subpopulation of Satb2 cells in the neocortex.

Satb2 expression is first detected at E11.5 within the mandibular and maxillar components of the first developing branchial arch and at E13.5, in the telencephalon, tongue muscles and a subpopulation of dorsal spinal cord neurons. At E13.5 Satb1 mRNA was detected in the entire spinal cord and in two groups of postmitotic cells of the ventral telencephalon. It was also strongly expressed in the transition zone between pons and medulla and in the cerebral cortex where its expression was mostly confined to the SVZ zone. At E15.5, Satb2 is expressed in the intermediate zone (IZ) and cortical plate (CP) while Satb1 expression is detected in the cells of the marginal zone (MZ), subplate of the developing hippocampus, piriform cortex and olfactory tubercle (Britanova et al., 2005). IHC analysis indicates that Satb1 and Satb2 are coexpressed in the cortical plate and subplate. Interestingly there is a minor subpopulation of cells located in the most upper part of the CP that express exclusively Satb1. At P0, Satb2 is expressed in UL of the cortex whereas Satb1+ cells are located above Satb2 expression domain where most cells seem not to express Satb2. The vast majority of the migrating neurons express both genes (Fig.4).

At P0, both genes are expressed in incisors and molars but Satb2 seems to be restricted to a subpopulation of Satb1 + cells in the dental epithelium. However, Satb1 is strongly expressed in this dental epithelium whereas Satb2 is mostly expressed in the dental mesenchyme.

In the septal cartilages overlying the upper jaw both proteins extensively colocalize although Satb1 is more strongly expressed than Satb2 in the medial epithelial seam (of palate) and in vomero-nasal organ (Fig.12 A-D).
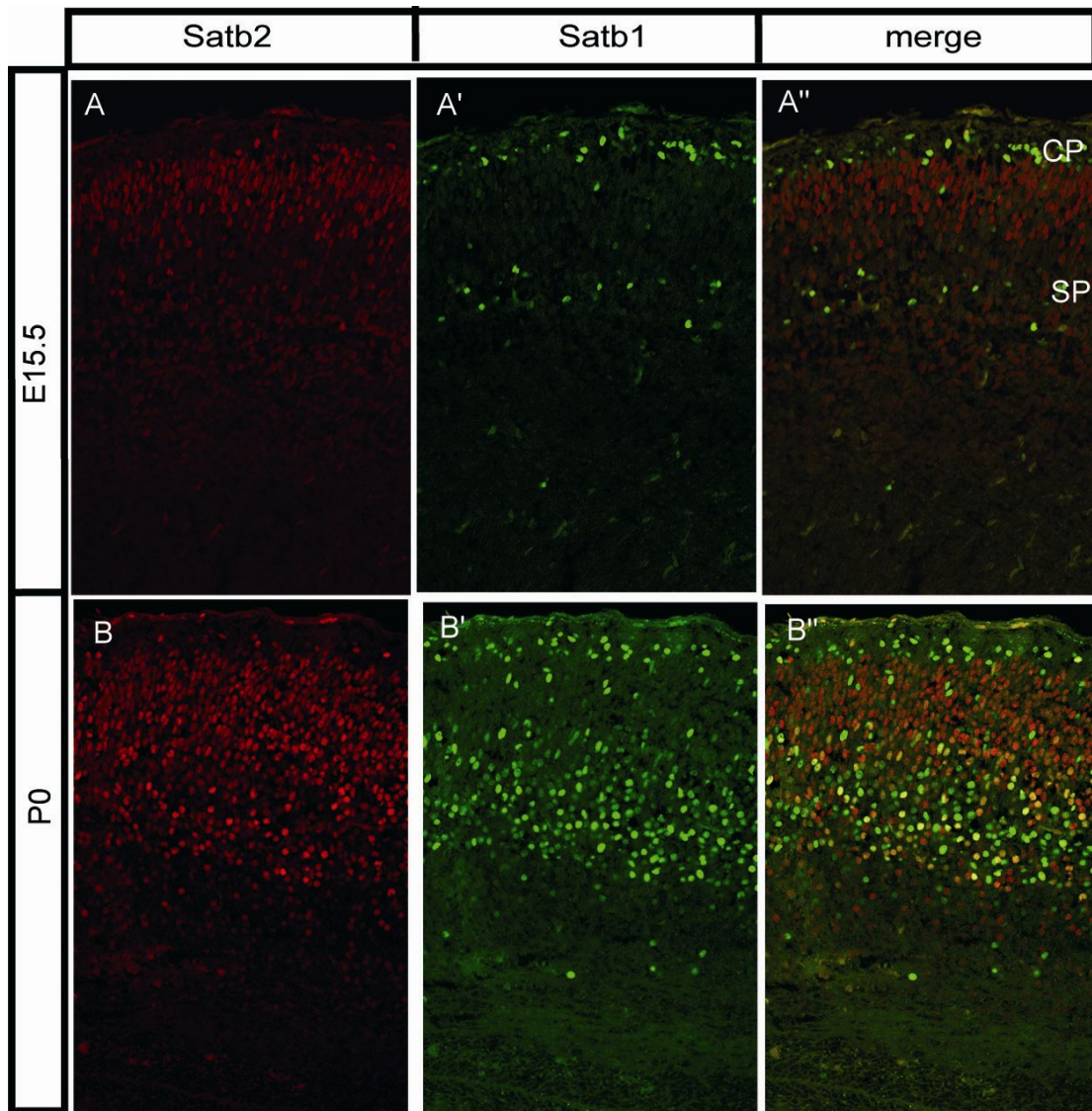
| Satb2 | Satb1 | merge |

FIG 4. Satb1 and Satb2 expression in mouse development.

Satb1 protein expression at E.15.5 (A) and at P0 (B) is restricted to a subpopulation of Satb2 in the neocortex.

4.1.2 Ctip2, Satb1 and Satb2 expression during development.

To relate Satb1 and Satb2 protein expression to certain DL neocortical subtypes more precisely, co-localization analysis of Satb1, Satb2 and Ctip2 by double IHC were performed. Satb1 and Satb2 were predominantly expressed in the UL neurons of neocortex starting from E13.5. The majority of neocortical Satb2+ neurons were born between E14.5 and E15.5 in the dorsal telencephalon although there were few Satb2+ cells in the CP already at E13.5 (Britanova et al., 2006a). At 15.5 the amount of neurons expressing Satb1 in the CP is still very low but the number increases as

development proceeds (Fig.5 E, H). Ctip2 is a transcription factor that is expressed by many cortical plate neurons already at early stages of corticogenesis. At later stages, its expression is mostly confined to layer 5 neurons that project to the spinal cord and tectum but not to corpus callosum (Arlotta et al., 2005). The onset of Satb1 and Satb2 expression in the dorsal telencephalon was detected at E13.5 (Fig.5A-B, E-F). At this stage, many Satb1 and Satb2 expressing cells were found within the CP, while there were many more Ctip2+ cells in this region. Most Satb1 and Satb2 neurons at this stage also expressed Ctip2.

At E15.5, the number of Satb2+ cells increased and most of them did not co-express Ctip2 (Fig.5C) whereas not many Satb1+ cells where found in the CP at this stage, and most of them continued to express Ctip2 (Fig5. G). Satb2 and Ctip2 double positive cells were found in the lower part of the Satb2 domain indicating that they could represent the same cell population that coexpresses both genes at E13.5. However, at P0 there were very few cells that expressed both proteins and they were also located in the lower part of the Satb2 domain (Fig. 5D). Interestingly, cells that expressed both proteins, expressed Ctip2 at lower levels than Ctip2+ cells that did not express Satb2 (Fig.5 A-D). On the other hand, cells expressing Satb1 and Ctip2 at P0 were distributed throughout layer V (Fig.5 H).

These results indicate that Satb2 and Ctip2 control mutually exclusive genetic programs of UL and DL cell type specification whereas Satb1 seems not to have any effect on Ctip2-mediated genetic program.

4.1.3 Satb2 seems not to be expressed in Svet + cells.

Satb2 protein expression was also analyzed in relation with Svet, a marker of a subpopulation of upper layer cells. Svet1+ cells reside in the SVZ until they begin to enter the CP at E18.5 and finish their migration by P2 (Tarabykin et al., 2001). In order to know whether Satb2 and Svet1 are expressed in the same cells, we combined IHC with Satb2 antibody and non-radioactive in situ hybridization with *Svet1* probe at developmental stages starting from E17.5 to P2. At these stages, both genes are expressed in the CP but any co-localization in the SVZ and IZ was detected. Most cells in the CP that expressed Svet1 at high level at P0 or P2 did not express Satb2 (Fig.6).
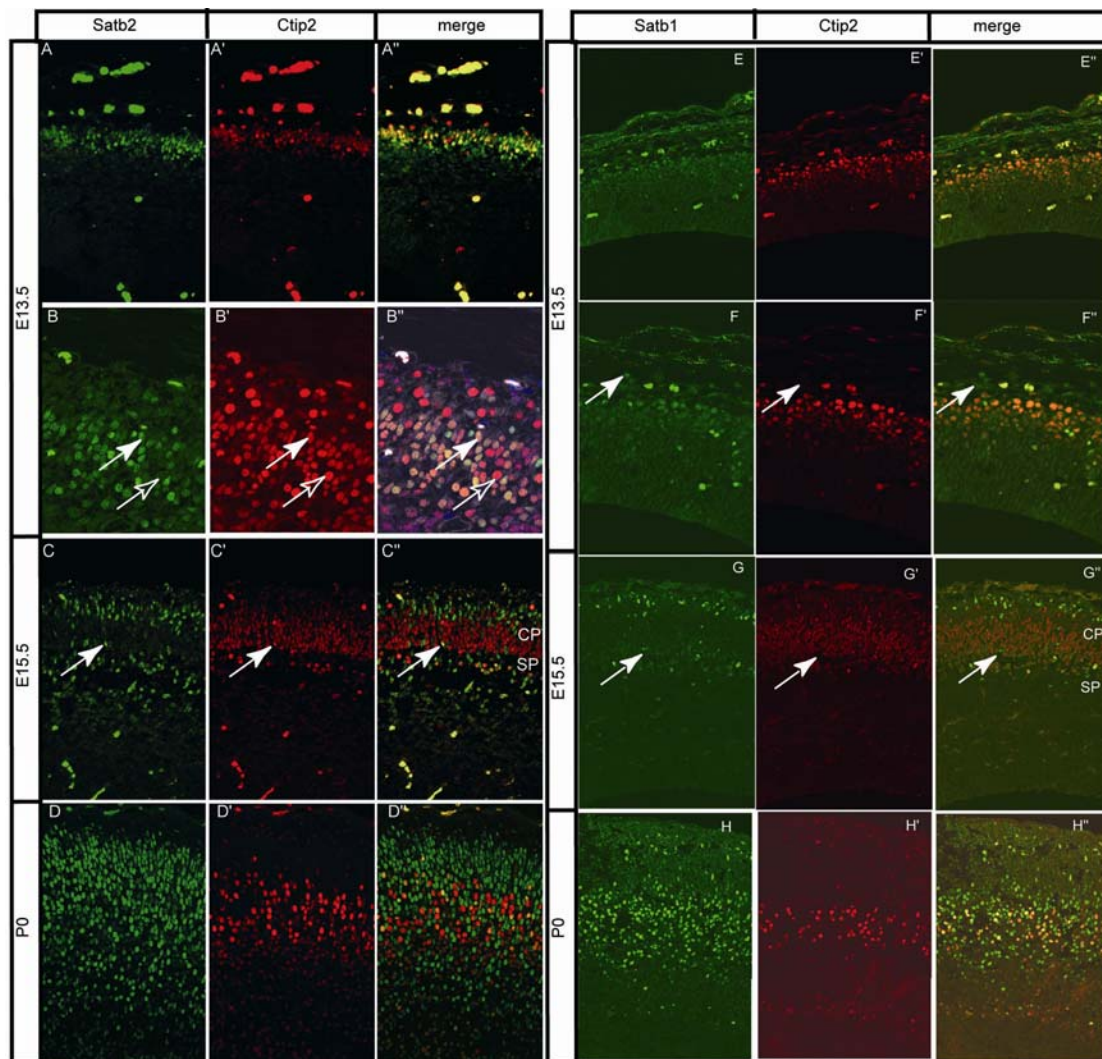
FIG 5. Satb2 and Ctip2 Label Distinct Subpopulations in the Developing Cortical Plate whereas Satb1 is expressed in Ctip2 expressing cells.
(A) Most CP cells at E13.5 express Ctip2, and some of them also express Satb2. (B) Higher magnification image of the CP at E13.5. Note that there are cells that coexpress Ctip2 and Satb2 (empty arrowheads) or express Ctip2 only (filled arrowheads). (C) At E15.5, Satb2+ cells occupy the subplate (SP) and the upper part of the CP. Most of the cortical cells are Ctip2+ (C') and few coexpress Satb2 in the subplate (arrowheads), but there are no double-labeled cells in the rest of the CP. (D) By P0, the proportion of Satb2+ cells is significantly increased as compared to Ctip2.(E) Satb1 expression at E13.5 (F) 63x magnification of E13.5 cortex. (G) Satb1 is expressed in Ctip2 cells at 15.5. (H) Layer V Ctip2 expressing cells colocalizes with Satb1. Note that there are cells that express Satb1 but not Ctip2 (filled arrowheads) (F, G).

Due to the nuclear staining of Satb2 and cytoplasmic staining of Svet1, it is not possible to completely rule out the possibility that there are some neurons in the CP that express both genes. However, no overlap between the two colors was ever detected although, in some cases, weak Svet1 signal was seen in close vicinity of Satb2 nuclei, indicating that some cells might express both genes in the CP.
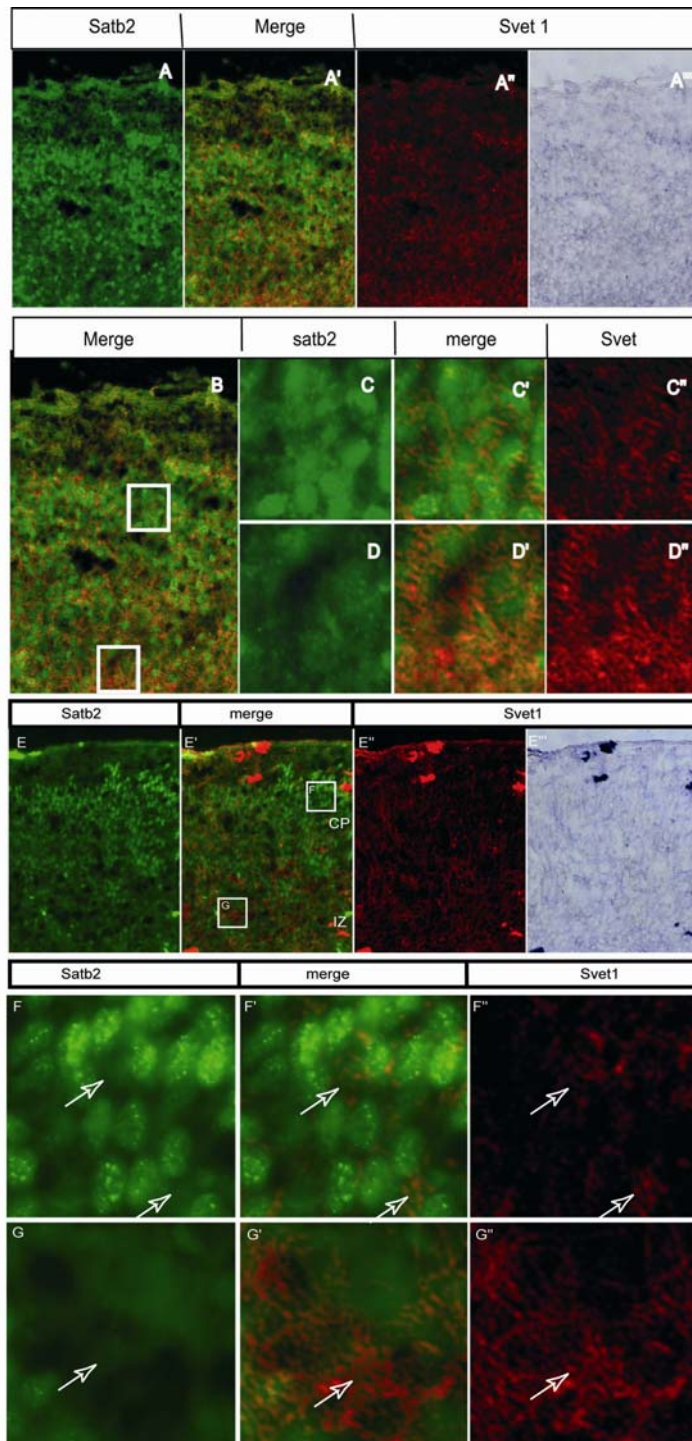
FIG 6. Satb2 and Svet seems to be expressed in different Cell Subpopulations in the Developing Cortical Plate
(A) Satb2 protein and Svet1 mRNA expression reveals no colocalization in the intermediate zone (IZ) and CP at P2. (C and D) Higher-magnification view of the boxed in B. area in (A), (A'), and (A'') are in a pseudocolor from (A''').
(E) Satb2 protein and Svet1 mRNA expression reveals no colocalization in the intermediate zone (IZ) and CP at P0 (empty arrows on [F] and [G]). (F and G) Higher-magnification view of the boxed area in (E'), (E''), (F''), and (G'') are in a pseudocolor from (E''').

Taken together, these results suggest that there are at least three distinct classes of neurons in the cortical plate characterized by the expression of: Ctip2 (some of them may also express Satb1 and Satb2), Svet1 and Satb2. Probably, some Svet1 positive cells also express Satb2. These data also suggest that presence of Satb2 in a subset of UL cells can help to distinguish between two subtypes of UL neurons.

4.2 Satb2 protein expression is not activated immediately after mitotic cycle exit

Satb2 is not expressed in proliferating cells within the dorsal telencephalon (Britanova et al., 2005; Szemes et al., 2006). In order to analyze whether Satb2 is expressed immediately after cells exit the cell cycle or at a later time point, we performed experiments where BrdU was injected into E15.5 pregnant mice. Double immunostaining for BrdU and Satb2 was done in order to analyze colocalization at 6h, 12h and 24h after BrdU pulse. It has been reported that the length of S phase and G2+M phases at E15.5 is around 4 and 2 hours respectively (Caviness et al., 1995). Accordingly, cells at the end S phase would be labeled within a time period of two hours after BrdU injection, while all postmitotic cells would incorporate BrdU within a period of six hours after injection. No BrdU/Satb2+ cells were found 6 hours after injection and very few cells were positive for both BrdU and Satb2 12 hours after injection whereas this number increased at 24 hours after injection (Fig.8). The double-labeled cells at the 12 hour time point were more advanced in the mitotic cycle, i.e. they were at the end S phase at the time of BrdU injection, as evident from the lower number of BrdU/Satb2+ cells 12 hours post injection as opposed to 24 hours. These data indicate that the "postmitotic waiting period" for the onset of Satb2 expression can be approximated to 9-10 hours after the last cell division (Fig.7). These experiments together with the Satb2/Ctip2 double staining suggest that Satb2 marks a distinctive subpopulation of UL neurons.

Satb2 was not present in new born neurons at least nine hours after mitotic cycle exit, but the expression was high during neuronal migration and axonal growth, indicating that Satb2 may be involved in the control of laminar cell-type identity, including connectivity.
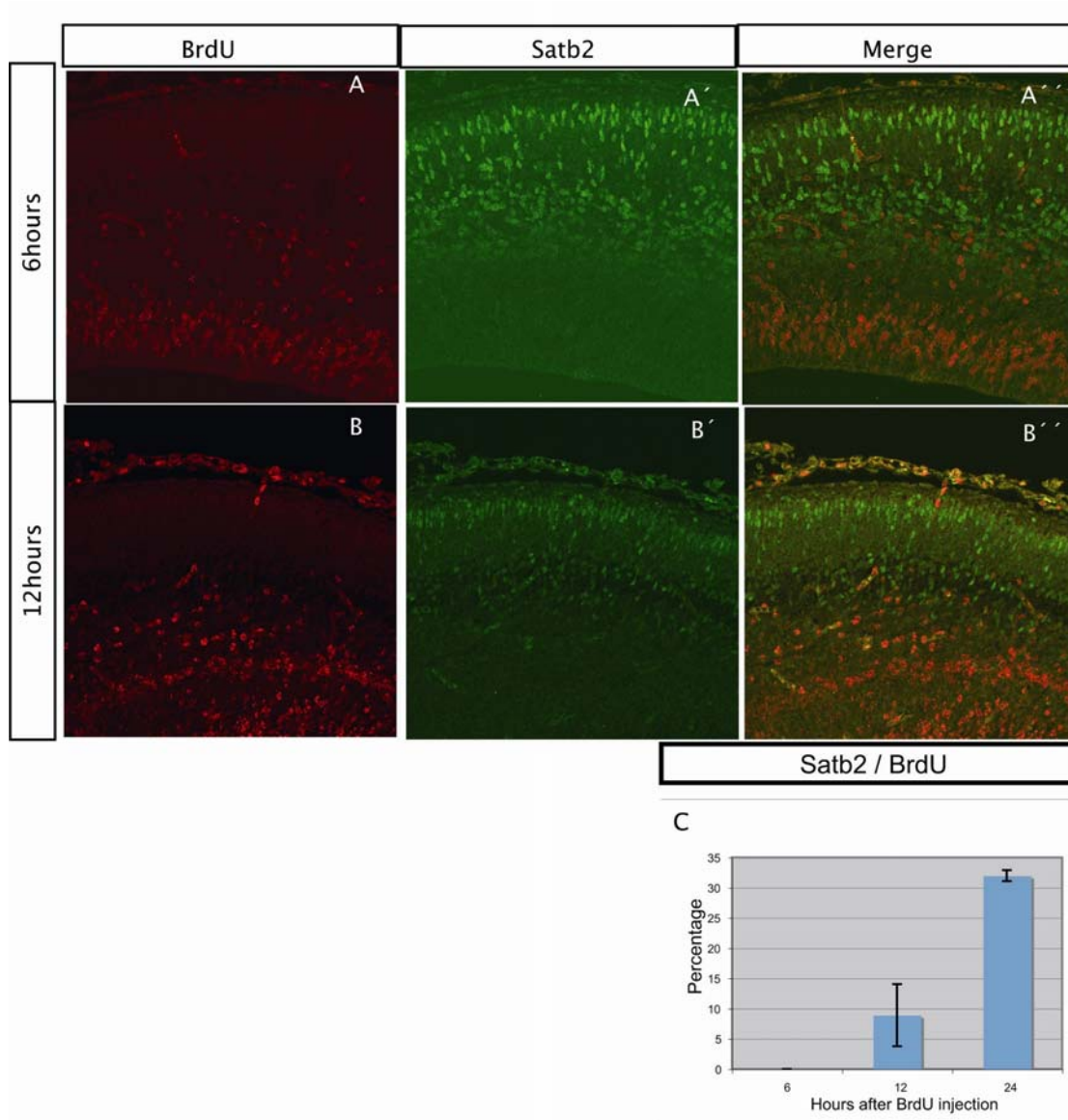
FIG. 7 Satb2 is a late postmitotic gene.
IHC of P0 brains 6 hours after BrdU injection (A) and after 12 hours (B). (C) Quantification of the percentage of BrdU/Satb2 double-labeled cells after BrdU pulse labelling showed that Satb2 is only expressed in postmitotic cells (mean ± SD, 6 hr 0 ± 0, n = 4; 12 hr 8.90 ± 5.12, n = 3; 24 hr 31.99 ± 0.91, n = 4).

4.3 Generation of Satb1 knock-in mouse line.

4.3.1 Generation of knockin construct and ES-cell screens

In order to delete *Satb2* and express *Satb1* ectopically in cells containing transcriptionally active *Satb2* promoter, a conventional knock-in construct was generated by Olga Britanova. Both 5′ and 3′ homology arms were produced by PCR

amplification from isolated ES-cell genomic DNA. The 5′ homology arm was 5120 bps long and contained sequences between the 2nd and 3rd exon, whereas the 3′ homology arm was aprox.2000 bps long and contained genomic sequences downstream of the third exon (Fig.8). This construct would delete exon 3 of *Satb2* gene; "IRES-Satb1-pA" cassette was inserted at the 3′ end of the 5′ homology arm to achieve a knock-in of '*Satb1*' into the *Satb2* locus.

This cassette contained its own polyA signal sequence to stop transcription and IRES (Internal Ribosome Entry Site) sequence to ensure that it will be translated independent of the open-reading frame of *Satb2* gene. Since this cassette would replace the *Satb2* sequence downstream of the 2nd exon where the 5′ homology ends, the transcription of *Satb1* gene would be under the control of transcriptional regulators of *Satb2* gene, and hence will mimic the latter's expression. A floxed "pGK-Neomycin-pA" cassette was placed between "IRES-Satb1-pA" cassette and the 3′homology arm for positive selection of recombined ES-clones. Within this cassette, neomycin gene has its own strong pGK promoter and polyA signal sequence.

The LoxP sites flanking the cassette, offers the possibility of removing it after the selection of ES cells and production of chimeras. For negative selection, a thymidine kinase (TK) cassette with its own promoter and polyA sequence was inserted downstream of the 3′homology arm (Fig.8).

The linearized construct was electroporated into (MPI-II) ES-cells. Positive selection for neomycin and negative selection for TK were done and the surviving clones were picked and grown separately. A total of 131 clones were frozen and a small amount of cell were grown in a feeder less 24 well plate in order to obtain DNA for analysis. Isolated genomic DNA was digested with NsiI, separated on agarose gels and transferred to nylon membranes. The membranes were hybridized separately with 5′ and 3′ external probes. Expected band sizes for the wild-type (WT) allele with both probes was 7.5 kb; while for mutant alleles with correct homologous recombination, the expected band sizes were 4.6 kb with the 5′ probe and 7.6 kb with the 3′ probe. After screening 131 ES-cell clones, only two positive clones were obtained (ES#44 and ES#134). (Fig.8)
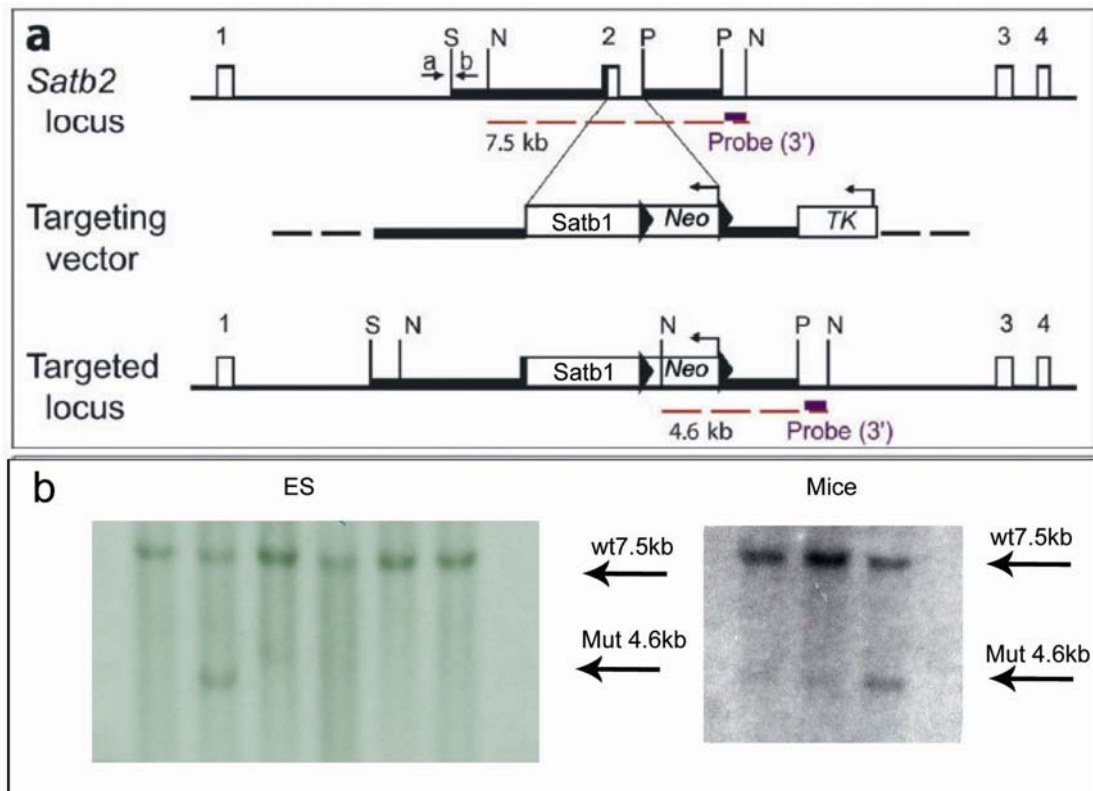
FIG 8. Design rationale for targeted replacement of *Satb2* by *Satb1*.
 a, Schematic representation of the *Satb2* locus, the targeting vector, and the targeted locus. Coding exons are shown as boxes. Restriction sites are *Sma*I (S), *Nsi*I (N), and *Pac*I (P). Oligonucleotides are indicated by arrows and are designated as "a" and "b." The expected fragments are indicated by the dashed red lines. The 3' external probe (*purple box*) identifies a 7.5-kb *Nsi*I fragment in the wild-type allele and a 4.6-kb fragment in the mutant allele. *b*, Analysis of transfected ES cells (*left*) and chimeras (*right*) by genomic Southern-blot analysis with a 3'external probe. Mut=mutant allele.

4.3.2 Generation of chimeras and screening for germline transmissions

Chimeras were created from ES-clones (ES#44 and ES#134) by 'Blastocyst Injection', since this method is known to yield chimeras with higher possibility of germline transmission. This was done in our departmental facilities. The blastocyst injection of ES#44 yielded three litters in which five chimeras were obtained out of ten in the first litter, two out of twelve in the second and one out of seven in the third. From clone ES#134 only one chimera was obtained out of 8 offsprings, a female. Five males derived from ES#44 revealed 65-80% chimerism while one other male and two females showed lower percentage. After several rounds of mating, three of the six male chimeras obtain from ES#44 resulted in germline transmissions (the ones that

showed 85% and 65% chimerism) (Fig. 8). The female chimera obtained from ES#134 was not analyzed.

4.4 Targeting of the Satb2 locus in knock out and knock in mice.

4.4.1 Cre recombinase expression recapitulates Satb2 expression in *Satb2*^{Wt/Cre} brains

In order to analyze the function of Satb2 in cortical development, a knock-out mouse where the second coding exon of *Satb2* was replaced by Cre recombinase cDNA, was generated in the Lab (Britanova et al., 2006b). In *Satb2*^{Wt/Cre} brains, Cre mRNA and protein were detected and both IHC and ISH revealed that its expression pattern was almost identical to that of Satb2 (Fig.9 A-C). Double IHC with anti-Satb2 and anti-Cre antibodies revealed some Satb2-expressing cells that did not express Cre reporter, however no ectopic Cre expression was found. Double IHC with anti-Satb2 and anti-Cre antibodies in *Satb2*^{Cre/Cre} brains demonstrate that Cre and Satb2 expression is mutually exclusive.

We did not found any differences between heterozygous and WT littermates in the neocortex, although *Satb2*^{Wt/Cre} animals display haploinsufficiency in jaw development, this implies that expression of *Satb2* from a single allele is sufficient to ensure normal cortical development and that the function of Satb2 is not dosage-dependent.

4.4.2 Expression of Satb1 recapitulates that of Satb2 in *Satb2* ^{Wt/Satb1} brains, but Satb2 expression persists in *Satb2* ^{Satb1/Satb1} brain.

In order to test for successful *Satb2* targeting and insertion of *Satb1* coding sequences, Satb1 expression was checked at the translational level by IHC. The deletion at the genomic DNA level was validated earlier by southern blotting (Fig.4) and PCR (Fig.4). Brains were isolated from heads of P0 pups. IHC with anti-Satb1 antibody in *Satb2*^{Wt/Satb1} brains revealed Satb1 expression in cortical cells that normally express Satb2 but not Satb1 (Fig 9 J-L). Although Satb1 ki construct is the same as Satb2 ko
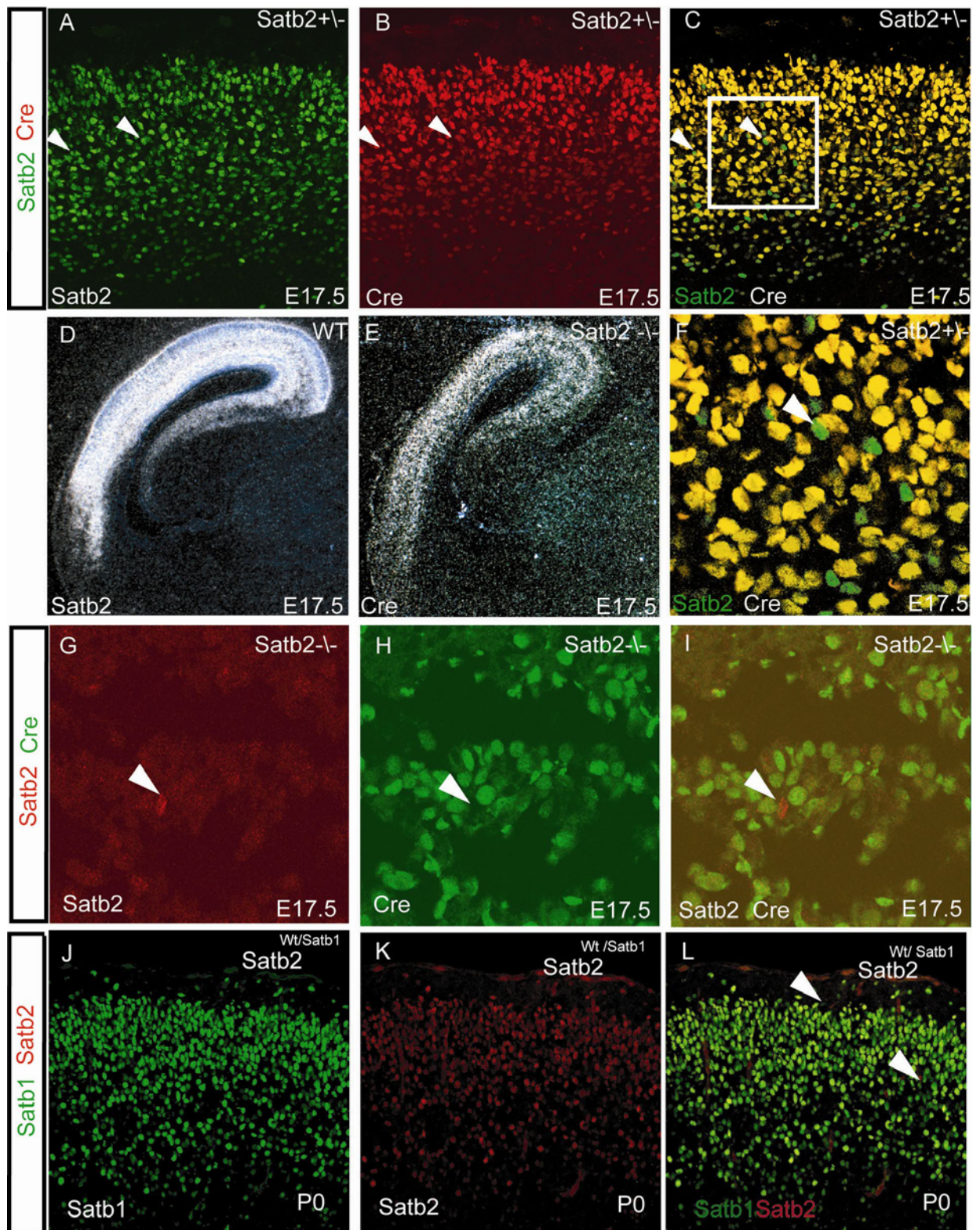
FIG 9. Cre Recombinase Expression Resembles Satb2 Expression in *Satb2* [Wt/Cre] Neocortex
(A–C and F) In *Satb2* [Wt/Cre] cortices, Satb2 (green) colocalizes with Cre (red), although there are a few cells that express Satb2 only (arrowheads). (F) Higher-magnification view of boxed area in (C). (D and E) ISH of Satb2 and Cre on E17.5 *Satb2* [Wt/Cre] sections also reveals a very similar pattern. (G–I) A small number of neurons in *Satb2* [Cre/Cre] neocortex maintain Satb2 expression due to a rare exon exclusion. The arrowhead indicates a cell that still expresses Satb2 but not Cre. (J–L) In *Satb2* [Wt/Satb1] cortices, Satb1 (green) colocalizes with Satb2 (red), although there are a few cells that express Satb1 or Satb2 only (arrowheads) (L).

construct, with the difference that cre recombinase was substituted by Satb1 coding region, Satb2 protein expression was also detected in *Satb2*^{Satb1/Satb1} brains (Data not shown). In order to reduce the dosage of Satb2 in *Satb2*^{Satb1/Satb1} mutant animals, crosses between this line and *Satb2*^{Wt/Cre} were performed. Mice with *Satb2*^{Cre/Satb1} genotype showed an ectopic expression of Satb1 in Satb2 expressing cells as well as some Satb2 expression. Appropriate embryonic or adult positive and negative control tissues were always included in the staining protocols (Fig.9).

4.5 Satb2 deletion in neocortical cell in *Satb2*$^{\text{Cre/Cre}}$ mice.

It has been shown that unlike in the branchial arch derivatives, Satb2 expression was not completely ablated in the developing spinal cord in *Satb2*$^{\text{Cre/Cre}}$ mice (Britanova et al., 2006b). Two Satb2 specific antibodies generated against two different parts of Satb2 protein Ab1 and Ab2 (Britanova et al., 2005) were used in order to probe the deletion of *Satb2* in *Satb2*$^{\text{Cre/Cre}}$ neocortex. Ab1 antibody did not reveal any staining in *Satb2*$^{\text{Cre/Cre}}$ brains whereas Ab2 antibody detected some scattered cells in the developing cortex. There was a variation among different areas of the mutant neocortex and among different animals in the number and distribution of cells expressing Ab2. (Fig.10). However, cells that did not inactivate *Satb2* expression in the *Satb2*$^{\text{Cre/Cre}}$ brains did not express Cre either.

This data suggests the idea of an alternatively spliced form of *Satb2*, so that while the Satb2 ko construct does express Cre protein, Satb2 is still detectable in *Satb2*$^{\text{Cre/Cre}}$ brains.
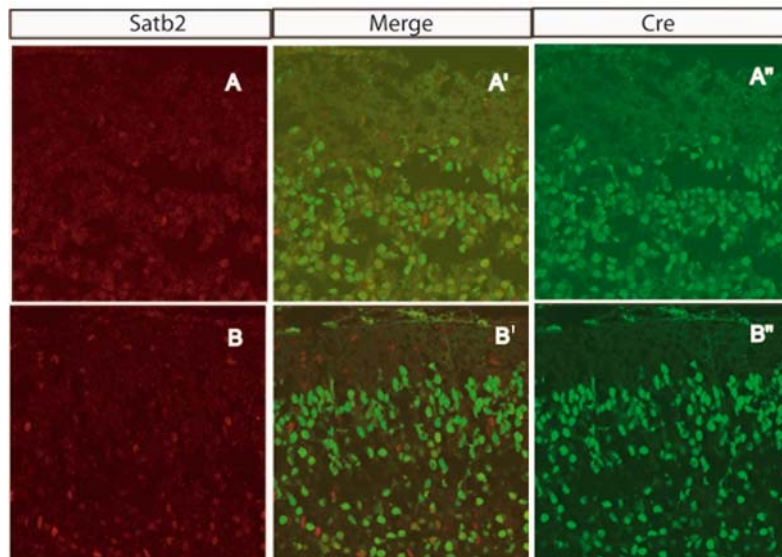
FIG.10. Distribution of cells that escape Satb2 deletion varies between different areas of the mutant neocortex.
IHC with Satb2 (A, B) and Cre (A´´, B´´) in *Satb2*^{Cre/Cre} brains.

4.6 Craniofacial phenotype of *Satb2*^{Cre/Satb1}.

In a C57Bl/6 background, *Satb2*^{Cre/Cre} neonates exhibit slight microcephaly, small mouths, premaxillary and nasocapsular hypoplasia, micrognathia, and variable incisor hypodontia and/or adontia (Britanova et al., 2006b). In *Satb2*^{Cre/Satb1} the craniofacial abnormalities are not as severe as in *Satb2*^{Cre/Cre}. The snout of adult *Satb2*^{Cre/Satb1} animals is strongly truncated and occasionally asymmetric (Fig.11C) and the animal also shows slight microcephaly accompanied by smaller cortex and thinner Corpus Callosum (Fig.11 D´´´).

Satb1 and Satb2 are expressed in the palate, which is formed from two primordia, the primary palate and the secondary palate. The secondary palate develops bilaterally as two vertical projections, the palate shelves, which become oriented horizontally as morphogenesis proceeds. The palate shelves approach each other and fuse medially. In *Satb2*^{Cre/Satb1} there is a failure of the palate shelves to fuse, leading to a cleft palate (Fig 12A, E). This problem can be due to misregulation of either the timing, rate or extent of outgrowth of the palate shelves. Cleft palate problems were already reported in *Satb2*^{Cre/Cre} and mice heterozygous for this mutation (Britanova et al., 2006b).

Another important event in craniofacial morphogenesis is tooth formation. This process is regulated by inducible tissue interactions between the oral epithelium and the subjacent mesenchyme of the first branchial arch where both, Satb1 and Satb2 are

expressed. One of the first steps in tooth formation is the invagination of the dental lamina into the underlying mesenchyme. $Satb2^{Cre/Satb1}$ shows abnormal convolutions in the dental epithelium as well as cell aggregate formation in the condensed mesenchyme (dental papilla) when compared with the wild type (Fig. 12C, G)

This data suggests that even thought Satb1 is expressed in the branchial arches, its overexpression doesn't compensate for the lack of Satb2. In $Satb2^{Wt\ /Satb1}$ the craniofacial morphology is not affected most probably due to the normal Satb2 expression in these animals. However, $Satb2^{Cre/Satb1}$ mice show abnormalities more severe than the normal heterozygous mice for $Satb2$ deletion. The midline structures connected to the upper and lower arcades are affected, as evident from the septal cartilages overlying the upper jaws and parasagittal elements. Incisors and their associated alveolar bone fail to form in each jaw quadrant (Fig.11 E'''). Overexpression of Satb1 seems unable to compensate for Satb2 function as regulator of murine jaw and palate development and morphogenesis.
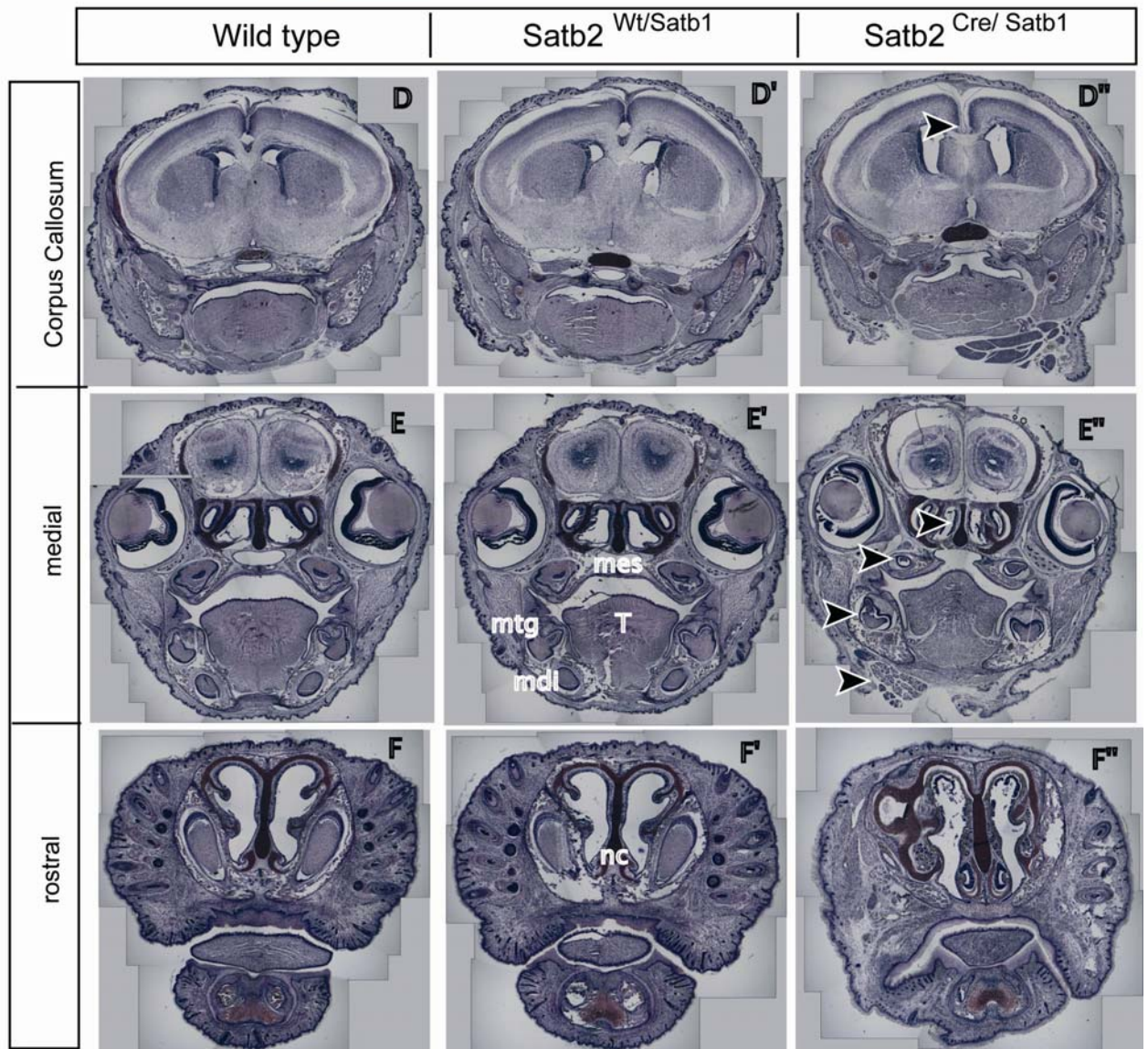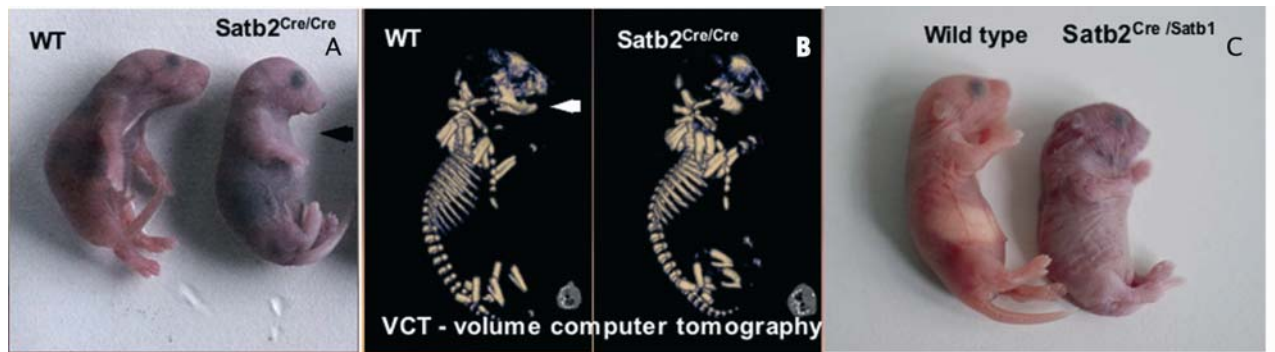
FIG. 11 Craniofacial phenotype
Phenotypical comparison between Wt and $Satb2^{Cre/Cre}$ (A) and $Satb2^{Cre/Satb1}$(C) mice. Arrowheads show lower jaw malformation. (B) Computer tomography of Satb2 $^{Cre/Cre}$ (Data from Olga Britanova)**.**
Comparative histological sections of nissel-stained wild-type, $Satb2^{Cre/Cre}$ and $Satb2^{Cre/Satb1}$ neonates (D-F) demonstrating the effect of gene dosage on upper jaw and palatal development. (E''') Highlighting loss of parasagittal hard- and soft-tissue structures in $Satb2^{Cre/Satb1}$. Arrowheads: midline nasal septum upper molar tooth or bud and lower molar tooth or bud. med-medial epithelial seam (of palate), mdi-mandibular incisor buds, mtg- molar tooth germ, nc-nasal cavity, t-tongue
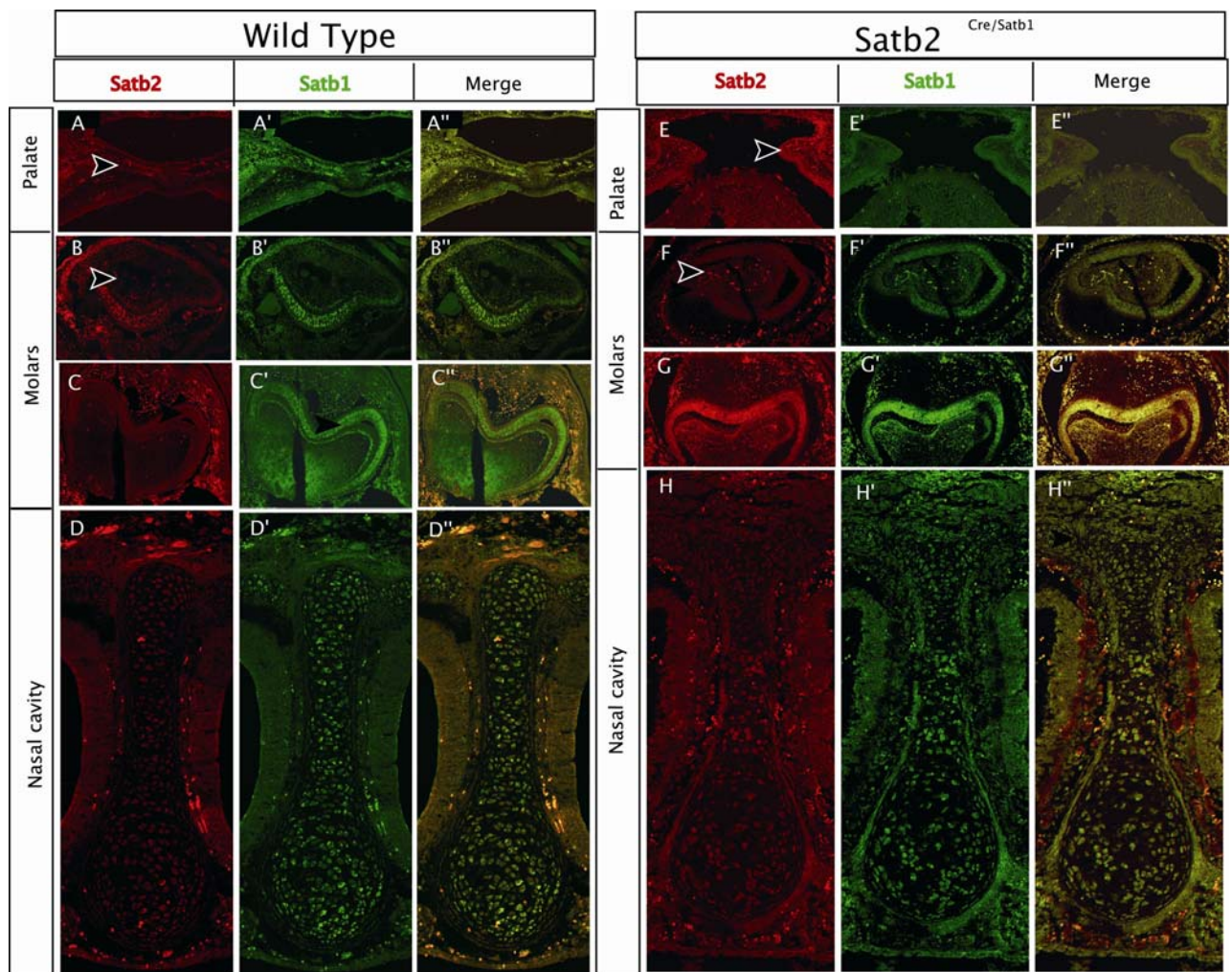
Fig 12. Satb1 and Satb2 expression in the midline structures connected to the upper and lower arcades

Comparison between Wt expression in Wt and *Satb2*Cre/Satb1 in the septal cartilages overlying the upper jaws (A,D,E;H) and parasagittal elements, such as incisors (B,F), molar (C,G) reveals several malformations including reduction in teeth size and bone formation failure in their associated alveolar bone in each jaw quadrant. Note the cell aggregates in the mutants (arrowheads)

4.7 Study of commissures in *Satb2*Cre/Cre, *Satb2*Satb1/wt and *Satb2*Cre/Satb1.

4.7.1. Satb2 mutants fail to form corpus callosum, but retain both hippocampal and anterior commissures.

During development three major axonal tracts connecting the two cortical hemispheres are formed: corpus callosum (C.C) hippocampal commissure (h.p) and anterior commissure (a.c). Lack of *Satb2* seems to affect two of them, C.C and a.c

Nissl staining based analysis of *Satb2*^{Cre/Cre} brains has shown lack of C.C, a frequent event in numerous mutations affecting cortical development (N=30). However, C.C was always present in both heterozygote (N=10) and WT (N=30). On the other hand, the a.c was thicker at the same rostro-caudal levels (Fig.14), whereas the hippocampal commissure, a bundle of axons located caudally from C.C was not affected. IHC staining of L1, a member of NCAM family of adhesion molecules that labels cortical axons (Fukuda et al., 1997; Molnar et al., 2002), did not reveal formation of a Probst bundle (Fig.14).This accumulation of fibers in the vicinity of the midline is associated with phenotypes involving absence of C:C, where fibers fail to cross the midline.

Further studies of commissural projections using lipophilic tracer DiI were performed with the help of Amanda Cheung. DiI travel along lipid membranes both anterogradely and retrogradely thus enabling examination of both fiber trajectories and cell morphologies. In experiments with P0 Wt animals where DiI was placed in the a.c, most of the back-labeled cortical neurons were located in the insular cortex, and 37% of them were Satb2+ (Fig. 13A). In *Satb2*^{Cre/Cre} brains where there is not C.C, 58% of DiI-labeled cells were Cre+, and they were seen originating from a more dorsal position in the cortex (e.g., parietal cortex , including putative somatosensory cortex) than in normal Wt brains (Fig.13). Moreover, when DiI was placed in the presumptive somatosensory area, allowing the anterograde labeling of corticofugal axons, cortical axons from this area were seen travelling via the external capsule to a.c in KO (Fig.13C) whereas in Wt, axons from the same area were seldom seen projecting to the a.c.(n=3) (Fig.13C, D). In WT, neurons from insular cortex also send callosally-projecting axons. In a DiI/DiD double-labeling experiment, with DiI placed in C.C and DiD placed in a.c, no double-labeled cell was found in the WT insular cortex (data not shown) indicating that there are no dual-projections from insular cortex neurons to both C.C and a.c.
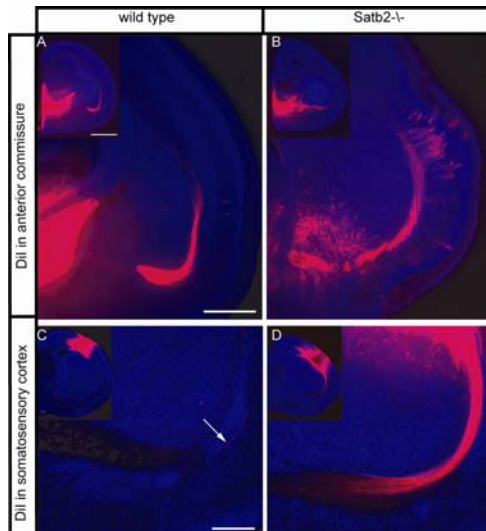
FIG 13. Commissural projection errors in *Satb2*^{Cre/Cre} mice.
DiI labelling (red) from the a.c at P0. In WT, very few DiI-labeled cells were found in the lateral cortex. No back-labeled cell was found in the dorsal cortex. In *Satb2*$^{Cre/Cre}$, more cells were back-labeled from the somatosensory cortex. (A and B) DiI labelling from the presumptive somatosensory cortex at P0. Cortical efferent fibers travelled via the external capsule to a.c. in *Satb2*$^{Cre/Cre}$, but this connection is almost absent in WT. All sections were counterstained with bisbenzimide (blue). Inset: DiI placement. Scale bars, 500 mm (A and B), 200 mm (C and D), and 1 mm (insets).

4.7.2. Analysis of *Satb2*$^{Satb1/wt}$ and *Satb2*$^{Cre/Satb1}$ brains do not reveal any commissural problem.

Analysis of Nissl stained *Satb2*$^{Satb1/wt}$ and *Satb2*$^{Cre/Satb1}$ brains did not reveal any malformation in the three major tracts that interconnect the two hemispheres of the cerebral cortex (Fig.14 C-D). We did however observed variable reduction in Satb2$^{Cre/Satb1}$ cortical size (D), but in none of the cases were any connections absent.
This data suggests that *Satb1* expression under *Satb2* promoter does not have an influence on normal axonal development.

4.8 Afferent and efferent cortical axonal connections in Satb2 mutants are misrouted

The expression of Satb2 coincides with the period of establishment of major cortical afferent and efferent connections, such as the corticothalamic and thalamocortical projections, and tracts passing through the cerebral peduncle. In experiments performed by Amanda Cheung, DiI was used to label different pathways from the
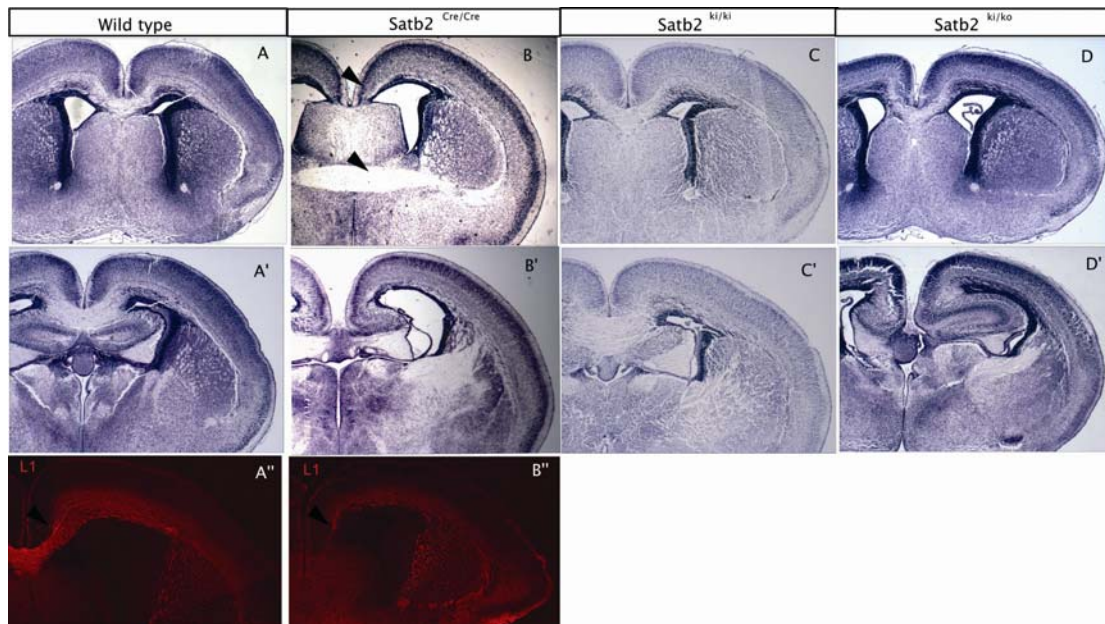
FIG 14. The Corpus Callosum and Anterior Commissure Are Affected by Satb2 Deletion but not for Satb1 overexpression.
Nissl staining of P0 WT, *Satb2*Cre/Cre, *Satb2*Satb1/wt and *Satb2*Satb1/Satb2 brains at rostral (A, B, C and D) and caudal level (A', B', C'and D'). Black arrowheads depict the c.c region (A'', B'' and B) and a.c. (B) ICH of L1 on P0 WT and *Satb2*Cre/Cre brains shows that the c.c is missing in *Satb2*Cre/Cre (arrowheads) (A''and B'').

cortex, thalamus, internal capsule and cerebral peduncle. DiI placed in the presumptive somatosensory area at P0, anterogradely labeled corticofugal axons (CFAs), and retrogradely labeled thalamocortical axons (TCAs). In Satb2Cre/Cre brains, corticofugal connection through the internal capsule shifted to a more caudal position and fewer cell bodies were labeled in the cortex when DiI was placed in the presumptive somatosensory area. On the other hand, S1 cortical crystal placements retrogradely-labeled cell bodies in the ventro-basal complex of thalamus (VB) and showed a normal innervation of the thalamic axons in Satb2 mutant cortex (Fig.15A-C). DiI placed in the VB or dorsal thalamus labeled TCAs and CFAs from somatosensory area by anterograde and retrograde transports respectively and TCAs traveled normally via the internal capsule to the cortex. However, similar to the corticofugal pathway, the trajectory of thalamocortical pathway was also shifted to a more posterior level in mutants. Thalamocortical innervation in the cortex was reduced, and there were also fewer back-labeled corticofugal neurons in the KO cortex (Fig. 15D-F).

A more careful examination of the distribution of subcortically projecting neurons, which predominantly originate from deep layers 5 and 6, was performed in Satb2

mutants. DiI was placed in the internal capsule or in the cerebral peduncle at P0. The number of subcortically-projecting neurons present in the differentiating cortical plate was increased from 1.69% to 6.10% in mutants when the cerebral peduncle was retrogradely labeled (N= 1047), and from 13.10% to 21.52% in internal capsule labeling (N=869) (Fig. 14 G, H). Colocalization of DiI labeling from the cerebral peduncle with Satb2 or Cre recombinase by immunostaining further showed that the lack of *Satb2* induced more neurons (from 37% in WT to 64% in KO) to send efferent connections to subcortical targets. There is a small population of cell that express both Satb2 and Ctip2, but Satb2+ cells were never seen projecting to the spinal cord in WT mice (N=87) (Fig. 15I). Since Satb2 mutants die after birth, we could not compare data between mutants and WT animals at later time points.

All DiI and IHC colocalization data (including the previous section) are summarized in Table 1. It indicates that Satb2-expressing neurons normally send their axons via the corpus callosum, anterior commissure, internal capsule, but never to the spinal cord. Without *Satb2*, the corpus callosum fails to form, and Cre-expressing UL neurons send axons to targets that are normally form connections with deep layer neurons, through the anterior commissure and cerebral peduncle.
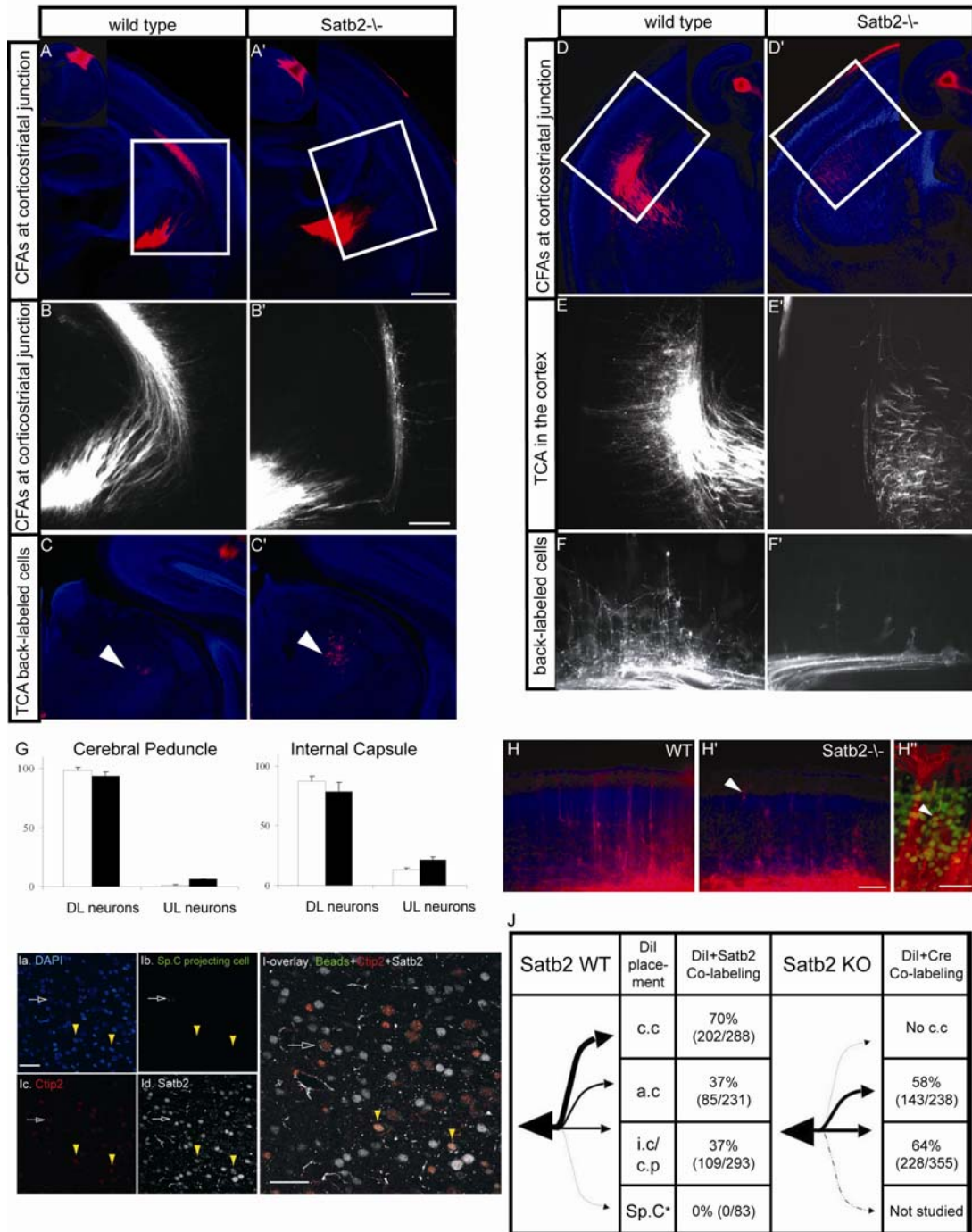
FIG 15. Abnormal Cortical Afferent and Efferent Connections in P0 *Satb2*^{Cre/Cre} Mice

(A–C) Axonal labeling from the presumptive somatosensory area. (A and A') Cortical neurons send projections via the internal capsule to various targets; however, the fibers were seen travelling at a more posterior level in *Satb2*^{Cre/Cre}. (B and B') Higher-magnification view of boxed areas in (A) and (A'). (C and C') Normal thalamocortical innervation in Satb2 KO was observed, as back-labeled cell bodies were found in the ventrobasal complex of thalamus (white arrows). (D–F) Axonal labelling from the ventrobasal complex of thalamus. (D and D') Thalamocortical axons travelled to the cortex via a more posterior level in *Satb2*^{Cre/Cre}, and fewer axons were seen innervating the cortex (E and E'). (F and F') Moreover, fewer back-labeled corticothalamic cells were seen in the cortex in *Satb2*^{Cre/Cre}. (G and H) The percentage (± standard error of the mean) of DiI-labeled neurons from upper or deep layers sending projections to the cerebral peduncle or the internal capsule shows that more neurons from the upper cortical plate (arrowhead) send projections to subcortical targets in *Satb2*^{Cre/Cre}. (H'') An example of a Cre-expressing neuron (green, arrowhead) being back-filled with DiI from subcortical targets. (I) Satb2 was never expressed in Ctip2+ spinal cord-projecting neurons in normal brains (white

arrow), although Satb2 and Ctip2 are coexpressed in some cells (yellow arrowheads). Scale bars, 500 mm (A and C), 200 mm (B, E, and F), 100 mm (H, H', and I), and 50 mm (H''). (J) A summary table showing the percentage of Satb2- or Cre-expressing cells projecting to different targets by DiI retrograde labelling in P0 Satb2 WT and KO brains, respectively. c.c, corpus callosum; a.c, anterior commissure; i.c, internal capsule; c.p, cerebral peduncle; Sp.C, spinal cord. * The Sp.C data were obtained by labelling P7 mouse spinal cord-projecting neurons with fluorescent latex microspheres from the spinal cord.

4.9 Satb2 deletion causes changes in Eph/ephrin expression.

Expression analyses of molecules that are normally expressed at the dorsal midline and regulate axon guidance (reviewed in Lindwall et al., 2007) were performed. In situ hybridization of control and $Satb2^{Cre/Cre}$ brains at P0 for several members of Ephrin-A and Ephrin-B gene families (Dufour et al., 2003) revealed changes in expression of some of these ephrins and their receptors (Fig 16).

In the absence of ephrin A5 and EphA4, a subset of rostral TC axons adopts the topographic behaviour of caudal TC axons in the ventral telencephalon. Projections of the rostral TC axons in ephrin A5/EphA4 DKOs show a more caudal pattern in the ventral epencephalon. While the bulk of TC axons from the rostral thalamus normally invade the rostral domains of ventral and dorsal telencephalon, in mutants they are present at more caudal levels both in the ventral and in the dorsal telencephalon (Dufour et al., 2003). This phenotype is also reproduced in $Satb2^{Cre/Cre}$, where the mutants display caudalization of TC axons (Fig 15 D-F). Analyses of the ephrin A5 and EphA4 RNA levels in $Satb2^{Cre/Cre}$ reveal a reduction in both of them throughout the CP (Fig.16 B, C), suggesting that the loss of Satb2 influences the levels of ephrin A5 and EphA4 and causes caudalization of the TC axons in $Satb2^{Cre/Cre}$ mutants. Further analysis of other members of Ephrin-A and Ephrin-B gene families has to be done but these preliminary results suggest that Satb2 may act in combination with these guidance molecules to control axon targeting of cells located in layers II-IV.
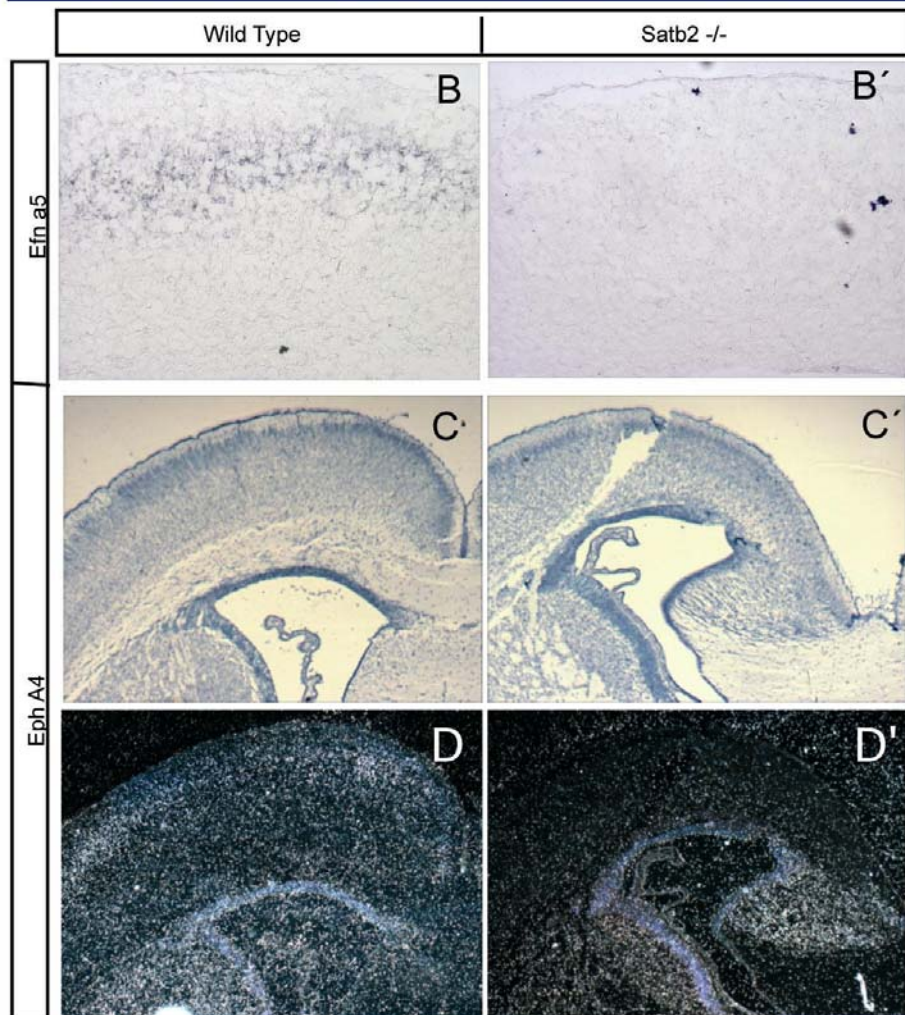
FIG 16. Eph/ephrins signalling.

(A) Alterations in the Expression of Genes Encoding Axon Guidance Ligands and Receptors in the P0 Satb2 Mutant Cortex as Determined by In Situ Hybridization. Expression of ephrin a5 (B) and Eph A4 (D) is lost in superficial CP and layer 5 neurons in *Satb2*[Cre/Cre] (B', D').

4.10 Migration problems in *Satb2*^{Cre/Cre}, *Satb2*^{Satb1/wt} and Satb2^{Cre/Satb1}.

4.10.1 *Satb2* ablation leads to impaired migration of upper layer neurons

In order to investigate whether lack of Satb2 can influence the migration of neurons in the cortex, additional BrdU pulse chase experiments were performed. BrdU was injected into pregnant females at E13.5, E15.5 and E17.5 and the brains were analyzed at P0. Cells undergoing the last mitotic cycle at the time of injection showed high levels of BrdU on immunostaining. The pattern of migration of these cells is indicated by the distribution of BrdU+ cells in the CP at later stages. Cells born at E13.5 mostly become DL neurons with the exception of a minor Satb2 + fraction (Britanova et al., 2006b). Injections at E13.5 show similar number and domain size of BrdU-labeled cells between WT and KO (Fig.17A, B). Although, the entire layer of BrdU+ cells was shifted towards the upper part of the CP in mutant animals while no BrdU+ cells were detected in this area in WT. These differences in the position of BrdU+ cells most probably are due to a problem in migration of later-born UL neurons that fail to migrate past early-born DL neurons, and end up occupying more superficial positions. Cells labeled at E15.5 did not migrate properly in the absence of Satb2. Most of the cells born at E15.5 occupied upper cortical layers in WT, but they were more dispersed in the KO (Fig.17 C, D).

Migration of cells born at E17.5 did not seem to be affected and BrdU+ cells were found in the VZ/SVZ, IZ and CP in WT and *Satb2*^{Cre/Cre} (Fig.17E, F).

In summary, Satb2 deficient cells failed to migrate past earlier born neurons and attain proper outer-layer position in *Satb2*^{Cre/Cre}.

4.10.2 Cells carrying *Satb2*^{Satb1/Satb1} and *Satb2*^{Cre/Satb1} mutations do not migrate properly.

In order to investigate whether neuronal migration was also affected in *Satb2*^{Satb1/wt} and *Satb2*^{Cre/Satb1} mutant animals, we performed similar BrdU pulse chase experiments as the ones done in *Satb2*^{Cre/Cre}. Pregnant females were injected with BrdU at E13.5, E15.5 and E17.5 and the brains were analyzed at P0.

Most cells born at E13.5 occupied similar domain in WT, $Satb2^{Wt/Satb1}$ and $Satb2^{Satb1/Cre}$. At this stage BrdU-labeled cells are mostly located in the UL of the cortical plate, and even if the number seems to be reduced, the distribution is not affected (Fig.17 G). There is reduction the number of cells born at E15.5 in $Satb2^{Cre/Satb1}$ and they are located in the UL of the cortex but not in the VZ, whereas $Satb2^{Wt/Satb1}$ shows a normal distribution of BrdU+ cells as compared to Wt (Fig.17 H). The distribution of BrdU + cells born at E17.5 does not seem to be affected in $Satb2^{Cre/Satb1}$ when compared with $Satb2^{Wt/Satb1}$; there is however a decrease in the number of BrdU+ cells in $Satb2^{Cre/Satb1}$ (Fig.17I).
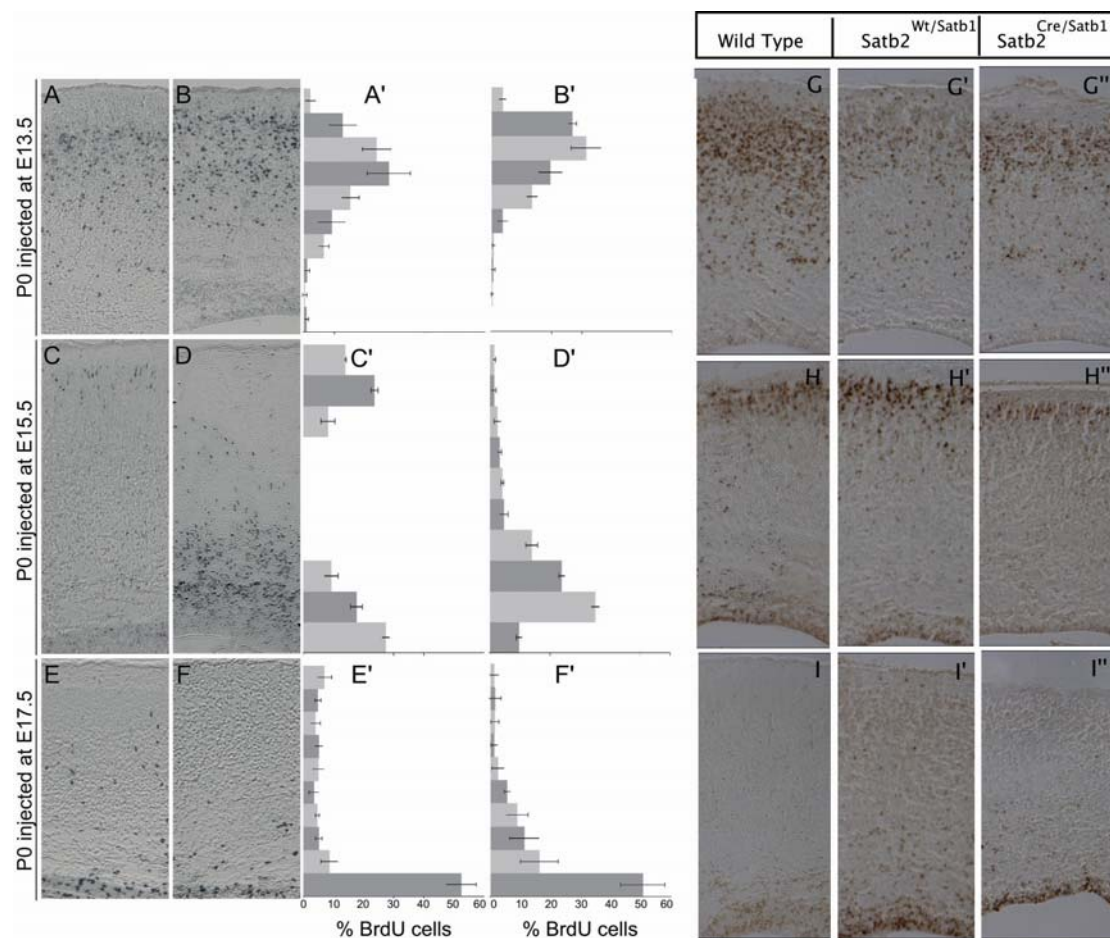

FIG 17. Abnormal Migration of UL Neurons in Satb2-targeted Cells

(A and B) BrdU pulse labelling shows that cells born at E13.5 migrate similarly in WT (A) and $Satb2^{Cre/Cre}$ (B) brains, but there are more cells in the superficial cortical plate (CP) in $Satb2^{Cre/Cre}$. (C and D) Cells born at E15.5 are found in the superficial CP in WT (C) but dispersed in $Satb2^{Cre/Cre}$ (D). (E and F) Cells born at E17.5 are distributed in both WT (E) and $Satb2^{Cre/Cre}$ (F) across the CP, intermediate zone (IZ), and ventricular zone/subventricular zone (VZ/SVZ).
(A'–F') The distribution of BrdU+ cells along the radial axis of P0 WT and $Satb2^{Cre/Cre}$ neocortex.
BrdU pulse labelling at E 13.5(G-G'''), E15.5 (H-H''') and E17.5 (I-I''') in Wt, $Satb2^{Wt/Satb1}$ and $Satb2^{Cre/Satb1}$ don't reveal major migration problems excepting E.15.5

These findings indicate that the migration of neurons was not affected by Satb1 overexpression whereas the number of proliferating cells seems to be reduced in *Satb2*$^{Cre/Satb1}$

4.11 Satb2 is required to maintain genetic program of upper layers.

In order to determine whether lack of Satb2 influences the genetic program of other cell types in the developing neocortex, the expression of several layer-specific genes was analyzed. Changes in the expression of genes normally expressed in upper layers, such as *Brn2* were analyzed by IHC and that of *Cux2* and *Svet1* by ISH (McEvilly et al., 2002; Nieto et al., 2004; Sugitani et al., 2002; Tarabykin et al., 2001; Zimmer et al., 2004). Analysis of *Satb2*$^{Cre/Cre}$ brains did not show significant differences in the number of Brn2+ or Cux2+ cells (Fig.18D, I). *Svet*1, that marks a subpopulation of upper layer cells that are not expressed in the CP before E18.5 (Tarabykin et al., 2001) was found to be ectopically activated in cells where Satb2 expression was abolish.

To determine whether the expression of DL genes was also affected in *Satb2*$^{Cre/Cre}$ mice, ISH and IHC with several deep layer markers was performed. ISH shows that the expression domains of layer V and VI markers, Er81 (Fig.19D, H) and RoRβ (not shown) in E15.5 and E17.5 mutant brains were not altered. Expression of Fezl was also not affected by *Satb2* mutation (not shown). Tbr1, a gene important for proper specification of layer VI, and is expressed at high levels in subplate and at low levels in some UL neurons, is not expressed by most Satb2 + cells at E15.5 (Britanova et al., 2006a; Hevner et al., 2001; Tarabykin et al., 2001). However, the expression of Tbr1 at P0 in UL cells was down-regulated whereas its expression in DL cells was not affected by Satb2 deletion. (Fig. 17 B, G). *Brn2* (and also *Brn1*) are expressed in both UL progenitors and postmitotic neurons with very similar expression patterns (McEvilly et al., 2002; Sugitani et al., 2002). At P0, most cells in the IZ and CP co-expressed Satb2 and Brn2, although there were also two minor cell populations that exclusively expressed either Satb2 or Brn2 (Fig.18D, I). The transcription factor *Nurr1*, normally expressed in the subplate medially and in upper layers laterally, was ectopically activated in Satb2 expressing cells in the medial part of the neocortex whereas in the lateral cortex Nurr1 expression was shifted into deeper layers of the

CP. However, the number of Nurr1 expressing cells in the lateral cortex does not seem to be affected significantly (Fig.19B, F). Additional *in situ* hybridization experiments with dorsal and medial cortex specific molecular markers (*Id2, Oct6, Fzd8, and Sfrp1*) did not reveal any abnormal area specification (Fig 19 I, J, K, and L).

Another gene that is expressed strongly in the developing neocortex and required for its normal development is *Sip1* (Miquelajauregui et al., 2007). It is highly expressed in virtually all UL neurons and at lower level in many DL neurons (Fig 18 C, H). Co-localization studies comparing Cre and Sip1 expression in *Satb2*$^{wt/Cre}$ mice showed that almost all Sip1+ neurons in upper layers co-expressed Cre. In deep layers a minor population of cells that expressed Sip1 at high levels also expressed Cre. However, most cells in deep layers expressed Sip1 at low levels, and did not express Cre. While Sip1 expression in *Satb2*$^{Cre/Cre}$ UL neurons was strongly downregulated, expression in DL cells was maintained. Interestingly, the scattered cells in upper layers that did not down-regulate Sip1 expression did not express Cre either, indicating that they still maintained Satb2 expression (Fig.18C, H).

Ctip2, a transcription factor that controls specification of DL neurons, is also required for formation of corticospinal tract (Arlotta et al., 2005). As mentioned before, most Satb2+ cells do not co-express Ctip2 at P0 (Fig5. D;Fig.18 A, F) but Satb2 ablation changes Ctip2 expression dramatically and virtually all Cre expressing cells became Ctip2+ in *Satb2*$^{Cre/Cre}$ (Fig. 18A, F).

Interestingly, single cells that did not show Ctip2 immunoreactivity in *Satb2*$^{Cre/Cre}$ were the same cells that retained Satb2 immunoreactivity.

In summary, these results indicate that Satb2 is required to activate genetic program of early UL neurons (high Sip1 expression, low Tbr1 expression) and conversely, inactivate expression of genes specific for other neocortical sublineages, such as DL cells (Ctip2 and Nurr1 expression) and late UL cells (Svet1 expression). Analysis of cells that failed to inactivate Satb2 in the mutant cortices indicates that Satb2 is required cell autonomously for specifying genetic program of early born UL neurons.
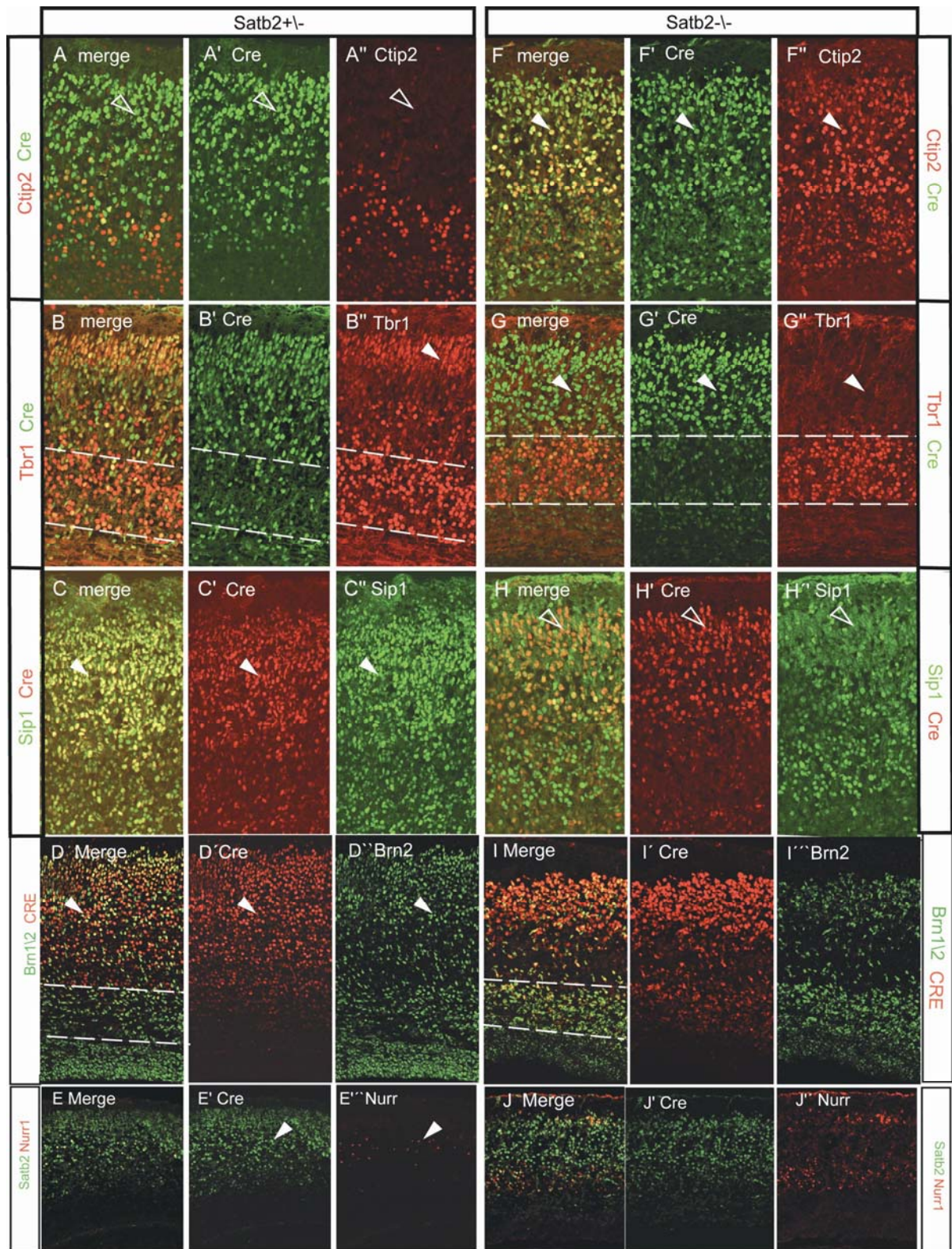
FIG 18. Ctip2, Tbr1, Sip1, Brn2 and Nurr1 Expression Levels Are Affected by Satb2 Deletion
(A and F) The majority of Cre-positive cells are Ctip2-negative in *Satb2*[wt/Cre] neocortex (empty arrowheads), whereas in *Satb2*[Cre/Cre] virtually all Cre+ cells coexpress Ctip2 in the cortical plate (filled arrowheads in [B] and [G]) The position of Tbr1-expressing cells of layers 5 and 6 (demarcated by dashed lines) is not affected, but the expression of Tbr1 is downregulated in the upper layers of *Satb2*[Cre/Cre] (filled arrowheads). (C and H) Most neurons in the upper layers coexpress Cre and Sip1 in *Satb2*[wt/Cre] (white arrowheads); however, Sip1 is strongly downregulated in *Satb2*[Cre/Cre]. There are few remaining Sip1-expressing neurons, but they do not coexpress Cre arrowheads. (D and I) Most cells in

the upper layers co-express Brn1/2 and Satb2 (D)The numbers of Brn1/2-positive cells is not significantly altered between $Satb2^{Wt/Cre}$ (D) and $Satb2^{Cre/Cre}$ cortex (I), but in$Satb2^{Cre/Cre}$ significantly more Brn1/2-positive cells are located in the intermediate zone (IZ). In contrast to $Satb2^{Wt/Cre}$ most cells in IZ of $Satb2^{Cre/Cre}$ are Cre/Brn1/2 double-positive. (E and J) Double-IHC of Nurr1 (red) with either Satb2 or Cre (green) in E18 WT and $Satb2^{Cre/Cre}$. Increased Nurr1 protein expression in the neocortex was also observed in the $Satb2^{Cre/Cre}$ neocortex. Arrowheads point to Nurr1/Satb2 or Nurr1/Cre double-labeled cells.
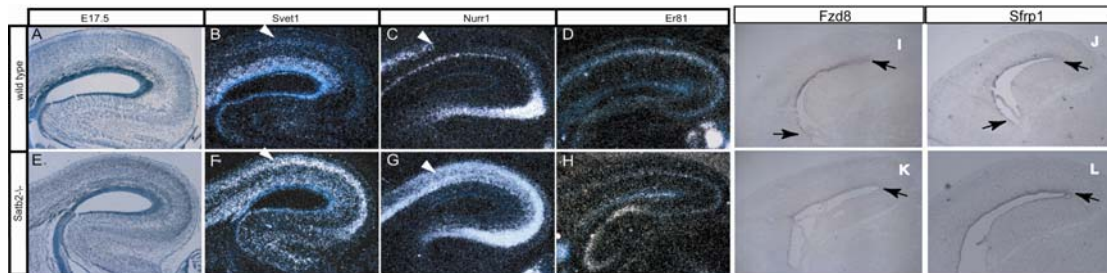

FIG.19 In Situ analysis of several cortical markers in $Satb2^{Cre/Cre}$
(A–I) Svet1 and Nurr1 are activated ectopically in the $Satb2^{Cre/Cre}$ neocortex. (A–D) In E17 WT, Svet1 mRNA is detected in the SVZ and IZ, but not CP, whereas Nurr1 is detected in layers 5 and 6 and Er81 only in layer 5. (G–J) In $Satb2^{Cre/Cre}$, both Svet1 and Nurr1 mRNAs are ectopically expressed in the CP (arrowheads). *In situ* hybridization experiments with molecular markers of the dorsal cortex. Fzd8 (I, K) and Sfrp1 (J, L) cortical domains of expression are not shifted in $Satb2^{Cre/Cre}$ (K, L) as compared to the $Satb2^{Wt/Cre}$ (I, J).

4.12 Effect of ectopic expression of Satb1 in the neocortex.

4.12.1 Ctip2 expression is not repressed in Satb1 and Satb2 expressing cells.

Double IHC was used to address whether Satb2+ cells co-express Ctip2 in $Satb2^{Wt/Satb1}$ and in $Satb2^{Cre/Satb1}$ brains (Fig.20A-C). While $Satb2$ ablation increase Ctip2 expression in virtually all Cre expressing cells in $Satb2^{Cre/Cre}$ mice, $Satb1$ ectopic expression doesn't change Ctip2 expression in the UL of the cortex. Interestingly, the number of cells that express both these genes is dramatically increased in $Satb2^{Cre/Satb1}$. To further investigate the effect of Satb1 in Ctip2 expressing cells and how its expression is affected in cells carrying $Satb2^{Cre/Satb1}$mutation, another double IHC was performed
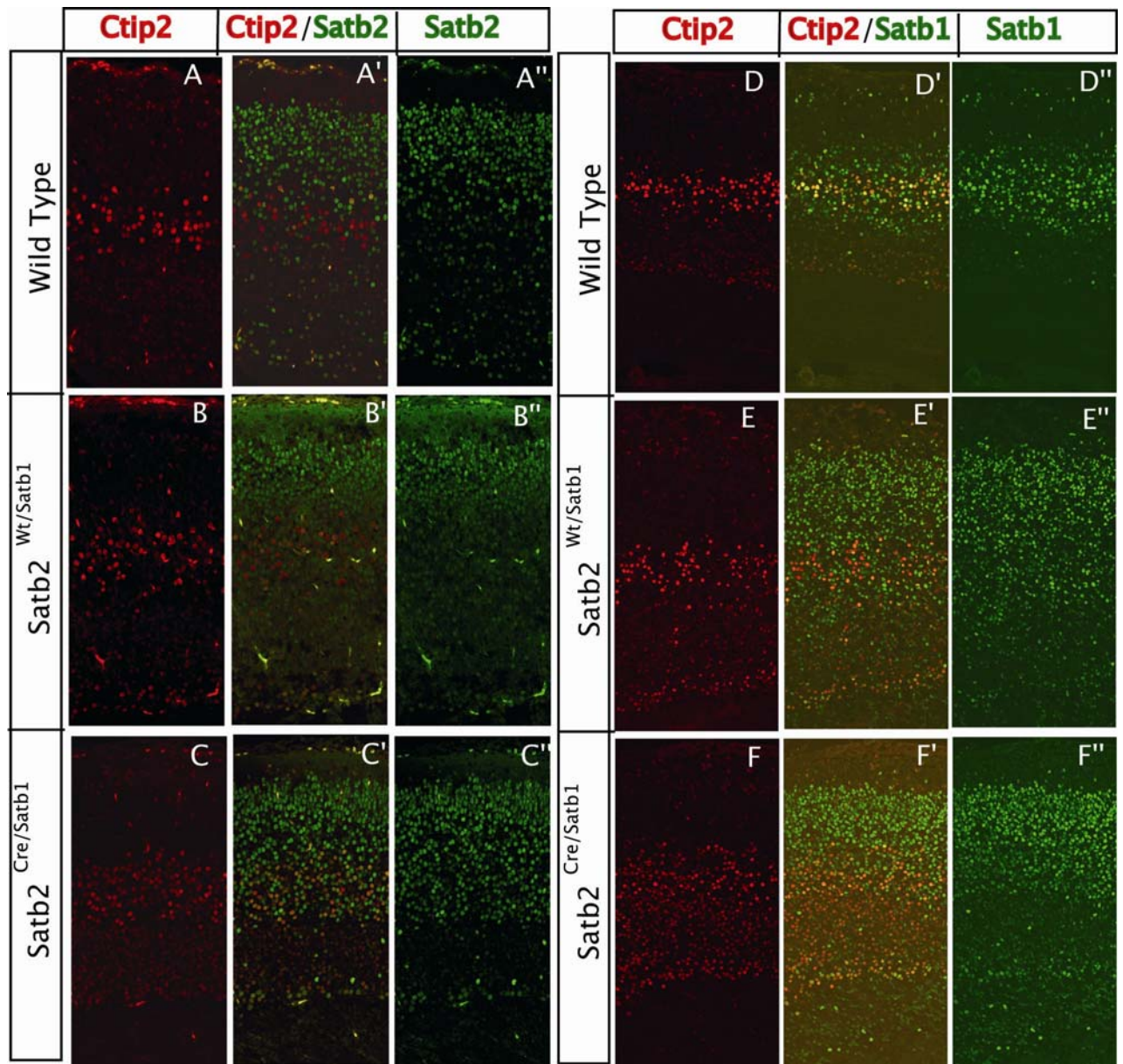
FIG.20 Satb1 and Satb2 expression related with Ctip2.

There is an increase in the number of cells expressing both Satb2 and Ctip2 genes in *Satb2*[Cre/Satb1] (C) in comparison with the Wt (A) and *Satb2*[Wt/Satb1] (B). Upper layers of the cortex are more sensitive than the deep layers to Satb2 dosage as evidenced by Ctip2 expression (A-C, D-F). Satb1 does not have an effect in Ctip2 expression (D-F).

FIG.21.Triple colocalization between Satb1, Satb2 and Ctip2.
Satb1, Satb2 and Ctip2 expression in Wt (A), *Satb2*[Wt/Satb1] (C) and *Satb2*[Cre/Satb1] (D). 63x magnification of Wt cortex. Arrowheads indicate that cells that colocalize Satb2 and Ctip2 and also express Satb1 (B´´´).

Virtually all Satb1+ cells did coexpress Ctip2 in the wild type, and this population of cells increased in *Satb2*$^{Wt/Satb1}$ and in *Satb2*$^{Cre/Satb1}$. Moreover, the upper layers of the cortex seem to be more sensitive to Satb2 dosage than the 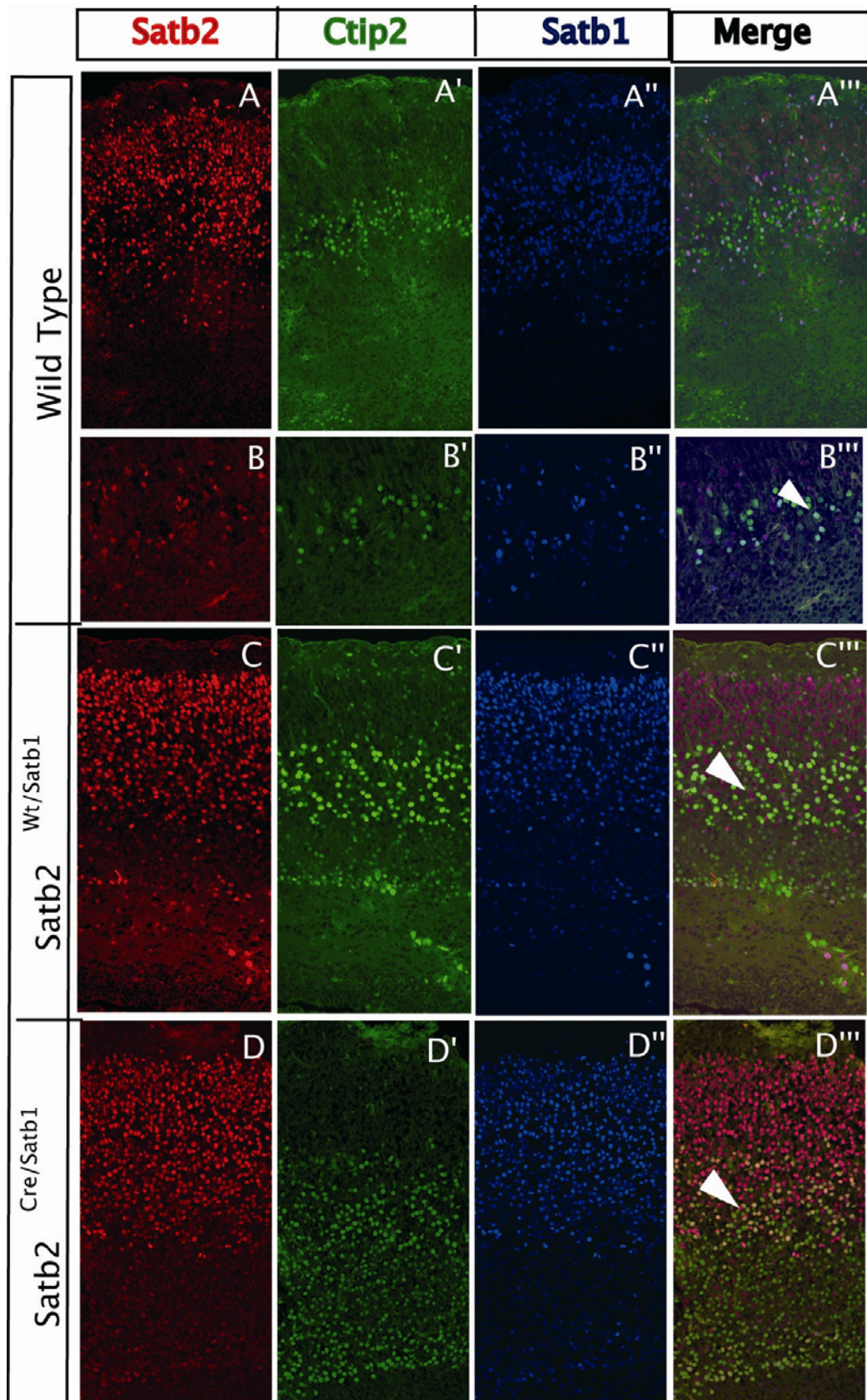deep layers (Fig.20D-F). Finally a triple IHC with Satb1, Satb2 and Ctip2 antibodies was performed in order to see if the cells coexpressing Satb1 and Satb2 are the ones that can not repress Ctip2 expression.

Analysis of the Wt brains reveals that almost all cells expressing both Satb1 and Satb2 did not inactivate Ctip2 expression (Fig21 A).

This data together with the fact that Satb1-Satb2 seems to form heterodimers (data not shown) suggest the possibility that these complexes may not activate transcription of Satb2 target genes.

4.12.2 Satb1 ectopic expression affects expression of Tbr 1 but not Sip1 or Brn2.

The expression of several layer-specific genes that were affected by *Satb2* deletion was analyzed. *Sip1, Tbr1, Brn2* expression was analyzed by IHC in order to determine whether the ectopic expression of *Satb1* under Satb2 promoter affects cell type specific genetic programs in the developing neocortex.

No significant differences were found in the number and distribution of Brn2+ cells in *Satb2*$^{Wt/Satb1}$ and *Satb2*$^{Cre/Satb1}$ whereas Sip1 expression seems to be reduced in the most upper part of the UL in both. Tbr1 is the gene most affected, with a severe reduction in the number of cells in *Satb2*$^{Wt/Satb1}$ brains and complete absence of expression in the case of *Satb2*$^{Cre/Satb1}$ mutant brains (Fig.22). These results suggest that Satb1 overexpression in Satb2+ cells alone can not inactivate genetic program of early UL neurons, but in combination with Satb2 dosage reduction it can affect Tbr1 expression in UL.
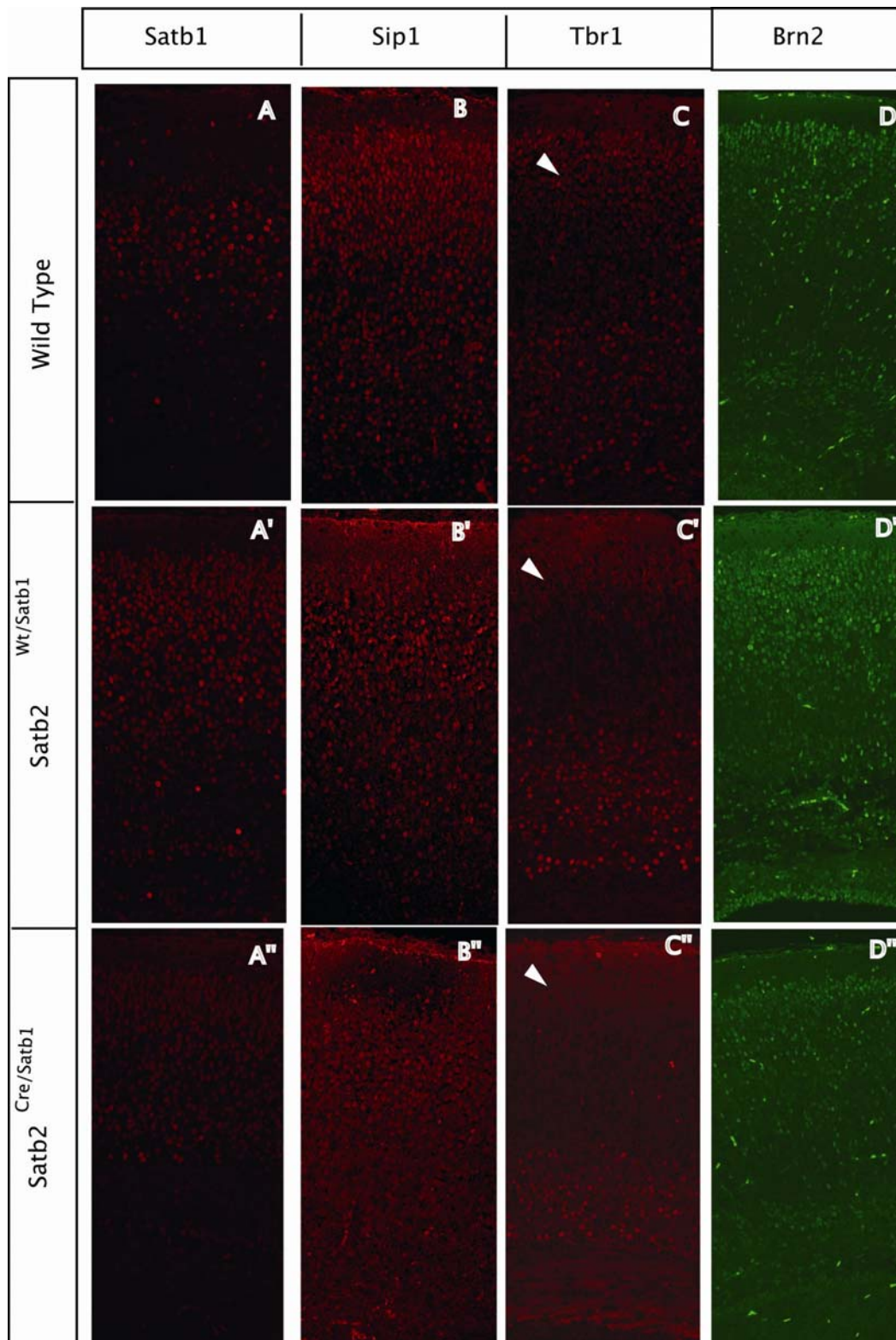
FIG.22 Tbr1 expression is affected in *Satb2*[Cre/Satb1]
Sip1 expression is reduced in most upper part of UL (B) in both *Satb2*[Wt/Satb1] (B') and *Satb2*[Cre/Satb1] (B''). Tbr 1 expression is abolish in *Satb2*[Cre/Satb1] (C''). Brn2 is not affected (D).

4.13 TSA treatment induces changes in Ctip2 expression in cultured cortical cells.

It is well established that histone modifications influence chromatin state and genome functions, generating synergistic or antagonistic interaction affinities for chromatin-associated proteins (Jenuwein and Allis, 2001). One of the most studied modifications is the deacetylation of lysines in the core histones, which is performed by histone deacetylases (HDACs). The most potent of the known histone deacetylase inhibitors (HDACIs) is trichostatin A (TSA), which belongs to the group of hydroxamic acids and is active at nanomolar concentrations *in vitro*. In order to investigate if expression of Ctip2 was repressed by Satb2 with the assistance of HDACs, *in vitro* experiments were performed. Cortical cells were first dissociated and plated on coverslips in order to establish the ideal concentration of cells for TSA treatment. After establishing that 0.8 million cells was a concentration sufficient to start any treatment, different concentration of TSA were applied at different time points (6h, 12h 24 h) at different embryonic stages (E14.5, E16.5, E18.5, P2). Finally the actual experiment was done at embryonic stage E18.5, during 24 h and with increasing concentration of TSA. In control coverslips several cells expressing Satb2 but not Ctip2 could be identified. After treatment with low dosage of TSA all cells started to express both proteins. High dosage of TSA resulted in a coexpression in an exclusive manner of Satb 2 and Ctip2 (Fig.23). However, spatially within the nucleus of such a cells, they can be detected in mutually exclusive domains.

A very strong and rapid enhancement of acetylated forms of H4 at the nuclear periphery is observed with a wide range of doses of (HDACIs) applied on a variety of cell types (Taddei et al., 1999). Pericentric heterochromatin in cycling cells is specifically responsive to prolonged treatment with HDACIs. At low doses, these defined regions relocate to the nuclear periphery and lose their properties of retaining heterochromatin protein 1 (HP1) proteins, which are spread throughout the nucleoplasm. Intriguingly, such an effect on centromere nuclear localization is not observed when the HDACI trichostatin A (TSA) is used for a short time or at high doses on non-proliferating cells (Gilchrist et al., 2004).

The acetylation state of a chromatin locus results from the antagonist activities of histone acetyltransferases (HATs) and histone deacetylases (HDACs) on pre-existing

nucleosomes. These two activities are locally regulated. Indeed, inhibiting deacetylases by trichostatin A (TSA) stabilizes the acetylation state of histone H4 in euchromatin regions with a very strong efficiency at the nuclear periphery, whereas it has no effect on heterochromatin regions (Taddei et al., 1999).

The concentration of parental histones must be diluted to generate a visible effect on the nuclear organization of pericentric heterochromatin regions. The use of HDACIs at high concentration (100 nM) prevents this by inducing immediate cell-cycle arrest on proliferating cells, and is not observed at all on quiescent cells (Gilchrist et al., 2004) This data suggest that, TSA has an effect on the regulation of Ctip2 by Satb2, but it is not clear if it is a direct interaction.
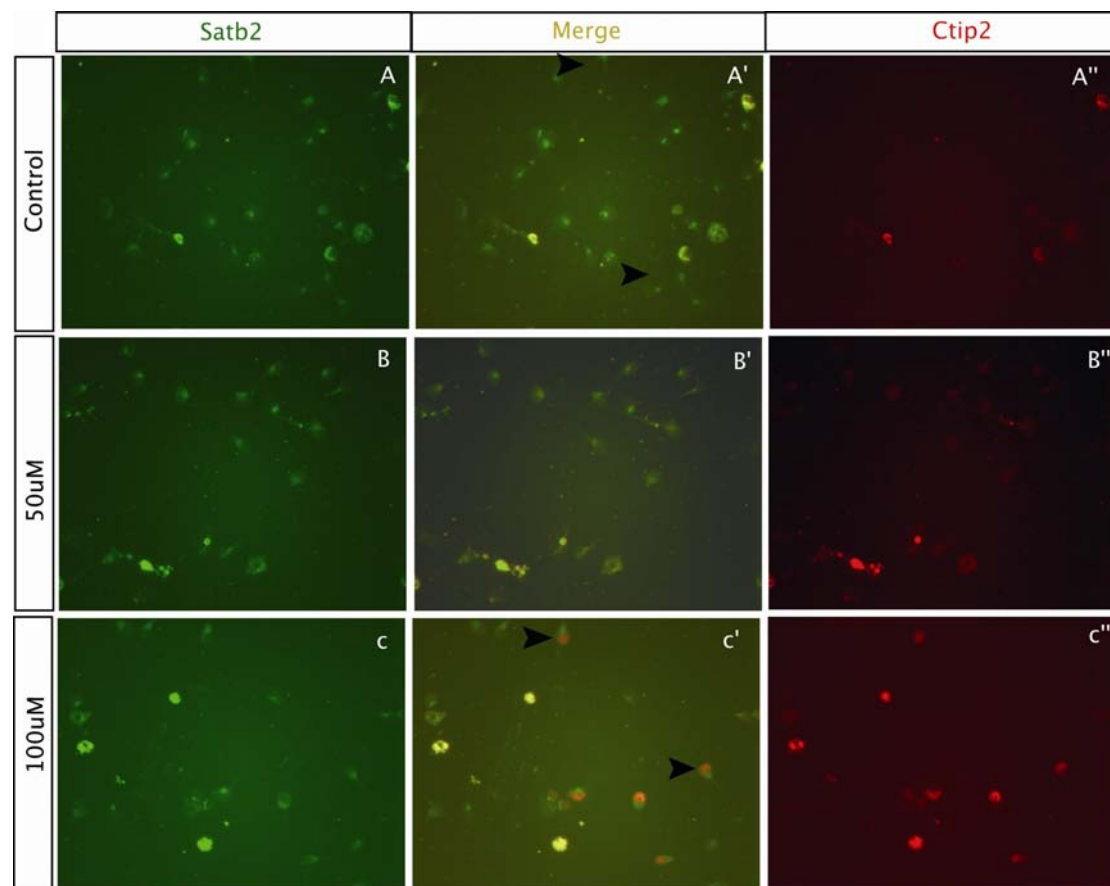
FIG 23. TSA treatment in Cortical Cells Affects Ctip2 regulation by Satb2
Immunocitochemistry with Satb2 (A-C) and Ctip2 (A''-C'') in cells treated with increasing TSA dosage. A' arrowheads shows cells that express Satb2 but not Ctip2 in wt cells without TSA treatment. C'' arrowheads point cells were the nucleus was compartmentalized due to an excess of TSA. In this cells Satb2 and Ctip2 coexpress but do not colocalizes in the nucleus.

4.14 Satb2 expression in DL cells induces Ctip2 down-regulation and impairs development of cortico-spinal tract.

Ex vivo electroporation approach was applied with the help of Manuela Schwark in order to study the effect of ectopic expression of *Satb2* in DL cells. In these experiments, Satb2 expressing plasmid was electroporated together with GFP plasmid into E13.5 lateral ventricles in "whole head" preparations. Electroporated brains were sectioned and slices were incubated for two or three days. Most GFP+ cells activated Satb2 expression (data not shown). The expression of Ctip2 was monitored in GFP expressing cells (Figure 24A and 24B), we found that ectopic Satb2 expression had a strong effect on Ctip2 as evident from the fact that only 12% of GFP-positive cells coexpressed Ctip2. In contrast, 55% of GFP-positive cells were found to express Ctip2 in control experiments where only GFP plasmid was electroporated.
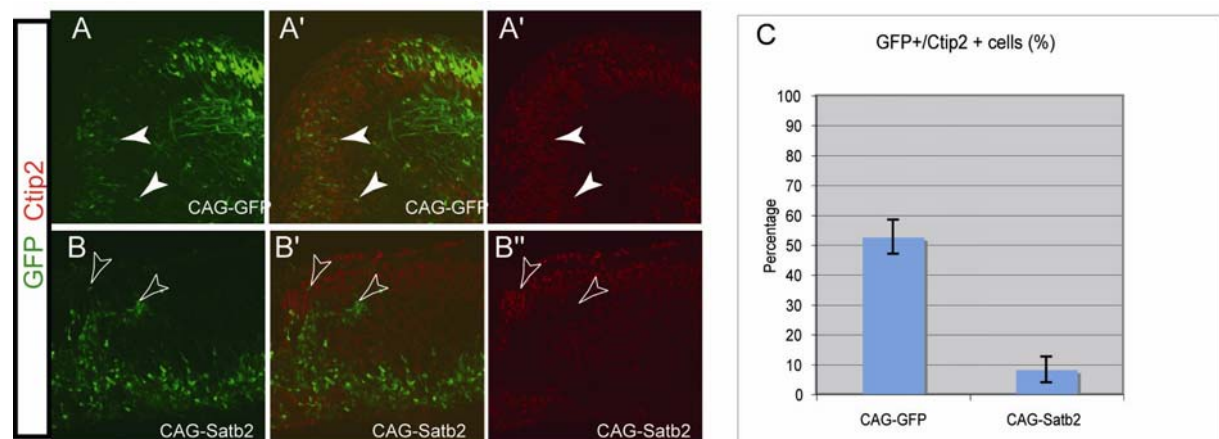

FIG 24. Overexpression of Satb2 inhibits Ctip2 expression and impairs the formation of corticospinal connections.
(A) GFP and Ctip2 (white arrowheads) coexpress on GFP-control brain slices electroporated at E13.5 (B) However, Ctip2 is not expressed in GFP+ cells that have been transfected with Satb2/GFP (empty arrowheads).

4.15 Satb2 interacts with both *Ctip2* promoter and histone deacetylase complex and controls chromatin remodeling.

Satb1, the closest homologue of Satb2, was shown to interact with specialized AT-rich DNA sequences (MARs/SARs and BURs) and controls the expression of multiple genes (Alvarez et al., 2000; Cai et al., 2003; de Belle et al., 1998; Yasui et al., 2002). It has been shown that in the cortex Satb2 is part of a protein complex that can interact with different MAR and AT-rich DNA sequences in vitro(Britanova et al., 2005; Szemes et al., 2006). Therefore, DNA sequences that can be recognized by Satb2-containing protein complex were investigated in the *Ctip2* genomic locus. Computer algorithm MAR-Wiz (http://www.futuresoft.org/MAR-Wiz) and SMARTest (http://www.genomatix.de/products/SMARTest/) were used to predict MARs in the vicinity of *Ctip2* transcription start site. Both programs revealed a single region located 3500 bp upstream of the *Ctip2* transcription start site. In experiments done by Olga Britanova, this DNA fragment was amplified by PCR, radioactively labeled, and subjected to a binding reaction with nuclear proteins extracted from E17.5 cortical cells. This assay resulted in a DNA mobility shift, indicating that there is a protein complex in cortical cells capable of interacting with the sequence. Addition of an unlabeled MAR DNA fragment in a concentration-dependent manner marred the appearance of this band, confirming the specificity of the DNA/protein interaction. Inclusion of an anti-Satb2-specific antibody in the DNA mobility shift assay ''supershifted'' the specific band (Figure 24B). Chromatin immunoprecipitation assay (ChIP) using a anti-Satb2 antibody was done by our collaborators Andrea Gyorgy and Denis Agoston, in order to confirm this interaction in vivo. A Satb2 protein/Ctip2 DNA complex was detected by semiquantitative PCR with several pairs of primers complementary to sites within 10 kb of the *Ctip2* upstream region. ChIP assay demonstrated that Satb2 protein binds within 3.5 kb upstream region of the *Ctip2* transcription start. However, this antibody failed to precipitate any DNA from *Satb2* mutant tissue (Figure 24C). We applied a similar approach to ask whether chromatin remodelling at the *Ctip2* locus was affected in the *Satb2*[Cre/Cre]mice. Using ChIP with antibodies specifically recognizing acetylated or methylated forms of histone H4, a strong hyperacetylation was demonstrated in *Ctip2* locus in cortical cells of *Satb2*[Cre/Cre]. In contrast, the level of H4 methylation of *Ctip2* locus did not

seem to be changed (Figure 24C). Satb1 has been shown to interact with components of the NURD chromatin remodelling complex (Yasui et al., 2002). We therefore immunoprecipitated nuclear proteins isolated from E18 rat cerebral cortex with a Satb2-specific antibody in order to detect possible binding of Satb2 to the NURD complex. The experiment was done using rather cerebral cortex to enable easier isolation of sufficient quantities of cortical tissue. Interaction of Satb2 with two members of the NURD complex, histone deacetylases HDAC1 and MTA2, was specifically tested using a coimmunoprecipitation assay. Immunoblots performed by Kenneth Y. Kwan showed that both MTA2 and HDAC1 are coprecipitated with Satb2 in the presence of anti Satb2 antibody (Figure 24 D). As no Satb2, HDAC1, or MTA2 immunoreactivity was detected when using the control antibody, these experiments indicate that, in the developing cortex, Satb2 interacts with HDAC1 and MTA2. Occupancy of HDAC1 and MTA2 at *Ctip2* locus in both wild-type and mutant P0 brains was then analyzed, in order to investigate whether the NURD chromatin remodelling complex interacted with the *Ctip2* locus and whether this interaction was affected by a *Satb2* deletion. ChIP experiments with HDAC1 and MTA2 antibodies revealed that both proteins interact with the *Ctip2* locus. Importantly, the interaction was substantially reduced (3- to 6-fold) although not completely abolished in *Satb2*$^{Cre/Cre}$ mice (Figure18A, F). This *in vivo* interaction is specific, since the negative control region (GAPDH) was not amplified from samples precipitated with either of the antibodies, but only from non-immunoprecipitated positive (input) control. There was no difference between *Satb2*$^{Cre/Cre}$ mice and the wild-type samples in this region. It is worth mentioning that in all ChIP experiments the entire cortex was used. Such samples also contain many cells that did not express Satb2. This suggests that differences in acetylation and NURD complex occupancy of the *Ctip2* locus specifically in UL cells are substantially higher than we detected. Together, these data strongly suggested that Ctip2 is a direct target of Satb2 in the developing neocortex and that Satb2 downregulates Ctip2 expression via the assembly of a NURD chromatin remodelling complex at the *Ctip2* locus.
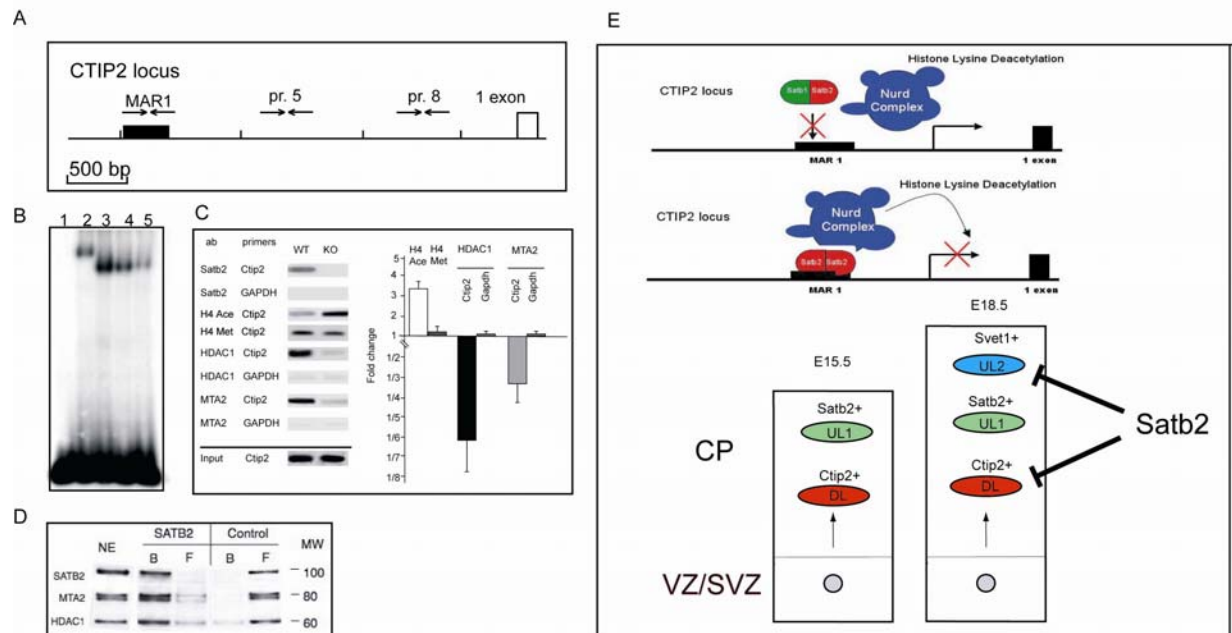
FIG 24. (A–D) Satb2 protein interacts with both the region upstream toCtip2 promoter upstream region and histone deacetylase complex and controls chromatin remodelling. (A) Position of putative Matrix Attachment Region (MAR, black box) within Ctip2 upstream region. Arrows show the location of PCR primers for ChIP experiments. (B) Interaction of Satb2-containing protein complex with MAR DNA from Ctip2 genomic locus in vitro. Gel mobility shift assay with radiolabeled MAR and nuclear protein extract isolated from E17.5 neocortex. Lane 1: DNA sample without nuclear protein. Lane 2: binding reaction with anti-Satb2 antibody and nuclear extract. Lane 3: binding reaction with nuclear extract but without antibody against Satb2. Lanes 4 and 5: same as lane 3 with increasing amount (50 and 200 ng) of specific unlabeled competitor DNA without Satb2 antibody. (C) Semiquantitative chromatin immunoprecipitation (ChIP) with Ctip2 locus DNA. ChIP assay was performed using whole-brain or cortical tissue from P0 WT or $Satb2^{Cre/Cre}$ brains. An _500 bp DNA fragment containing upstream part of Ctip2 DNA region (primer pair MAR1) or a negative control region (GAPDH) was amplified from samples that were immunoprecipitated with anti-SATB2, anti-HDAC1, anti-MTA2 as well as with antibodies against acetylated (H4 Ace) or methylated (H4 Met) forms of histone H4, or normal rabbit serum as a negative control (data not shown). Left part of (C) shows gel images of semiquantitative PCR; right part of (C) shows quantification of fold changes for ChIP with H4 Ace, H4 Met, HDAC, and MTA2 antibodies. (D) Satb2 binds both HDAC1 and MTA2 in vivo. Nuclear extracts (NE) from the E18 rat cortex were immunoprecipitated using either anti-Satb2 or control antibodies. Following immunoprecipitation, bound (B) and free (F) fractions were separated on gels and analyzed by immunoblotting using antibodies specific to Satb2, HDAC1, and MTA2. The positions of Satb2, MTA2, and HDAC1 immunoreactive bands are marked on the left. Molecular weight (MW) is shown in kDa on the right side.

(E) Model of Satb1 and Satb2 function in the cortical lamination. Satb2 is required to assemble NURD chromatin remodeling complex on Ctip2 locus. This induces deacetylation of histones and inactivation of Ctip2 expression but when its form heterodimers with Satb1 Ctip2 is not repressed. There are three major subpopulations of neocortical neurons: DL neurons express Ctip2, some of them also coexpress Satb2; UL1 neurons express Satb2 but not Ctip2; UL2 neurons express Svet1 but not Satb2. Satb2 inhibits UL2 and DL genetic programs.

5. Discussion

5.1. Satb2 is required for cell-type specification of UL neurons in the neocortex.

Satb2-deficient UL neurons upregulate expression of at least two transcription factors, Ctip2 and Nurr1, which are normally only expressed by DL neurons. Presence of Satb2 and Ctip2 is mutually exclusive in most neocortical cells at the time when they start to establish connections with other neurons. However, there are some Satb2-expressing cells that coexpress Ctip2. These double-positive cells seem to be the oldest Satb2+ cells in the cortex. Our data suggest that these cells also contain Satb1, offering the possibility of formation of Satb1- Satb2 heterodimers that may not be able to repress Ctip2 expression anymore. We have shown that almost all cells in *Satb2*$^{Cre/Cre}$ mice that have lost their normal expression of Satb2 activate Ctip2 ectopically, implying that Satb2 is a negative regulator of Ctip2. On the other hand, Satb1 has no effect on Ctip2 expression. Interestingly, cells that escape Satb2 inactivation do not activate Ctip2 expression, while cells that expressed Satb2 ectopically in our electroporation experiments failed to turn on Ctip2 expression. These results indicate that Satb2 controls Ctip2 expression in a cell autonomous fashion. The transcription factor Sip1 that is expressed in both UL and DL neurons, acts downstream of Satb2 in UL neurons. Downregulation of Sip1 in UL but not DL neurons in *Satb2*$^{Cre/Cre}$ suggests that Satb2 is required for Sip1 expression in UL neurons. This seems to be mediated through a cell-autonomous regulatory mechanism, since expression of Sip1 was maintained in those cells of the upper layers that did not inactivate Satb2

The expression of Satb1 ectopically in Satb2 expressing cells does not completely compensate for Satb2 function in the maintenance of UL genetic program. Experiments with *Satb2*$^{Cre/Satb1}$ did not reveal any major changes in Sip 1 and Brn2 expression, although Tbr1+ subpopulation of UL cells seems to be abolished as in *Satb2*$^{Cre/Cre}$ while Ctip2 shows an increase in expression in DL neurons. *Satb2*$^{Wt/Satb1}$ showed milder phenotype or no changes at all when compared to *Satb2*$^{Cre/Satb1}$. These data suggest that Tbr1 and Ctip2 are more sensitive to Satb2, and that the defects

caused due to reduction in Satb2 expression can not be fully compensated for by Satb1.

5.2 Satb2 deletion leads to misrouting of UL projections to the internal capsule and cerebral peduncle.

Satb2-deficient UL neurons failed to form the corpus callosum, a major fiber tract that interconnects UL neurons between the cerebral hemispheres, some of this neurons send their axons towards the cerebral peduncle, a feature normally associated exclusively with layer 5 neurons. We have also shown an increase in the thickness of the anterior commissure, another bundle of fibers interconnecting the two hemispheres, in *Satb2*$^{Cre/Cre}$. As shown in the DiI tract labelling experiment performed with the help of Amanda Cheung, this could be due to a misrouting of c.c fibers towards the a.c from a more dorsal region of the cortex (e.g., from parietal and frontal cortical areas). The absence of Probst bundles can be explained by a reduction in the number of callosal axons that arrive at the midline. Moreover, Satb2 deficient mice display a caudalization phenotype, as evident in the present of axons at more posterior levels. We have shown that Satb2 influences the expression of several axonal guidance molecules of the Eph/ephrins family. It has been reported in ephrinA5/EphA4 DKOs that deletion of these two genes leads to a caudalization of TC axons (Dufour et al., 2003). This data prompted us to hypothesize that the caudalization of TC fibers in Satb2 deficient mice is due to a reduction in EphA4 and ephrin A5 expression.

It has been shown that Ctip2-deficient layer 5 neurons fail to extend projections to the spinal cord (Arlotta et al., 2005). Ctip2 is not expressed in callosal neurons; therefore, ectopic activation of Ctip2 in UL neurons of *Satb2*$^{Cre/Cre}$ mice may be the major reason for the misrouting of UL projections to the internal capsule and cerebral peduncle. Analysis of axonal projections of Satb2-positive cells shows those not only do most callosally projecting cells but also many cells projecting to the anterior commissure, as well as to internal and external capsules, express Satb2. Conversely, spinal cord projecting neurons did not express Satb2. We conclude that Satb2 is necessary for callosal connections, as its deletion results in rerouting of callosal axons toward the anterior commissure, but does not prevent axons from going toward the

internal capsule, the anterior commissure, or the external capsule. However, we can not rule out the possibility that the increase in the number of anterior commissure axons in $Satb2^{Cre/Cre}$ mice is a secondary, non-cell-autonomous effect of Satb2 ablation.

$Satb2^{Cre/Satb1}$ mice do not show a severe axonal misrouting. All major fiber tracts are present although there is a reduction in the size of C.C that wasn't observed in $Satb2^{Wt/Cre}$ indicating that Satb1 does not play a role in axonal connectivity.

5.3 Role of Satb2 in cortical lamination.

Our findings that Satb2 protein is not detected in young neurons for at least 9 hr after exit from the mitotic cycle and deletion of such a late postmitotic gene leads to maintenance of some aspects of DL laminar fate are surprising. It suggests that aspects of laminar fate, such as the specificity of connections, are not terminally determined at the level of progenitors, but rather at the level of postmitotic neurons. Moreover, CP neurons might have the potential to maintain some characteristics of both DL and UL longer than presently thought. This finding is unexpected because it has been shown that the decision on whether a cell becomes a UL or DL neuron is taken at the time of the terminal mitotic division, and UL progenitors cannot generate DL neurons (Desai and McConnell, 2000).

5.4 Satb2 affects migration of cortical neurons.

Many Satb2-deficient UL neurons failed to migrate into their normal superficial location and settled instead within the DL territory while the migration of DL neurons does not seem to be affected in $Satb2^{Cre/Cre}$ mutants. This data indicates that the effect of Satb2 on migration is cell-autonomous.

The differences in the position of DL neurons (cells labeled by BrdU at E13.5) between WT and $Satb2^{Cre/Cre}$ brains most probably reflect the fact that the migration of later-born UL neurons is affected. In fact, when later-born UL cells fail to migrate past early-born DL neurons, DL neurons end up occupying more superficial positions. However, it is not clear whether abnormal migration of UL neurons in $Satb2^{Cre/Cre}$ mice is due to a general delay of migration of UL cells or to mistargeted migration

into deep layers. The expression of Brn1 and Brn2, transcription factors that have been shown to control migration of UL neurons, was not affected by Satb2 deletion. Interestingly, migration of UL neurons as well as expression of Brn2 was not very much affected in $Satb2^{Cre/Satb1}$. These data suggest that ectopic expression of Satb1 may be able to rescue the defective migration seen in $Satb2^{Cre/Cre}$

5.5. Craniofacial dysmorfologies in $Satb2^{Cre/Satb1}$ mice

It has been shown that $Satb2^{Cre/Cre}$ mice displays several craniofacial abnormalities (Britanova et al., 2006b). It seems that $Satb2^{Cre/Satb1}$ partially display a similar phenotype. Morphological analysis of $Satb2^{Cre/Satb1}$ mice revealed that they show a stronger phenotype that the one seen in $Satb2^{Wt/Cre}$ mice. We observed microcephaly, hipodontia and defects in molar dental buds and the incisors in the $Satb2^{Cre/Satb1}$ mice. Generally all midline structures connected with the upper and lower arcades such as septal cartilages and parasagital elements are reduced and the animals display cleft palate.

These data indicate that Satb1 cannot fully rescue the function of Satb2 in the jaw and palate development, even though it is expressed in the same regions of the branchial arches.

5.6 Satb2 protein interacts with the NuRD complex.

Satb2, as its homolog Satb1, can interact with HDAC1 and MTA2, members of the NuRD chromatin remodelling complex. The NuRD complex deacetylates histones in its vicinity, converting the chromatin to an inactivate state. Satb2 deletion leads to hyperacetylation of the Ctip2 locus and decreases HDAC1 and MTA2 levels at this locus. Moreover, we have shown that Satb2 can interact with a MAR region at the Ctip2 locus. These results strongly suggest that Satb2 is required to recruit the NuRD complex to the Ctip2 locus in order to repress its expression.

5.7 Satb2 is required to initiate UL1-specific genetic program and repress Ctip2 expression.

Expression analysis of *Satb2*^{Cre/Cre} mice indicates that, even if UL neurons in *Satb2*^{Cre/Cre} cortex lose their UL identity, they do not change completely into DL neurons as evident from the finding that early UL neurons in *Satb2*^{Cre/Cre} mutants activate Svet1 expression. Our data indicate that there are at least two distinct UL subpopulations. One subpopulation, which we term ''UL1,'' is mostly born between E14.5 and E15.5 and expresses Satb2. UL1 cells do not seem to reside in the SVZ for a long time, as we detected many of these cells in the CP as early as E14.5. Another subpopulation, ''UL2,'' expresses Svet1. UL2 cells were first detected at E13.5 in the SVZ, but seem to stay several days at this location before migrating to the CP at E17.5 (Tarabykin et al., 2001). Colocalization experiments demonstrate that the expression of Svet1 and Satb2 is mutually exclusive in the CP. However, it is possible that Satb2 cells express Svet1 in the SVZ but downregulate it before starting their migration. In *Satb2*^{Cre/Cre} mice, Svet1 expression is ectopically activated in the CP as early as E15.5 and is very strong at E17.5 although it was not possible to colocalize Svet1 and Satb2 in the mutant brains, it is more likely that there is ectopic activation of Svet1 expression in cells lacking Satb2 rather than premature migration of Svet1-expressing cells from the SVZ towards CP. BrdU pulse experiments support the idea that there is a delay rather than acceleration in the migration of UL neurons and rule out the possibility of premature migration.

Satb2-deficient UL1 neurons represent a mixed identity as evident from its upregulation of both DL- and UL2-specific gene expression. On the other hand, Satb2 is required to suppress other ''non-Satb2+'' cortical cell fates. In summary, our data suggest that Satb2 is a crucial mediator for the specification of UL1 neurons. It is required to initiate UL1-specific genetic program and to inactivate the expression of DL- and UL2-specific genes. Our data also suggest that, at the molecular level, Satb2 is required to assemble the NuRD chromatin remodelling complex in order to prevent expression of DL-specific genes in UL of the cortex.

6. Conclusions

In the current study we investigated the role of Satb1 and Satb2 in the developing neocortex. Molecular analysis shows that Satb1 is mostly expressed in a subpopulation of Satb2 expressing cells in the cortex whereas Satb2, Svet1 and Ctip2 are expressed in different cell types.

Our work also shows that the lack of Satb2 leads to abnormal cell migration as well as cortical connectivity. Corpus callosum and anterior commissure are the structures more affected implicating a role of Satb2 in axonal connectivity. *Satb2*^{Cre/Satb1} animals show a partial restoration of the axonal tracts but we can not rule out the possibility that it is due to the residual Satb2 expression still present in this kind of mice.

The craniofacial abnormalities observed in *Satb2*^{Cre/Cre} mice are still present in *Satb2*^{Cre/Satb1} animals, but the degree of malformation is reduced as compared to *Satb2*^{Cre/Cre} animals. However, the phenotype is more severe than the one observed in *Satb2*^{Wt/Cre} animals indicating that overexpression of Satb1 in the branchial arches does not completely rescue the craniofacial abnormalities observed in the Satb2 knockouts.

Also, in *Satb2*^{Cre/Cre} mice, cortical expression of genes like Ctip2, Tbr1, Sip1 and Brn2 is affected, suggesting a role for Satb2 in the specification of laminar cell type identity. Our data also indicates that the ectopic expression of Satb1 under Satb2 promoter cannot fully compensate for Satb2 function in cortical lamination.

We observed a dramatic upregulation of Ctip2 (a gene that plays a crucial role in specifying the identity of corticospinal neurons) in cells where Satb2 was ablated. We used several biochemical approaches in order to show the direct interaction of Satb2 with a MAR situated 3.500 bp away from exon 1 of *Ctip2* gene. Moreover, we could prove the direct interaction of Satb2 with MT1 and HDAC1, two of the components of the histone deacetylase complex, NuRD. Therefore, we conclude that Ctip2 is a direct downstream target of Satb2 and that Satb2 represses Ctip2 expression by assembling the NURD chromatin remodelling complex at Ctip2 locus. Our findings also suggest the possibility that Satb1 and Satb2 form heterodimers that may not activate transcription of Satb2 target genes, as evident from the inability of Satb2 to repress Ctip2 in cells coexpressing Satb1.

We believe that Satb2 is a crucial mediator for specification of a subclass of UL neurons (UL1) and is required to initiate the UL1-specific genetic program and repress the expression of DL and UL2 specific genes.

7. References

Agoston, D. V., and Dobi, A. (2000). Complexity of transcriptional control in neuropeptide gene expression; enkephalin gene regulation during neurodevelopment. Biochem Soc Trans *28*, 446-451.

Alvarez, J. D., Yasui, D. H., Niida, H., Joh, T., Loh, D. Y., and Kohwi-Shigematsu, T. (2000). The MAR-binding protein SATB1 orchestrates temporal and spatial expression of multiple genes during T-cell development. Genes Dev *14*, 521-535.

Allendoerfer, K. L., and Shatz, C. J. (1994). The subplate, a transient neocortical structure: its role in the development of connections between thalamus and cortex. Annu Rev Neurosci *17*, 185-218.

Andres, V., Nadal-Ginard, B., and Mahdavi, V. (1992). Clox, a mammalian homeobox gene related to Drosophila cut, encodes DNA-binding regulatory proteins differentially expressed during development. Development *116*, 321-334.

Angevine, J. B., Jr., and Sidman, R. L. (1961). Autoradiographic study of cell migration during histogenesis of cerebral cortex in the mouse. Nature *192*, 766-768.

Arlotta, P., Molyneaux, B. J., Chen, J., Inoue, J., Kominami, R., and Macklis, J. D. (2005). Neuronal subtype-specific genes that control corticospinal motor neuron development in vivo. Neuron *45*, 207-221.

Avram, D., Fields, A., Pretty On Top, K., Nevrivy, D. J., Ishmael, J. E., and Leid, M. (2000). Isolation of a novel family of C(2)H(2) zinc finger proteins implicated in transcriptional repression mediated by chicken ovalbumin upstream promoter transcription factor (COUP-TF) orphan nuclear receptors. J Biol Chem *275*, 10315-10322.

Avram, D., Fields, A., Senawong, T., Topark-Ngarm, A., and Leid, M. (2002). COUP-TF (chicken ovalbumin upstream promoter transcription factor)-interacting protein 1 (CTIP1) is a sequence-specific DNA binding protein. Biochem J *368*, 555-563.

Beverdam, A., Brouwer, A., Reijnen, M., Korving, J., and Meijlink, F. (2001). Severe nasal clefting and abnormal embryonic apoptosis in Alx3/Alx4 double mutant mice. Development *128*, 3975-3986.

Blochlinger, K., Bodmer, R., Jack, J., Jan, L. Y., and Jan, Y. N. (1988). Primary structure and expression of a product from cut, a locus involved in specifying sensory organ identity in Drosophila. Nature *333*, 629-635.

Bode, J., Benham, C., Knopp, A., and Mielke, C. (2000). Transcriptional augmentation: modulation of gene expression by scaffold/matrix-attached regions (S/MAR elements). Crit Rev Eukaryot Gene Expr *10*, 73-90.

Bode, J., Kohwi, Y., Dickinson, L., Joh, T., Klehr, D., Mielke, C., and Kohwi-Shigematsu, T. (1992). Biological significance of unwinding capability of nuclear matrix-associating DNAs. Science *255*, 195-197.

Britanova, O., Akopov, S., Lukyanov, S., Gruss, P., and Tarabykin, V. (2005). Novel transcription factor Satb2 interacts with matrix attachment region DNA elements in a tissue-specific manner and demonstrates cell-type-dependent expression in the developing mouse CNS. Eur J Neurosci *21*, 658-668.

Britanova, O., Alifragis, P., Junek, S., Jones, K., Gruss, P., and Tarabykin, V. (2006a). A novel mode of tangential migration of cortical projection neurons. Dev Biol *298*, 299-311.

Britanova, O., de Juan Romero, C., Cheung, A., Kwan, K. Y., Schwark, M., Gyorgy, A., Vogel, T., Akopov, S., Mitkovski, M., Agoston, D., *et al.* (2008). Satb2 is a

postmitotic determinant for upper-layer neuron specification in the neocortex. Neuron *57*, 378-392.

Britanova, O., Depew, M. J., Schwark, M., Thomas, B. L., Miletich, I., Sharpe, P., and Tarabykin, V. (2006b). Satb2 Haploinsufficiency Phenocopies 2q32-q33 Deletions, whereas Loss Suggests a Fundamental Role in the Coordination of Jaw Development. Am J Hum Genet *79*, 668-678.

Cai, L., Hayes, N. L., Takahashi, T., Caviness, V. S., Jr., and Nowakowski, R. S. (2002). Size distribution of retrovirally marked lineages matches prediction from population measurements of cell cycle behavior. J Neurosci Res *69*, 731-744.

Cai, S., Han, H. J., and Kohwi-Shigematsu, T. (2003). Tissue-specific nuclear architecture and gene expression regulated by SATB1. Nat Genet *34*, 42-51.

Campbell, T. N., and Robbins, S. M. (2008). The Eph receptor/ephrin system: an emerging player in the invasion game. Curr Issues Mol Biol *10*, 61-66.

Casarosa, S., Fode, C., and Guillemot, F. (1999). Mash1 regulates neurogenesis in the ventral telencephalon. Development *126*, 525-534.

Caviness, V. S., Jr., Takahashi, T., and Nowakowski, R. S. (1995). Numbers, time and neocortical neuronogenesis: a general developmental and evolutionary model. Trends Neurosci *18*, 379-383.

Cockerill, P. N., and Garrard, W. T. (1986). Chromosomal loop anchorage sites appear to be evolutionarily conserved. FEBS Lett *204*, 5-7.

Coussens, A. K., Hughes, I. P., Wilkinson, C. R., Morris, C. P., Anderson, P. J., Powell, B. C., and van Daal, A. (2008). Identification of genes differentially expressed by prematurely fused human sutures using a novel in vivo - in vitro approach. Differentiation *76*, 531-545.

Chen, B., Schaevitz, L. R., and McConnell, S. K. (2005a). Fezl regulates the differentiation and axon targeting of layer 5 subcortical projection neurons in cerebral cortex. Proc Natl Acad Sci U S A *102*, 17184-17189.

Chen, Y., Zhang, T., Li, T., Han, W., Zhang, Y., and Ma, D. (2005b). Preparation and characterization of a monoclonal antibody against CKLF1 using DNA immunization with in vivo electroporation. Hybridoma (Larchmt) *24*, 305-308.

Chilton, J. K. (2006). Molecular mechanisms of axon guidance. Dev Biol *292*, 13-24.

de Belle, I., Cai, S., and Kohwi-Shigematsu, T. (1998). The genomic sequences bound to special AT-rich sequence-binding protein 1 (SATB1) in vivo in Jurkat T cells are tightly associated with the nuclear matrix at the bases of the chromatin loops. J Cell Biol *141*, 335-348.

De Carlos, J. A., and O'Leary, D. D. (1992). Growth and targeting of subplate axons and establishment of major cortical pathways. J Neurosci *12*, 1194-1211.

Denhardt, D. T. (1966). A membrane-filter technique for the detection of complementary DNA. Biochem Biophys Res Commun *23*, 641-646.

Dent, E. W., and Gertler, F. B. (2003). Cytoskeletal dynamics and transport in growth cone motility and axon guidance. Neuron *40*, 209-227.

Desai, A. R., and McConnell, S. K. (2000). Progressive restriction in fate potential by neural progenitors during cerebral cortical development. Development *127*, 2863-2872.

Dickinson, L. A., Joh, T., Kohwi, Y., and Kohwi-Shigematsu, T. (1992). A tissue-specific MAR/SAR DNA-binding protein with unusual binding site recognition. Cell *70*, 631-645.

Dietz, A., Kay, V., Schlake, T., Landsmann, J., and Bode, J. (1994). A plant scaffold attached region detected close to a T-DNA integration site is active in mammalian cells. Nucleic Acids Res *22*, 2744-2751.

Dobreva, G., Chahrour, M., Dautzenberg, M., Chirivella, L., Kanzler, B., Farinas, I., Karsenty, G., and Grosschedl, R. (2006). SATB2 is a multifunctional determinant of craniofacial patterning and osteoblast differentiation. Cell *125*, 971-986.

Dobreva, G., Dambacher, J., and Grosschedl, R. (2003). SUMO modification of a novel MAR-binding protein, SATB2, modulates immunoglobulin mu gene expression. Genes Dev *17*, 3048-3061.

Dufour, A., Seibt, J., Passante, L., Depaepe, V., Ciossek, T., Frisen, J., Kullander, K., Flanagan, J. G., Polleux, F., and Vanderhaeghen, P. (2003). Area specificity and topography of thalamocortical projections are controlled by ephrin/Eph genes. Neuron *39*, 453-465.

Earnshaw, W. C. (1988). Mitotic chromosome structure. Bioessays *9*, 147-150.

Englund, C., Fink, A., Lau, C., Pham, D., Daza, R. A., Bulfone, A., Kowalczyk, T., and Hevner, R. F. (2005). Pax6, Tbr2, and Tbr1 are expressed sequentially by radial glia, intermediate progenitor cells, and postmitotic neurons in developing neocortex. J Neurosci *25*, 247-251.

FitzPatrick, D. R., Carr, I. M., McLaren, L., Leek, J. P., Wightman, P., Williamson, K., Gautier, P., McGill, N., Hayward, C., Firth, H., *et al.* (2003). Identification of SATB2 as the cleft palate gene on 2q32-q33. Hum Mol Genet *12*, 2491-2501.

Freiman, R. N., and Tjian, R. (2003). Regulating the regulators: lysine modifications make their mark. Cell *112*, 11-17.

Fujita, N., Jaye, D. L., Geigerman, C., Akyildiz, A., Mooney, M. R., Boss, J. M., and Wade, P. A. (2004). MTA3 and the Mi-2/NuRD complex regulate cell fate during B lymphocyte differentiation. Cell *119*, 75-86.

Fukuda, T., Kawano, H., Ohyama, K., Li, H. P., Takeda, Y., Oohira, A., and Kawamura, K. (1997). Immunohistochemical localization of neurocan and L1 in the formation of thalamocortical pathway of developing rats. J Comp Neurol *382*, 141-152.

Galande, S., Dickinson, L. A., Mian, I. S., Sikorska, M., and Kohwi-Shigematsu, T. (2001). SATB1 cleavage by caspase 6 disrupts PDZ domain-mediated dimerization, causing detachment from chromatin early in T-cell apoptosis. Mol Cell Biol *21*, 5591-5604.

Gale, N. W., Holland, S. J., Valenzuela, D. M., Flenniken, A., Pan, L., Ryan, T. E., Henkemeyer, M., Strebhardt, K., Hirai, H., Wilkinson, D. G., *et al.* (1996). Eph receptors and ligands comprise two major specificity subclasses and are reciprocally compartmentalized during embryogenesis. Neuron *17*, 9-19.

Gasser, S. M., and Laemmli, U. K. (1987). Improved methods for the isolation of individual and clustered mitotic chromosomes. Exp Cell Res *173*, 85-98.

Ghosh, H. S., Spencer, J. V., Ng, B., McBurney, M. W., and Robbins, P. D. (2007). Sirt1 interacts with transducin-like enhancer of split-1 to inhibit nuclear factor kappaB-mediated transcription. Biochem J *408*, 105-111.

Gilchrist, S., Gilbert, N., Perry, P., and Bickmore, W. A. (2004). Nuclear organization of centromeric domains is not perturbed by inhibition of histone deacetylases. Chromosome Res *12*, 505-516.

Goldshmit, Y., McLenachan, S., and Turnley, A. (2006). Roles of Eph receptors and ephrins in the normal and damaged adult CNS. Brain Res Rev *52*, 327-345.

Gotz, M., and Barde, Y. A. (2005). Radial glial cells defined and major intermediates between embryonic stem cells and CNS neurons. Neuron *46*, 369-372.

Gyorgy, A. B., Szemes, M., de Juan Romero, C., Tarabykin, V., and Agoston, D. V. (2008). SATB2 interacts with chromatin-remodeling molecules in differentiating cortical neurons. Eur J Neurosci *27*, 865-873.

Han, H. J., Russo, J., Kohwi, Y., and Kohwi-Shigematsu, T. (2008). SATB1 reprogrammes gene expression to promote breast tumour growth and metastasis. Nature *452*, 187-193.

Harada, R., Dufort, D., Denis-Larose, C., and Nepveu, A. (1994). Conserved cut repeats in the human cut homeodomain protein function as DNA binding domains. J Biol Chem *269*, 2062-2067.

Haubensak, W., Attardo, A., Denk, W., and Huttner, W. B. (2004). Neurons arise in the basal neuroepithelium of the early mammalian telencephalon: a major site of neurogenesis. Proc Natl Acad Sci U S A *101*, 3196-3201.

Hawkins, S. M., Kohwi-Shigematsu, T., and Skalnik, D. G. (2001). The matrix attachment region-binding protein SATB1 interacts with multiple elements within the gp91phox promoter and is down-regulated during myeloid differentiation. J Biol Chem *276*, 44472-44480.

Heroult, M., Schaffner, F., and Augustin, H. G. (2006). Eph receptor and ephrin ligand-mediated interactions during angiogenesis and tumor progression. Exp Cell Res *312*, 642-650.

Hevner, R. F., Shi, L., Justice, N., Hsueh, Y., Sheng, M., Smiga, S., Bulfone, A., Goffinet, A. M., Campagnoni, A. T., and Rubenstein, J. L. (2001). Tbr1 regulates differentiation of the preplate and layer 6. Neuron *29*, 353-366.

Hong, W., Nakazawa, M., Chen, Y. Y., Kori, R., Vakoc, C. R., Rakowski, C., and Blobel, G. A. (2005). FOG-1 recruits the NuRD repressor complex to mediate transcriptional repression by GATA-1. Embo J *24*, 2367-2378.

Jaenisch, R., and Bird, A. (2003). Epigenetic regulation of gene expression: how the genome integrates intrinsic and environmental signals. Nat Genet *33 Suppl*, 245-254.

Jarman, A. P., and Higgs, D. R. (1988). Nuclear scaffold attachment sites in the human globin gene complexes. Embo J *7*, 3337-3344.

Jenuwein, T., and Allis, C. D. (2001). Translating the histone code. Science *293*, 1074-1080.

Jezewski, P. A., Vieira, A. R., Nishimura, C., Ludwig, B., Johnson, M., O'Brien, S. E., Daack-Hirsch, S., Schultz, R. E., Weber, A., Nepomucena, B., *et al.* (2003). Complete sequencing shows a role for MSX1 in non-syndromic cleft lip and palate. J Med Genet *40*, 399-407.

Kehle, J., Beuchle, D., Treuheit, S., Christen, B., Kennison, J. A., Bienz, M., and Muller, J. (1998). dMi-2, a hunchback-interacting protein that functions in polycomb repression. Science *282*, 1897-1900.

Kissinger, C. R., Liu, B. S., Martin-Blanco, E., Kornberg, T. B., and Pabo, C. O. (1990). Crystal structure of an engrailed homeodomain-DNA complex at 2.8 A resolution: a framework for understanding homeodomain-DNA interactions. Cell *63*, 579-590.

Klehr, D., Maass, K., and Bode, J. (1991). Scaffold-attached regions from the human interferon beta domain can be used to enhance the stable expression of genes under the control of various promoters. Biochemistry *30*, 1264-1270.

Koester, S. E., and O'Leary, D. D. (1993). Connectional distinction between callosal and subcortically projecting cortical neurons is determined prior to axon extension. Dev Biol *160*, 1-14.

Kohwi-Shigematsu, T., deBelle, I., Dickinson, L. A., Galande, S., and Kohwi, Y. (1998). Identification of base-unpairing region-binding proteins and characterization of their in vivo binding sequences. Methods Cell Biol *53*, 323-354.

Kohwi-Shigematsu, T., and Kohwi, Y. (1990). Torsional stress stabilizes extended base unpairing in suppressor sites flanking immunoglobulin heavy chain enhancer. Biochemistry *29*, 9551-9560.

Kohwi-Shigematsu, T., and Kohwi, Y. (1992). Detection of non-B-DNA structures at specific sites in supercoiled plasmid DNA and chromatin with haloacetaldehyde and diethyl pyrocarbonate. Methods Enzymol *212*, 155-180.

Kohwi-Shigematsu, T., Maass, K., and Bode, J. (1997). A thymocyte factor SATB1 suppresses transcription of stably integrated matrix-attachment region-linked reporter genes. Biochemistry *36*, 12005-12010.

Kullander, K., and Klein, R. (2002). Mechanisms and functions of Eph and ephrin signalling. Nat Rev Mol Cell Biol *3*, 475-486.

Kumar, P. P., Purbey, P. K., Ravi, D. S., Mitra, D., and Galande, S. (2005). Displacement of SATB1-bound histone deacetylase 1 corepressor by the human immunodeficiency virus type 1 transactivator induces expression of interleukin-2 and its receptor in T cells. Mol Cell Biol *25*, 1620-1633.

Lee, J., Klase, Z., Gao, X., Caldwell, J. S., Stinski, M. F., Kashanchi, F., and Chao, S. H. (2007). Cellular homeoproteins, SATB1 and CDP, bind to the unique region between the human cytomegalovirus UL127 and major immediate-early genes. Virology *366*, 117-125.

Leid, M., Ishmael, J. E., Avram, D., Shepherd, D., Fraulob, V., and Dolle, P. (2004). CTIP1 and CTIP2 are differentially expressed during mouse embryogenesis. Gene Expr Patterns *4*, 733-739.

Leonard, W. J., Depper, J. M., Crabtree, G. R., Rudikoff, S., Pumphrey, J., Robb, R. J., Kronke, M., Svetlik, P. B., Peffer, N. J., Waldmann, T. A., and et al. (1984). Molecular cloning and expression of cDNAs for the human interleukin-2 receptor. Nature *311*, 626-631.

Liu, J., Bramblett, D., Zhu, Q., Lozano, M., Kobayashi, R., Ross, S. R., and Dudley, J. P. (1997). The matrix attachment region-binding protein SATB1 participates in negative regulation of tissue-specific gene expression. Mol Cell Biol *17*, 5275-5287.

Luo, J., Su, F., Chen, D., Shiloh, A., and Gu, W. (2000). Deacetylation of p53 modulates its effect on cell growth and apoptosis. Nature *408*, 377-381.

Luskin, M. B., and Shatz, C. J. (1985). Studies of the earliest generated cells of the cat's visual cortex: cogeneration of subplate and marginal zones. J Neurosci *5*, 1062-1075.

Mackarehtschian, K., Lau, C. K., Caras, I., and McConnell, S. K. (1999). Regional differences in the developing cerebral cortex revealed by ephrin-A5 expression. Cereb Cortex *9*, 601-610.

Mallamaci, A., and Stoykova, A. (2006). Gene networks controlling early cerebral cortex arealization. Eur J Neurosci *23*, 847-856.

Marin, O., Plump, A. S., Flames, N., Sanchez-Camacho, C., Tessier-Lavigne, M., and Rubenstein, J. L. (2003). Directional guidance of interneuron migration to the cerebral cortex relies on subcortical Slit1/2-independent repulsion and cortical attraction. Development *130*, 1889-1901.

McConnell, S. K. (1995). Plasticity and commitment in the developing cerebral cortex. Prog Brain Res *105*, 129-143.

McConnell, S. K., and Kaznowski, C. E. (1991). Cell cycle dependence of laminar determination in developing neocortex. Science *254*, 282-285.

McEvilly, R. J., de Diaz, M. O., Schonemann, M. D., Hooshmand, F., and Rosenfeld, M. G. (2002). Transcriptional regulation of cortical neuron migration by POU domain factors. Science *295*, 1528-1532.

Mielke, C., Kohwi, Y., Kohwi-Shigematsu, T., and Bode, J. (1990). Hierarchical binding of DNA fragments derived from scaffold-attached regions: correlation of properties in vitro and function in vivo. Biochemistry *29*, 7475-7485.

Miquelajauregui, A., Van de Putte, T., Polyakov, A., Nityanandam, A., Boppana, S., Seuntjens, E., Karabinos, A., Higashi, Y., Huylebroeck, D., and Tarabykin, V. (2007). Smad-interacting protein-1 (Zfhx1b) acts upstream of Wnt signaling in the mouse hippocampus and controls its formation. Proc Natl Acad Sci U S A *104*, 12919-12924.

Miyata, T., Kawaguchi, A., Saito, K., Kawano, M., Muto, T., and Ogawa, M. (2004). Asymmetric production of surface-dividing and non-surface-dividing cortical progenitor cells. Development *131*, 3133-3145.

Molnar, Z., Lopez-Bendito, G., Small, J., Partridge, L. D., Blakemore, C., and Wilson, M. C. (2002). Normal development of embryonic thalamocortical connectivity in the absence of evoked synaptic activity. J Neurosci *22*, 10313-10323.

Molyneaux, B. J., Arlotta, P., and Macklis, J. D. (2007). Molecular development of corticospinal motor neuron circuitry. Novartis Found Symp *288*, 3-15; discussion 15-20, 96-18.

Murawsky, C. M., Brehm, A., Badenhorst, P., Lowe, N., Becker, P. B., and Travers, A. A. (2001). Tramtrack69 interacts with the dMi-2 subunit of the Drosophila NuRD chromatin remodelling complex. EMBO Rep *2*, 1089-1094.

Nadarajah, B., Alifragis, P., Wong, R. O., and Parnavelas, J. G. (2003). Neuronal migration in the developing cerebral cortex: observations based on real-time imaging. Cereb Cortex *13*, 607-611.

Nakagomi, K., Kohwi, Y., Dickinson, L. A., and Kohwi-Shigematsu, T. (1994). A novel DNA-binding motif in the nuclear matrix attachment DNA-binding protein SATB1. Mol Cell Biol *14*, 1852-1860.

Nakashima, K., Zhou, X., Kunkel, G., Zhang, Z., Deng, J. M., Behringer, R. R., and de Crombrugghe, B. (2002). The novel zinc finger-containing transcription factor osterix is required for osteoblast differentiation and bone formation. Cell *108*, 17-29.

Nelson, W. G., Pienta, K. J., Barrack, E. R., and Coffey, D. S. (1986). The role of the nuclear matrix in the organization and function of DNA. Annu Rev Biophys Biophys Chem *15*, 457-475.

Neufeld, E. J., Skalnik, D. G., Lievens, P. M., and Orkin, S. H. (1992). Human CCAAT displacement protein is homologous to the Drosophila homeoprotein, cut. Nat Genet *1*, 50-55.

Nguyen, L., Besson, A., Roberts, J. M., and Guillemot, F. (2006). Coupling cell cycle exit, neuronal differentiation and migration in cortical neurogenesis. Cell Cycle *5*, 2314-2318.

Nieto, M., Monuki, E. S., Tang, H., Imitola, J., Haubst, N., Khoury, S. J., Cunningham, J., Gotz, M., and Walsh, C. A. (2004). Expression of Cux-1 and Cux-2 in the subventricular zone and upper layers II-IV of the cerebral cortex. J Comp Neurol *479*, 168-180.

Noctor, S. C., Martinez-Cerdeno, V., Ivic, L., and Kriegstein, A. R. (2004). Cortical neurons arise in symmetric and asymmetric division zones and migrate through specific phases. Nat Neurosci *7*, 136-144.

Noctor, T. A., Pham, C. D., Kaliszan, R., and Wainer, I. W. (1992). Stereochemical aspects of benzodiazepine binding to human serum albumin. I. Enantioselective high performance liquid affinity chromatographic examination of chiral and achiral binding interactions between 1,4-benzodiazepines and human serum albumin. Mol Pharmacol *42*, 506-511.

O'Leary, D. D. (1993). Adding neurons to the adult mammalian brain. Proc Natl Acad Sci U S A *90*, 2101-2102.

O'Leary, D. D., Schlaggar, B. L., and Tuttle, R. (1994). Specification of neocortical areas and thalamocortical connections. Annu Rev Neurosci *17*, 419-439.

Park, J. W., Cai, J., McIntosh, I., Jabs, E. W., Fallin, M. D., Ingersoll, R., Hetmanski, J. B., Vekemans, M., Attie-Bitach, T., Lovett, M.*, et al.* (2006). High throughput SNP and expression analyses of candidate genes for non-syndromic oral clefts. J Med Genet *43*, 598-608.

Peters, H., Neubuser, A., and Balling, R. (1998). Pax genes and organogenesis: Pax9 meets tooth development. Eur J Oral Sci *106 Suppl 1*, 38-43.

Plachez, C., and Richards, L. J. (2005). Mechanisms of axon guidance in the developing nervous system. Curr Top Dev Biol *69*, 267-346.

Poljak, L., Seum, C., Mattioni, T., and Laemmli, U. K. (1994). SARs stimulate but do not confer position independent gene expression. Nucleic Acids Res *22*, 4386-4394.

Prakash, N., Vanderhaeghen, P., Cohen-Cory, S., Frisen, J., Flanagan, J. G., and Frostig, R. D. (2000). Malformation of the functional organization of somatosensory cortex in adult ephrin-A5 knock-out mice revealed by in vivo functional imaging. J Neurosci *20*, 5841-5847.

Rakic, P. (1972). Mode of cell migration to the superficial layers of fetal monkey neocortex. J Comp Neurol *145*, 61-83.

Rakic, P. (1974). Neurons in rhesus monkey visual cortex: systematic relation between time of origin and eventual disposition. Science *183*, 425-427.

Rakic, P. (2003). Developmental and evolutionary adaptations of cortical radial glia. Cereb Cortex *13*, 541-549.

Rash, B. G., and Richards, L. J. (2001). A role for cingulate pioneering axons in the development of the corpus callosum. J Comp Neurol *434*, 147-157.

Rosenfeld, M. G. (1991). POU-domain transcription factors: pou-er-ful developmental regulators. Genes Dev *5*, 897-907.

Roy, K., Kuznicki, K., Wu, Q., Sun, Z., Bock, D., Schutz, G., Vranich, N., and Monaghan, A. P. (2004). The Tlx gene regulates the timing of neurogenesis in the cortex. J Neurosci *24*, 8333-8345.

Sasaki, T., Nishihara, H., Hirakawa, M., Fujimura, K., Tanaka, M., Kokubo, N., Kimura-Yoshida, C., Matsuo, I., Sumiyama, K., Saitou, N.*, et al.* (2008). Possible involvement of SINEs in mammalian-specific brain formation. Proc Natl Acad Sci U S A *105*, 4220-4225.

Satokata, I., and Maas, R. (1994). Msx1 deficient mice exhibit cleft palate and abnormalities of craniofacial and tooth development. Nat Genet *6*, 348-356.

Scott, M. P., Tamkun, J. W., and Hartzell, G. W., 3rd (1989). The structure and function of the homeodomain. Biochim Biophys Acta *989*, 25-48.

Scheuermann, R. H., and Garrard, W. T. (1999). MARs of antigen receptor and co-receptor genes. Crit Rev Eukaryot Gene Expr *9*, 295-310.

Schuffenhauer, S., Leifheit, H. J., Lichtner, P., Peters, H., Murken, J., and Emmerich, P. (1999). De novo deletion (14)(q11.2q13) including PAX9: clinical and molecular findings. J Med Genet *36*, 233-236.

Senawong, T., Peterson, V. J., Avram, D., Shepherd, D. M., Frye, R. A., Minucci, S., and Leid, M. (2003). Involvement of the histone deacetylase SIRT1 in chicken ovalbumin upstream promoter transcription factor (COUP-TF)-interacting protein 2-mediated transcriptional repression. J Biol Chem *278*, 43041-43050.

Shen, Q., Wang, Y., Dimos, J. T., Fasano, C. A., Phoenix, T. N., Lemischka, I. R., Ivanova, N. B., Stifani, S., Morrisey, E. E., and Temple, S. (2006). The timing of

cortical neurogenesis is encoded within lineages of individual progenitor cells. Nat Neurosci *9*, 743-751.

Smart, I. H. (1973). Proliferative characteristics of the ependymal layer during the early development of the mouse neocortex: a pilot study based on recording the number, location and plane of cleavage of mitotic figures. J Anat *116*, 67-91.

Soriano, P. (1999). Generalized lacZ expression with the ROSA26 Cre reporter strain. Nat Genet *21*, 70-71.

Southern, E. M. (1975). Long range periodicities in mouse satellite DNA. J Mol Biol *94*, 51-69.

Stenman, J., Toresson, H., and Campbell, K. (2003). Identification of two distinct progenitor populations in the lateral ganglionic eminence: implications for striatal and olfactory bulb neurogenesis. J Neurosci *23*, 167-174.

Sturm, R. A., Das, G., and Herr, W. (1988). The ubiquitous octamer-binding protein Oct-1 contains a POU domain with a homeo box subdomain. Genes Dev *2*, 1582-1599.

Sugitani, Y., Nakai, S., Minowa, O., Nishi, M., Jishage, K., Kawano, H., Mori, K., Ogawa, M., and Noda, T. (2002). Brn-1 and Brn-2 share crucial roles in the production and positioning of mouse neocortical neurons. Genes Dev *16*, 1760-1765.

Szemes, M., Gyorgy, A., Paweletz, C., Dobi, A., and Agoston, D. V. (2006). Isolation and characterization of SATB2, a novel AT-rich DNA binding protein expressed in development- and cell-specific manner in the rat brain. Neurochem Res *31*, 237-246.

Taddei, A., Roche, D., Sibarita, J. B., Turner, B. M., and Almouzni, G. (1999). Duplication and maintenance of heterochromatin domains. J Cell Biol *147*, 1153-1166.

Tarabykin, V., Stoykova, A., Usman, N., and Gruss, P. (2001). Cortical upper layer neurons derive from the subventricular zone as indicated by Svet1 gene expression. Development *128*, 1983-1993.

Valarche, I., Tissier-Seta, J. P., Hirsch, M. R., Martinez, S., Goridis, C., and Brunet, J. F. (1993). The mouse homeodomain protein Phox2 regulates Ncam promoter activity in concert with Cux/CDP and is a putative determinant of neurotransmitter phenotype. Development *119*, 881-896.

van den Boogaard, M. J., Dorland, M., Beemer, F. A., and van Amstel, H. K. (2000). MSX1 mutation is associated with orofacial clefting and tooth agenesis in humans. Nat Genet *24*, 342-343.

Vanderhaeghen, P., Lu, Q., Prakash, N., Frisen, J., Walsh, C. A., Frostig, R. D., and Flanagan, J. G. (2000). A mapping label required for normal scale of body representation in the cortex. Nat Neurosci *3*, 358-365.

Walther, C., and Gruss, P. (1991). Pax-6, a murine paired box gene, is expressed in the developing CNS. Development *113*, 1435-1449.

Wang, B., Dickinson, L. A., Koivunen, E., Ruoslahti, E., and Kohwi-Shigematsu, T. (1995). A novel matrix attachment region DNA binding motif identified using a random phage peptide library. J Biol Chem *270*, 23239-23242.

Weissman, T., Noctor, S. C., Clinton, B. K., Honig, L. S., and Kriegstein, A. R. (2003). Neurogenic radial glial cells in reptile, rodent and human: from mitosis to migration. Cereb Cortex *13*, 550-559.

Wen, J., Huang, S., Rogers, H., Dickinson, L. A., Kohwi-Shigematsu, T., and Noguchi, C. T. (2005). SATB1 family protein expressed during early erythroid differentiation modifies globin gene expression. Blood *105*, 3330-3339.

Wimmer-Kleikamp, S. H., and Lackmann, M. (2005). Eph-modulated cell morphology, adhesion and motility in carcinogenesis. IUBMB Life *57*, 421-431.

Wu, J., and Luo, H. (2005). Recent advances on T-cell regulation by receptor tyrosine kinases. Curr Opin Hematol *12*, 292-297.

Xue, Y., Wong, J., Moreno, G. T., Young, M. K., Cote, J., and Wang, W. (1998). NURD, a novel complex with both ATP-dependent chromatin-remodeling and histone deacetylase activities. Mol Cell *2*, 851-861.

Yang, X., and Karsenty, G. (2004). ATF4, the osteoblast accumulation of which is determined post-translationally, can induce osteoblast-specific gene expression in non-osteoblastic cells. J Biol Chem *279*, 47109-47114.

Yao, Y. L., and Yang, W. M. (2003). The metastasis-associated proteins 1 and 2 form distinct protein complexes with histone deacetylase activity. J Biol Chem *278*, 42560-42568.

Yasui, D., Miyano, M., Cai, S., Varga-Weisz, P., and Kohwi-Shigematsu, T. (2002). SATB1 targets chromatin remodelling to regulate genes over long distances. Nature *419*, 641-645.

Yun, K., Garel, S., Fischman, S., and Rubenstein, J. L. (2003). Patterning of the lateral ganglionic eminence by the Gsh1 and Gsh2 homeobox genes regulates striatal and olfactory bulb histogenesis and the growth of axons through the basal ganglia. J Comp Neurol *461*, 151-165.

Zhang, Y., Ng, H. H., Erdjument-Bromage, H., Tempst, P., Bird, A., and Reinberg, D. (1999). Analysis of the NuRD subunits reveals a histone deacetylase core complex and a connection with DNA methylation. Genes Dev *13*, 1924-1935.

Zhang, Y., and Reinberg, D. (2001). Transcription regulation by histone methylation: interplay between different covalent modifications of the core histone tails. Genes Dev *15*, 2343-2360.

Zimmer, C., Tiveron, M. C., Bodmer, R., and Cremer, H. (2004). Dynamics of Cux2 expression suggests that an early pool of SVZ precursors is fated to become upper cortical layer neurons. Cereb Cortex *14*, 1408-1420.

8. Acknowledgements

To Dr. Victor Tarakykin, for supervising my work and giving me the opportunity to do my PhD in his lab.

To Professor. Dr. Ernst August Wimmer for accepting to act as my Referee at the Faculty of biology and for his support with all formalities concerning the doctoral thesis. I would also like to thank Professor. Dr. Thomas Pieler, not only for being my Co-referee but also for his support and critical evaluation of my work.

I offer my special thanks to Professor Dr. Walter Stühmer, for being more than a supervisor, a friend and for his constant help, moral support and encouragement.

I wish to extend my gratitude to all our collaborators in England, United States and Russia, who performed several of the experiments that I mencion here and whose efforts have made the Neuron publication possible.

I am also indebted to the CMPB, for providing financial support for this project.

To my former colleagues: Sridhar Boppana ("Siji") for putting a smile on my face each and every day that we worked together; Pavlos Alifragis (" Little Pavlos") for his incredible help and support, he motivated me to do my best and improve, step by step, day by day and also to Anton Karabinos, Amaya Miquelajauregui and Olga Britanova.

To my colleagues: Anjana Nityanandam, we spent a lot of time together, comparing our different cultures, helping each other not only with the research but also sharing everyday life; Manuela Schwark, not only for her amazing technical help but also for creating such a friendly environment in the lab, and Mallte Puhan ("the man in black"), Gerd-Marten Kuscher (" Superhero"), Lena and Vivi.

To my long-standing friends Ana Magaz, Rebeca Garcia and Ana Machin for motivating me.

To my friends Maria Valero and Eva Herrero for making me feel at home in Goettingen.

Special thanks are due to the people in the MBNS department for sharing everything and creating such a good environment, especially to the people on the first floor, Milena, Ye, Miso and Roser , who helped me a lot in my work and also personally. I would also like to thank all my friends at the Max Planck Institute for Experimental Medicine.

To Alberto for believing in me when I was just a biology student and for accompanying me during most of my PhD; to Gena, without his help, I would not have started my PhD career in goettingen.

At the end, not as a matter of importance but only because they already know they are the first, a huge thanks to my family. My parents, Francisca Romero and Francisco Juan, they stood by me in all, good and bad moments throughout my entire career. My sister Rocio, for her moral support; my brother Raul, who was always there to remind me why I was doing this thesis, for encouraging me and helping me to stand up every time I fell and my sister Elena, for helping me everytime when I needed her technical and moral support and for showing me how to enjoy life outside the lab.

9. Curriculum vitae

Meury del Camino de Juan Romero

Born on 14 December 1979, León, Spain.

Education:

Sep 1997 – Jun 2003:   Master of Science in Biology,
León University, Spain.

Jan 2004 - Dec 2004:   Jr. research fellow, Prof. Dr. Depert / Cagatay
Günes. HPI, Hamburg, Germany.

Jan 2005 – Present: PhD student, Prof. Dr. Walter Stühmer/ Victor
Tarabykin, Max Planck Institute, Göttingen,
Germany.

Publications:

Britanova O*, de Juan Romero C*, Cheung A, Kwan KY, Schwark M, Gyorgy A, Vogel T, Akopov S, Mitkovski M, Agoston D, Sestan N, Molnár Z, Tarabykin V.
Satb2 is a postmitotic determinant for upper-layer neuron specification in the neocortex.
Neuron. (2008)Feb 7;**57**:378-92.

Gyorgy AB, Szemes M, de Juan Romero C, Tarabykin V, Agoston DV. SATB2 interacts with chromatin-remodeling molecules in differentiating cortical neurons.
Eur J Neurosci. (2008) Feb;**27** 865-73.

* This Authors contributed equally to this work.

LEBENSLAUF

Name	**Meury del Camino de Juan Romero**
Gerburtsdatum	14.12.1979
Gerburtsort	León (Spanien)
Familienstand	ledig

Schule:

1985 - 1993   Colegio Jesus Maestro MM. Josefinas.
                     León , Spain.

1993 - 1997   Instituto de Bachillerato Padre Isla
                     León , Spain.

Studium:

Sep 1997 – Jun 2003:   Licenciatura in Biology,
                         University of León, Spain.

Promotion:

Jan 2005 – Present: Georg-August Universität Göttingen, MPI Exp. Med
                        Thema: "Functional characterization of Satb1 and Satb2
                        in the developing neocortex" (Dr. Victor Tarabykin).

Berufstätigkeit:

Jan 2004 - Dec 2004:   Jr. Research fellow, Prof. Dr. Depert / Cagatay
                        Günes. HPI, Hamburg, Germany.

Datum des Meldetages: 15.09.2008

_____

Camino de Juan Romero